Promotor: Prof. Dr. Ir. J. Bouma
                   Hoogleraar in de bodeminventarisatie en landevaluatie.

Co-Promotor: Dr. Ing. H.W.G. Booltink
                   Universitair docent bij het Laboratorium voor Bodemkunde en Geologie.

Samenstelling promotiecommissie:
Prof. Dr. G. Várallyay, Research Institute for Soil and Agricultural Chemistry, Budapest, Hungary
Dr. C.J. Ritsema, Alterra, Wageningen, The Netherlands
Prof. Dr. Ir. R.A. Feddes, Wageningen University, The Netherlands
Prof. Dr. Ir. Stroosnijder, Wageningen University, The Netherlands

Irrigation practices affecting land degradation in Sicily

Giuseppina Crescimanno

Proefscrift
ter verkrijging van de graad van doctor
op gezag van de rector magnificus
van Wageningen Universiteit,
Prof. Dr. Ir. L. Speelman,
in het openbaar te verdedigen
op maandag 17 September 2001
des namiddags te 16.00 uur in de Aula

Propositions

1. To estimate the hydraulic parameters of clay soils, laboratory and optimization techniques accounting for macropores and shrinkage processes are necessary.
this thesis

2. The concept of "critical ESP threshold" needs reconsideration, because soil degradation upon increasing ESP is a continuum.
this thesis

3. Simulation models to evaluate management options in Mediterranean clay soils lead to irrelevant results when bypass flow is not considered.
this thesis

4. Alternating application of water of different qualities during irrigation is effective in preventing accumulation of salts when bypass flow occurs.
this thesis

5. The efficiency of Sodium removal by leaching is highest when the soil is dry and cracked, allowing rapid vertical movement of water along air-filled cracks.
this thesis

6. Scientists are not in a position to provide unequivocal "solutions" to problems. Rather, they can be helpful in formulating precise questions and problems and in developing options from which users can make a choice which best fits their priorities.

7. Our job as soil scientists requires us to be always critical about results obtained by established measuring and modelling methods, using field observations as starting points for innovative approaches to soil and water studies.

8. Interaction between scientists and policy makers is necessary to make efforts in combating desertification more effective. Scientists should be prepared to contribute different qualitative and quantitative sets of information to the interaction process.

9. In combating desertification and drought, active participation of local communities and local organizations is crucial. Researchers have a particular responsibility to make sure that links with regulatory and political organizations at regional and national level are maintained.

10. Current members of the European Union (EU) should be prepared to grant the same opportunities to the new members from Eastern Europe as were available to themselves in earlier years, even if this means that they will receive less funds from an enlarged EU in future.

11. Our knowledge of land degradation in Southern Europe is rich in some ways, and completely insufficient in others. The main focus has been on the role of climate, but the role of physical properties has not been sufficiently explored.

12. The best guarantee for being able to function well in the future is to look modestly but proudly to what has been achieved in the past, not being completely guided by judgements of others.

G. Crescimanno – Irrigation practices affecting land degradation in Sicily
Wageningen, 17 September 2001

Acknowledgments

Contents

Abstract

The available amount of fresh water for agriculture, and specifically for irrigation, is decreasing all over the world. The quality of irrigation water is deteriorating, and saline/sodic waters are increasingly used in many arid and semi-arid regions of the world. Salinization is closely associated with the process of desertification.

Sustainable land management practices are urgently needed to preserve the production potential of agricultural land while safeguarding environmental quality. In cracking soils sustainable management should take into account the occurrence of bypass flow and the influence that land use may have on soil structure and bypass flow phenomena.

Measurement of vertical and horizontal shrinkage in confined soil cores was found to be suitable for determining the Soil Shrinkage Characteristic Curve (SSCC) and for incorporating shrinkage in the soil hydraulic parameters/functions determined on confined undisturbed soil samples. An optimization procedure based on multi-step outflow experiments with inverse modelling was developed for determining the soil hydraulic characteristics (HC). The need for accounting for structural porosity and shrinkage processes was recognized on the basis of hydraulic conductivity values determined by the suction crust infiltrometer method and of the SSCC determined on confined soil cores.

Analysis of the response of clay soils to ESP values up to 15, showed that the concept of critical thresholds needs reconsideration, because increasing soil degradation upon increasing ESP appeared to be a continuum. A major hazard of deterioration of structural and hydraulic properties was recognized even at low ESP values (ESP<5) in dilute solutions. In addition, the major influence that reductions in hydraulic conductivity due to salinity and/or sodicity may have in water transport in the soil-crop system was also documented by application of the LEACHM model.

The relevance of bypass flow on the water balance in a Mediterranean climatic context as that occurring in Sicily, was evaluated by application of the FLOCR model. The results showed that bypass flow corresponded with about 70-74% of cumulative yearly rainfall, and that models not accounting for bypass flow may lead to a significant overprediction of crop evapotranspiration and underestimation of the hazard of land degradation and desertification.

Results of bypass flow measurements performed in a Mediterranean cracking soil under alternated use of a high salinity solution to distilled water showed that exchange of solutes occurred at the contact surfaces between the macropores/cracks walls and the incoming solution in concomitance with bypass fluxes. These exchanges were effective in determining leaching of solutes and removal of Sodium, and in preventing salinization and sodification in part of the soil volume that is in contact with the roots.

Combined use of morphometric and physical techniques made it possible to explore the effect of irrigation on soil structure and bypass flow phenomena of a Sicilian cracking soil under two different irrigation systems, i.e. drip and micro-sprinkler. Different vertical distributions of cracks was found under the two irrigation systems. In agreement with these observations, different flow behaviour was observed in the laboratory in cylindrical soil cores taken from the irrigated micro-sprinkler field. No bypass flow or lower amounts of

bypass flow were observed in the micro-sprinkler irrigated field compared to the drip irrigation treatment. Chemical dispersion of clay particles and detachment of these particles from the surface and their movement into the cracks were the mechanisms responsible for the partial or total occlusion of the (macro) pores in the micro-sprinkler irrigated field.

In conclusion, this study showed that drip irrigation alternatively using high and low salt water was most effective in maintaining the productive capacity of the clay soil being studied, particularly when this water was applied to a cracked soil. Combined use of morphometric and physical methods was necessary to understand the underlined highly dynamic flow behaviour in these complex soils.

Chapter 1

General Introduction

General Introduction

The available amount of fresh water for agriculture, and specifically for irrigation, is decreasing all over the world. The quality of irrigation water is also deteriorating, and saline/sodic waters are increasingly used in many arid and semi-arid regions of the world.

Salinization represents a hazard not only for agriculture, but also for the whole environment (Szabolcs, 1989). According to the estimates of FAO and UNESCO, as many as half of the current irrigation systems of the world are more or less under the influence of secondary salinization, sodification and waterlogging. Salinization is closely associated with the process of desertification, defined as "land degradation in arid, semi-arid and dry sub-humid areas resulting from climatic variations and human activities", with the term "land" including soil, water resources, crops and natural vegetation (UNEP, 1991).

Sustainable land management practices are urgently needed to preserve the production potential of agricultural land while safeguarding environmental quality. According to one of the various definitions given by FAO (1993), sustainable land management combines "technologies, policies and activities aimed at integrating socio-economic principles with environmental concern so as to protect the potential of natural resources and prevent degradation of soil and water quality".

Soil, as a part of a complex ecosystem, plays a crucial role in defining sustainable management practices. Water is the most important carrier of pollutants and salts in our soils. Rates of soil water movement in various soil water flow processes (infiltration, redistribution, root uptake and dynamics) are important for making practical soil management decisions to minimise potential groundwater contamination and degradation of soil quality from land applied chemicals.

Swelling/shrinking clay soils change volume (V) with changes in water content (Murray and Quirk, 1980), and during dry periods extensive cracks will form in the field (Bronswijk, 1988). These volumetric changes cause modifications in the geometry of some if not all the soil pores (Berndt and Coughlan, 1976), affecting the bulk density/water content relationship (Allbrook, 1992), and soil mechanical properties (Yong and Warkentin, 1975).

Soil cracks alter the pore-size distribution through intermittent wetting, acting as significant pathways for water and solutes and determining the occurrence of bypass flow, i.e. the rapid transport of water and solutes via shrinkage-cracks to subsoil and to groundwater through an unsaturated soil matrix (Beven and Germann, 1982; Bouma, 1991).

The Soil Shrinkage Characteristic curve: measurement and prediction

Knowledge of the Soil Shrinkage Characteristic Curve (SSCC), defined as the relationship between specific volume of soil clods per unit mass of soil (v) and gravimetric water content (U) (Mitchell, 1992), is fundamental to calculate the volumetric water content in swelling/shrinking soils, to predict cracking and subsidence under field conditions (Bronswijk, 1988), and to incorporate soil deformation in the soil hydraulic characteristics (HC) (Kim et al, 1992; Crescimanno and Iovino, 1995).

17

Different methods have been proposed to determine the SSCC. The method proposed by Brasher et al.(1966), based on the use of resin-coated natural aggregates, represents a fast and widely used measurement technique (Reeve et al., 1980; McGarry and Daniells, 1987; Bronswijk and Evers-Vermeer, 1990; Crescimanno et al., 1995). The measurement of surface subsidence and horizontal shrinkage, which is time-consuming compared to the use of resin-coated aggregates, has been used less frequently (Yule and Ritchie, 1980a; Bronswijk, 1990).

Comparisons need to be performed between the SSCCs measured on resin-coated aggregates and confined cores, the determination of which could be affected not only by the larger volume of the cores, but also by the different geometry and by the action of the inflexible ring containing the samples compared to the flexible resin wrapping the clods. Making this comparison will constitute the first objective of this research.

The possibility to predict the SSCC of confined cores from routinely measured soil physical properties will also be investigated as measurement of SSCC in confined cores is time-consuming compared to that performed on resin-coated clods.

Hydraulic characterization of structured soils

Models simulating transport of water and solutes in unsaturated soil require, in addition, the knowledge of soil hydraulic characteristics (HC), i.e. the water retention curve $\theta(h)$ and the hydraulic conductivity function $K(\theta)$.

The multistep (MSTEP) outflow method with inverse modeling (Kool et al. (1985; 1987) is increasingly used to determine the soil hydraulic properties (van Dam et al., 1990), but specific optimization techniques accounting for the presence of preferential pathways and incorporating shinkage processes (Kim et al., 1992) need to be developed for accurate determination of soil HC in clay soils.

Booltink et al. (1991) proposed the suction crust infiltrometer method (SCIM) to determine the hydraulic conductivity of structured soils in the near-saturation range.

Optimization procedures based on MSTEP experiments and incorporating some measurement of the saturated/unsaturated hydraulic conductivity performed by the SCIM on large soil cores ($\emptyset$=20 cm, h=20 cm) will be investigated in this study. Soil Shrinkage Characteristic Curves determined on soil samples having the same geometry as those used for MSTEP experiments (Crescimanno & Provenzano, 1999) will be used to incorporate shrinkage in the estimated hydraulic parameters/functions.

Swelling/shrinking clay soils in the saline/sodic environment

Sodium in the exchange complex may negatively affect soil structure, and aggregate stability (Abu-Sharar et al., 1987a; Baiamonte and Crescimanno, 1997), causing swelling (Murray and Quirk, 1980), dispersion of the clay particles (Shainberg et al., 1981), and slaking of unstable aggregates (Abu-Sharar et al., 1987b; Agassi et al., 1981).

An Exchangeable Sodium Percentage (ESP) greater than 15 (US Salinity Laboratory, 1954) is considered to affect the soil structural and hydraulic characteristics, but some investigations suggested that this concept of "critical threshold" may need reconsideration, because soil degradation can take place even at low ESP values in dilute solutions (Quirk and Schoefield, 1955; Shainberg et al., 1981).

Determination of quantitative relationships between soil (structural and hydraulic) properties and ESP is necessary to develop management strategies aimed to combat and prevent degradation of soil quality.

Analysis of the response of clay soils to ESP values up to 15, in terms of structural and hydraulic characteristics will be investigated in this study to verify existence of critical ESP threshold(s), or the hypothesis of a continuous soil behaviour at increasing ESP(s).

Water and solute transport in saline/sodic clay soils

Irrigation with saline-sodic waters is practiced in Sicily in many areas where these waters represent the only source of available water; clay soils with variably swelling/shrinking properties are widespread in these areas (Crescimanno and Provenzano, 1995). Great attention is focused in Sicily on the possible environmental adverse effects of irrigation such as secondary salinization and sodification (Crescimanno et al., 1995b; Baiamonte and Crescimanno, 1997).

Evaluation of the influence that reductions in hydraulic conductivity due to salinity and/or sodicity may have on water transport in the soil-crop system will be achieved by application of the LEACHM model (Wagenet and Hutson, 1992), simulating water flow and crop conditions. The possibility to use LEACHM to predict the hazard of salinization and/or sodification will be also explored in a Sicilian profile where irrigation with saline/sodic waters is a current practice.

Bypass flow as a relevant term in the water balance under Mediterranean conditions

The relevance that bypass flow, i.e. "the rapid transport of water and solutes via macropores or shrinkage-cracks to subsoil and to groundwater (Bouma, 1991)", may have on water flow, solute or pesticide transport is becoming increasingly recognized (Ahuja et al., 1991; Stenhuise and Parlange, 1991). In structured soils bypass flow is dominated by soil hydrological processes, such as rain intensity, initial pressure head of the soil, surface storage of rain, and hydraulic conductivity of the soil matrix. Bypass flow occurs when, during a rain event, rainfall intensity is higher than the adsorption capacity on the soil surface (Booltink et al., 1993). Magnitude of bypass flow processes can be particularly relevant in some Mediterranean climatic contexts characterized by high values of the rainfall intensity, low amounts of the annual rainfall, high values of the rainfall intensity, and clay soils with a low hydraulic conductivity.

In this study, assessment of the relevance of bypass flow as a term of water balance will be performed by a simulation model accounting for shrinkage/cracks and predicting bypass flow under specific soil and climatic conditions (Bronswijk, 1988). Using these models the influence of neglecting bypass flow on water transport and crops (evapo)transpiration will be evaluated.

Influence of bypass flow on salt-accumulation and salt- leaching in cracking soils

When saline/sodic waters are used for irrigation, conjunctive or alternated use of different- quality irrigation waters can be applied to reduce salt-accumulation in the root zone through

19

adequate leaching (Prendergast, 1995), and to keep the cationic concentration (C) of the pore solution at thresholds compatible with the crops tolerance (Maas, 1990).

However, in clay soils high velocity fluxes travelling through cracks may have less opportunity than slower moving water to leach salts from the root zone. Little work has been done to determine the extent at which bypass flow contributes to leaching of salts in the root zone (White, 1985). In order to simplify calculations of water loss below the root zone, some researchers assumed that bypass flow does not contribute to leaching (van der Molen, 1973; Thorburn and Rose, 1990). Yet in one field experiment on a heavy clay soils, it was suggested that bypass flow provided the primary mechanism for leaching (McIntire et al., 1982a,b).

The role of bypass flow on salt-accumulation and salt-leaching will therefore be investigated in this study in order to find management practices that are suitable to prevent salinization and sodification in cracking soils.

Sustainable management of irrigation in cracking soils

Sustainable management of irrigation in cracking soils should take into account the occurrence of bypass flow and the influence that land use may have on soil structure and bypass flow phenomena.

The sprinkler irrigation system is recognized to induce deterioration in soil structure because of clay dispersion, compaction under raindrop impact and surface sealing (Al-Quinna and Abu-Awwad, 1998).

Clay dispersion and migration of the detached particles may affect soil structure (Baiamonte and Crescimanno, 1997) and modify (macro)pores distribution, decreasing the soil hydraulic conductivity (Crescimanno et al., 1995; Lima et al. 1990), thereby affecting water flow and/or solute transport (Crescimanno and Iovino, 1995; McCoy and Cardina, 1997).

Flow patterns associated with bypass flow can be morphologically characterized using tracers such as methylene blue (Bouma and Dekker, 1978; Booltink and Bouma, 1991). Bypass flow can be measured in undisturbed soils columns under different rates of water application (Booltink et al., 1993).

Research is focused in this study wether coupling morphometric techniques with outflow measurements can be useful to investigate the effect of different irrigation systems on the macropores/cracks distribution and on the bypass flow behaviour of cracking soils, and to find sustainable management options in areas susceptible to desertification.

Research objectives

This thesis aims to contribute to hydrological and environmental research focused on prevention of land degradation and desertification in arid and semi-arid regions, with special attention to specific conditions occurring in Sicily, where a project funded by the EU is currently running (Crescimanno, 1998). Objective of the project is to derive management options and associated methodologies suitable to control and to prevent the extent of salinization and sodification in areas irrigated with saline/sodic waters.

The thesis is structured into three main parts. Part 1 focuses on the development of laboratory methodologies suitable for determination of basic soil physical/hydraulic properties. Part 2 focuses (i) on the interaction between salinity and sodicity and soil physical properties and (ii) on the analysis of water and solute transport in cracking soils. Part 3 focuses on a combination of laboratory techniques and field investigations with the purpose to derive sustainable management options suitable to prevent land degradation.

Specifically, in Part 1 (Chapters 2 and 3), measurement techniques suitable to measure shrinkage properties in clay soils and to determine hydraulic parameters/functions accounting for structural porosity and volume changes are developed.
In Part 2 (Chapters 4 and 5), (i) the influence of salinity and sodicity on soil structural and hydraulic properties of two Sicilian Vertisols is assessed by using measurement techniques developed in Part 1. The influence of salt-affected hydraulic characteristics (HC) on water transport is evaluated by a physically-based simulation model; the chemistry version of the same model is then used to predict the hazard of salinization and sodification for a Sicilian Vertisol irrigated with saline/sodic waters.
In Part 3 (Chapters 6, 7 and 8) the relevance that bypass flow may have on water transport is analyzed under climatic conditions characteristics of a Mediterranean environment like Sicily.
The role of bypass flow on the processes of salt-accumulation and salt-leaching is investigated, and combined use of morphometric and physical techniques is used to explore the effect of two different irrigation systems, i.e. drip and micro-sprinkler, on soil structure and bypass flow phenomena of a Mediterranean cracking soil.

Outline of the thesis
In Chapter 2 (Crescimanno and Provenzano, 1999), differences between the SSCC obtained on resin-coated natural aggregates (volume $V= 20-30$ cm^3) and on cylindrical confined cores having a volume (650 cm^3) which is close to the volume of the cores used for HC laboratory determination, are investigated using twenty-one Sicilian soils of variable shrink/swell behaviour.

In Chapter 3 (Crescimanno and Iovino, 1995; Crescimanno and Baiamonte, 1999), the applicability of the inverse method based on one-step and on multi-step outflow experiments for determining the soil water characteristic curve $\theta(h)$ and the hydraulic conductivity/water content $K(\theta)$ functions, is investigated for some Sicilian cracking soils.
An optimization procedure based on MSTEP experiments and incorporating some measurements of the saturated/unsaturated hydraulic conductivity performed by the Suction Crust Infiltrometer Method (SCIM) is then explored to account for the influence of structural porosity in clay soils.

In Chapter 4 (Crescimanno et al., 1995) the response of two Sicilian Typic Haploxererts to ESP values up to 15 is evaluated, at a low cationic concentration, in order to verify if a critical ESP threshold can be found, or if the hypothesis of a continuous behaviour is more

appropriate. The investigation is focused on aggregate stability, rating of soil shrink-swell potential and on both saturated and unsaturated hydraulic conductivity.

In Chapter 5 (Crescimanno, 2000) the influence of salt-affected soil hydraulic characteristics on water transport in the soil-crop system, is explored by application of the water flow version of the simulation model LEACHM (Wagenet and Hutson, 1992). The possibility to use the LEACHM model to predict the hazard of salinization and sodification connected with the use of saline/sodic waters is then explored and a comparison between predicted and measured values is performed for a Sicilian Vertisol.

In Chapter 6 (Crescimanno and Provenzano, 2000) the relevance of bypass flow as a term of the water balance under climatic conditions such as those occurring in a Mediterranean region as Sicily, is analysed by application of the FLOCR model (Oostindie and Bronswijk, 1992). These climatic conditions are characterized by high rainfall intensities, low annual rainfall and high rates of maximum evapotranspiration. The influence of bypass flow on water balance and on the hazard of land degradation and desertification is quantified.

In Chapter 7 (Crescimanno et al., 2000) the role of bypass flow in the process of salt-accumulation and/or salt-leaching in a Sicilian cracking soil where irrigation with saline-sodic waters is practised is investigated to check (i) if alternated application of high salinity and low salinity waters is effective for preventing the hazard of salt-accumulation and (ii) to explore the role of cracking in the process of solutes and Sodium removal under the occurrence of bypass fluxes.

In Chapter 8 (Crescimanno et al., 2000) the influence of two different irrigation systems, i.e. drip and micro-sprinkler, on soil structure and bypass flow phenomena is studied. Field application of methylene blue and laboratory measurements of bypass flow is used to investigate the effect of the two irrigation systems on the macropores/cracks distribution and on the bypass flow behaviour of a Sicilian cracking soil under the two irrigation systems.

Chapter 2

Soil Shrinkage Characteristic Curve in clay soils: measurement and prediction

Soil Shrinkage Characteristic Curve in clay soils: measurement and prediction

G. Crescimanno and G. Provenzano
Università di Palermo, Dipartimento ITAF, Sezione Idraulica. Palermo, Italy

Abstract

Laboratory determination of soil hydraulic characteristics (HC) is performed on cylindrical confined soil cores, while resin-coated small natural aggregates are prevalently used for determining the Soil Shrinkage Characteristic Curve (SSCC). Because of the different geometry and volume of clods and cores, incorporation of shrinkage in HC of clay soils could be affected by the use of SSCC determined on natural aggregates or on confined cores.

The objectives of this paper were (i) to investigate differences between the SSCC obtained on resin-coated natural aggregates (volume V= 20-30 cm³) and on cylindrical confined cores having a volume (650 cm³) close to that of cores used for HC laboratory determination; (ii) to test the performance of different models proposed for analytical interpretation of the SSCC and (iii) to derive regression equations predicting the SSCC from routinely measured soil physical properties.

Using twenty-one Sicilian soils of variable shrink/swell behavior, we found significantly larger specific volume (v), indicating less shrinkage, in the cylindrical confined cores. The investigation also proved the good fitting of a two-line model to the measured SSCC, and the possibility to predict the basic shrinkage line from the clay content.

These results suggest that incorporation of shrinkage in HC of clay soils should be based on the SSCC measured or predicted on cores with geometry and dimensions as those used for routine laboratory measurement of HC.

Introduction

Swelling/shrinking clay soils change volume (V) with changes in water content (Murray and Quirk, 1980), and during dry periods extensive cracks will form in the field (Bronswijk, 1990). These volumetric changes cause modifications in the geometry of some if not all the soil pores (Berndt and Coughlan, 1976), affecting the bulk density/water content relationship (Allbrook, 1992), and soil mechanical properties (Yong and Warkentin, 1975).

An important consequence of shrinkage is the preferential transport of water and solutes via shrinkage-cracks to subsoil and to groundwater (Beven and Germann, 1982).

Mitchell (1992) proposed to express the volume changes by the relationship between specific volume of soil clods per unit mass of soil (v) and gravimetric water content (U), defining this relationship the Soil Shrinkage Characteristic Curve (SSCC).

Assessment of soil volume change as a function of water content has been the subject of much research (Chan, 1982; McGarry and Malafant, 1987; Dasog et al., 1988; McGarry, 1988; Mitchell and van Genuchten, 1992).

Different methods have been proposed to determine the SSCC. The method proposed by Brasher et al.(1966), based on the use of resin-coated natural aggregates, represents a fast and widely used measurement technique (Reeve et al., 1980; McGarry and Daniells, 1987; Bronswijk and Evers-Vermeer, 1990; Crescimanno et al., 1995). The measurement of surface subsidence and horizontal shrinkage, which is time-consuming compared to the use of resin-coated aggregates, has been used less frequently. This measurement includes undisturbed soil cores (Yule and Ritchie, 1980a), large lysimeters (Bronswijk, 1990) or measurement under field conditions (Mitchell and van Genuchten 1992).

There is an increasing evidence of the influence that swelling-shrinkage processes may have on measurement of soil hydraulic characteristics, HC, (Bouma, 1983; Bronswijk, 1988). The need for incorporating soil deformation in the hydraulic parameters estimated by inverse techniques based on the evaporation or on the outflow method was recently confirmated by Garnier et al.(1997).

Procedures for incorporating volume changes in soil HC were proposed by Kim et al.(1992b), using the evaporation method, and by Crescimanno and Iovino (1995), using the parameter estimation method based on multi-step outflow experiments. In these studies, the SSCC was determined by separate experiments performed on small resin-coated aggregates, while both the evaporation and the outflow method are based on use of cylindrical confined cores with a volume ranging from 283.7 to 652.6 cm³.

Comparisons between SSCCs determined on small or larger confined cores (Yule and Ritchie 1980a, b) or under laboratory or field conditions (Mitchell and van Genuchten, 1992), showed differences in the SSCCs according to the volume of the soil samples used.

No comparisons appear to have been performed between SSCCs measured on resin-coated aggregates and confined cores, the determination of which could be affected not only by the larger volume of the cores, but also by the different geometry and by the action of the inflexible ring containing the samples compared to the flexible resin wrapping the clods.

Different models have been proposed for describing the SSCC: (i) the Three-Straight-Lines-Model (TSLM) (McGarry and Malafant, 1987); (ii) the Logistic model (LM) (Nelder, 1961, 1962) and (iii) the model proposed by Kim et al. (KM) (1992a).

The TSLM has mathematical properties which are consistent with the physical conditions operating within each of the three shrinkage zones, and the derived parameters have a physical meaning (McGarry and Malafant, 1987).

The TSLM (Fig. 1) is represented by the following equations:

$$v = \alpha + r\,U \qquad 0 < U < U_A \tag{1a}$$

$$v = k + n\,U \qquad U_A < U < U_B \tag{1b}$$

$$v = \gamma + s\,U \qquad U_B < U < U_S \tag{1c}$$

where:

- r, n and s are slopes of the SSCC in the residual, basic and structural zones, respectively;

$-U_A$, U_B and U_s represent the residual inflexion point, structural inflexion point and saturated water content, and α, k and γ are empirical constants.

The TSLM reduces to a two-line model if structural shrinkage is absent or negligible, as often observed (McGarry and Daniells, 1987). In this case the structural inflexion point (U_b) coincides with the saturated water content (U_s).

The Logistic Model (LM) represents the SSCC by an "S" shaped continuous curve with a gradual flattening of the relationship at either end and with a relatively straight section in between, corresponding to the basic shrinkage zone.

The equation is:

$$v = a + \frac{c}{1+\exp\left[-b\left(U-m\right)\right]} \tag{2}$$

where a, b, c and m are empirical constants.

The model proposed by Kim et al. (KM) is represented by the following equation:

$$v = \frac{1}{\rho_S} + \frac{1}{\rho_S \exp[\alpha' \rho_S U]} + b'U \tag{3}$$

with ρ_s particle density (Mg/m3) and a', α' and b' empirical parameters.
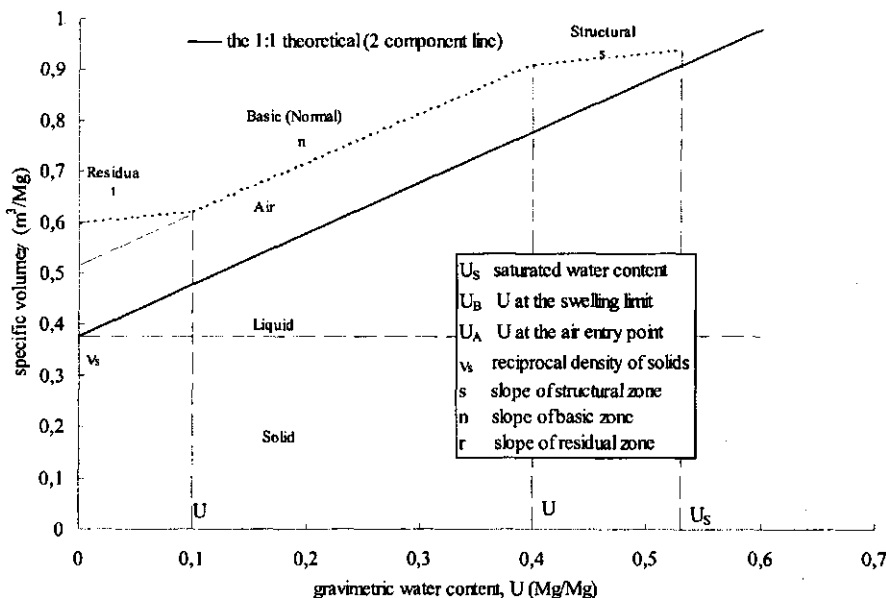
Fig.1 General form of the Three-Straight-Lines-Model (TSLM) with the three shrinkage phases.

Adapting an equation to the (U,v) experimental values is useful not only for analytical interpretation of the SSCC but also for exploring the possibility of relating the models' parameters to routinely determined soil physical properties, in order to predict the SSCC.

The literature reports relationships between the volume change (ΔV) or the coefficient of linear extensibility (COLE) and soil physical properties (De Jong et al., 1992; Parker et al., 1977; Schafer and Singer, 1976), but no attempts appear to have been made to relate the models' parameters to soil physical properties.

The objectives of this paper were (i) to compare the SSCC determined on natural aggregates to that obtained on confined cores having the same geometry and approximately the same dimensions as those used for laboratory determination of soil hydraulic characteristics; (ii) to test the performance of the TSLM, LM and KM models for the analytical interpretation of the SSCC; (iii) to investigate the possibility of predicting the SSCC from routinely measured soil physical properties.

Materials and methods

Twenty-one soils belonging to seven Sicilian irrigated areas were considered. Table 1 reports the classification and some physico-chemical characteristics of these soils.

Large undisturbed clods, sampled at a water content approaching field capacity, were equilibrated at a matric pressure of -0.2 kPa in a Stakman apparatus (Stakman et al., 1969). Three small aggregates were extracted from each large saturated clod. The aggregates, each representing a structural elementary unit, with a volume variable between 20 and 30 cm³, were immersed in SARAN F-310 resin (Brasher et al., 1966), using a resin to solvent ratio 1:5 (w/w).

The SARAN-coated clods were air-dried for about one hour and then re-saturated in the Stakman apparatus. By weighing in air and under water, both the weight and volume of the clods were determined non destructively at different stages of shrinkage. When weight losses became negligible, the SARAN-coated clods were oven-dried in order to determine final dry volume and dry weight.

The SSCC curve was expressed as specific volume v (m³/Mg⁻¹), which is the reciprocal of the bulk density ρb (Mg/m³), vs. gravimetric water content U (Mg/Mg⁻¹).

Ten soils, representative of different textural classes, were chosen for measurement of vertical and horizontal shrinkage (Yule and Ritchie, 1980a). Two replicated undisturbed soil cores, measuring 11.5 cm in height and 8.5 cm in diameter, were sampled on the same dates as the large undisturbed clods with a thin-wall hydraulic sampler, and equilibrated at a matric pressure of -0.2 kPa in the Stakman apparatus.

Vertical shrinkage (Δz) was determined daily during the drying period by measuring nine marked surface positions with a dial vernier caliper bolted to a fixed bar. A microswitch, glued to the shaft of the caliper, which could be read to a precision of 0.1 mm., was activated by contact with the soil surface. The weight of the cores was recorded daily. When the cores were approaching air-dryness, the steel tube was removed and the circumference of the core was measured with a flexible tape. Finally, the cores were oven-

dried and Δz was re-measured.

The geometry factor (r_s), which accounts for the relative amount of the vertical shrinkage caused by the changes in total volume shrinkage (ΔV), was determined (Rijniersce, 1983):

$$r_s = \frac{\log\left(1 - \dfrac{\Delta V}{V}\right)}{\log\left(1 - \dfrac{\Delta z}{z}\right)} \tag{4}$$

where V (cm3) and z (cm) are initial volume and height respectively.

Table 1 - Classification and main physico-chemical characteristics of the soils studied

Soil	Classification†	Horizon	Clay [%]	Silt [%]	Sand [%]	OM†† [%]	CEC§ [cmol$_c$/kg]
DELIA 1	Typic Haploxerert	Ap (0-30 cm)	57	35	8	3,55	39,2
DELIA 1	Typic Haploxerert	A1 (30-60 cm)	64	29	7	3,79	41,3
DELIA 2	Calcixerollic Xerochrepts	Ap1 (0-20 cm)	26	17	57	0,87	19,6
DELIA 2	Calcixerollic Xerochrepts	Ap2 (20-65 cm)	28	21	51	1,09	18,1
DELIA 3	Vertic Xerofluvent	Ap (0-20 cm)	22	11	67	1,16	22,5
DELIA 4	Typic Xerofluvent	Ap (0-30 cm)	22	19	59	0,84	25,0
DELIA 5	Typic Xerochrepts	Ap (0-30 cm)	35	26	39	1,42	29,0
DELIA 6	Typic Rhodoxeralfs	Ap (0-30 cm)	18	34	48	1,65	25,0
GELA 1	Typic Haploxerert	Ap (0-27 cm)	54	27	19	3,47	35,3
GELA 1	Typic Haploxerert	A1 (27-60 cm)	57	24	19	1,21	34,1
GELA 2	Typic Xerofluvent	Ap1 (0-20 cm)	21	14	65	0,66	31,9
GELA 3	Typic Chromoxerert	Ap (0-30 cm)	60	22	18	1,27	47,2
GELA 4	Typic Xerofluvent	Ap (0-30 cm)	29	19	52	0,91	25,0
GELA 5	Vertic Xerofluvent	Ap (0-30 cm)	50	23	27	0,64	49,0
GELA 6	Typic Chromoxerert	Ap (0-30 cm)	42	34	24	1,37	31,6
GELA 7	Typic Pelloxerert	Ap (0-30 cm)	46	28	26	1,30	34,1
GIBBESI 14	Vertic Xerochrepts	Ap (0-40 cm)	50	30	20	0,88	n.d.
GIBBESI 15	Calcixerollic Xerochrepts	Ap (0-20 cm)	20	40	40	1,68	n.d.
GORGO 1	Typic Chromoxerert	Ap (0-13 cm)	41	26	33	2,44	30,6
GORGO 1	Typic Chromoxerert	A1 (13-30 cm)	42	29	29	2,10	25,9
GORGO 2	Typic Xerofluvent	Ap (0-12 cm)	16	12	72	0,61	25,0
MISILMERI	Typic Xerochrepts	Ap (0-30 cm)	53	30	17	1,27	28,4
TIMETO 8	Typic Xerochrepts	Ap (0-30 cm)	57	25	18	2,35	45,0
TIMETO A3	Typic Xerochrepts	Ap (0-30 cm)	41	20	39	1,20	32,8
ZAFFERANA 1	Typic Chromoxerert	Ap (0-35 cm)	44	32	24	2,74	38,1
ZAFFERANA 1	Typic Chromoxerert	A1 (35-70 cm)	45	28	27	2,76	36,9

†   Soil Taxonomy (Soil Survey Staff, 1992)
†† OM = organic matter
§   CEC = cation exchange capacity
     n.d. = not determined

The Δz values measured during air-drying together with the determined rs were used for calculating the total volume shrinkage (ΔV) corresponding to each U value, and the specific volume v at fixed U.

Models (1), (2) and (3) were fitted to the (U,v) values obtained on the replicated clods of the different soils (Systat, 1992) and their performance was evaluated by comparing the Residual Mean Square (RMS) associated with each fitted equation, accounting for the number of parameters in each equation. The same analyses were performed on the (U,v) values obtained on the replicated cores. Further analyses were based on the results of the best fitting model (BFM).

Table 2 - Residual Mean Square (RMS) associated with the TSLM, with the LM, and with the KM fitted to specific volume (v) vs. gravimetric water content U (clods)

Soil	N†	10^3 RMS		
		TSLM	LM	KM
DELIA 1 a	16	0,072	0,115	0,118
DELIA 1 b	47	0,358	1,166	1,265
DELIA 2 a	27	0,083	0,237	0,213
DELIA 2 b	35	0,225	0,589	0,463
DELIA 3	20	0,074	0,095	0,101
DELIA 4	30	0,221	0,505	0,452
DELIA 5	41	0,116	0,500	0,471
DELIA 6	40	0,216	0,700	0,930
GELA 1 a	16	0,030	0,024	0,054
GELA 1 b	44	0,048	0,213	0,686
GELA 2 a	39	0,309	0,833	0,952
GELA 3	58	0,138	0,765	1,111
GELA 4	27	0,049	0,180	0,174
GELA 5	30	0,105	0,421	0,426
GELA 6	20	0,530	0,714	0,659
GELA 7	29	0,239	0,489	0,540
GIBBESI 14	30	0,049	0,124	0,290
GIBBESI 15	29	0,270	0,372	0,504
GORGO 1 a	16	0,114	0,059	0,054
GORGO 1 b	48	0,102	0,311	0,296
GORGO 2	29	0,206	0,392	0,361
MISILMERI	26	0,324	1,008	0,891
TIMETO 8	44	0,187	0,570	0,535
TIMETO A3	58	0,061	0,284	0,339
ZAFFERANA 1 a	16	0,115	0,114	0,165
ZAFFERANA 1 b	45	0,197	0,705	0,682
		0.171††	0.442††	0.490††

† N=number of measurements

†† average

For each soil, the significance of the differences between the SSCCs measured on clods and on cores was analysed by ANOVA performed on the BFM parameters.

The possibility of predicting the SSCC from routinely determined physico-chemical properties was investigated by simple and multiple regression equations (Statistix, 1994) between the parameters of the BFM and the following variables: clay content (C), organic matter (OM), cation exchange capacity (CEC).

The accuracy of the predictive equations was tested by analysing the significance of the differences between the v measured and those predicted, at fixed U.

Results and discussion

Table 2 reports the Residual Mean Square (RMS) associated with the TSLM, the LM and the KM fitted to the replicated clods of the different soils. Table 3 reports the results obtained on the confined cores.

Tables 2 and 3 show the best performance of the TSLM with regard to the LM and the KM, the poorer fit to the data being that of the KM.

Table 3 - Residual Mean Square (RMS) associated with the TSLM, with the LM, and with the KM fitted to specific volume (v) vs. gravimetric water content U (confined cores)

Soil	N†	10^3 RMS		
		TSLM	LM	KM
DELIA 1 a	23	0,055	0,396	0,464
DELIA 1 b	20	0,364	0,331	0,379
DELIA 2 a	41	0,237	0,223	0,232
DELIA 3	20	0,073	0,078	0,074
DELIA 4	30	0,228	0,386	0,229
DELIA 5	24	0,108	0,109	0,111
DELIA 6	20	0,137	0,145	0,147
GELA 6	22	0,042	0,075	0,109
GELA 7	24	0,156	0,171	0,166
ZAFFERANA 1 a	21	0,112	0,173	0,176
		0.151††	0.209††	0.208††

† N=number of measurements

†† average

Figures 2a and 2b illustrate some examples of the TSLM and of the LM fitted to the (U,v) measured on the clods of two soils. The KM model is also represented for sake of comparison. Figures 3a and 3b illustrate the same models fitted to the (U,v) measured on the confined cores of the same soils.

Fig.2 (a,b). Three-Straight-Lines-Model (TSLM), Logistic Model (LM) and model proposed by Kim (KM) fitted to the (U,v) values measured on clods.
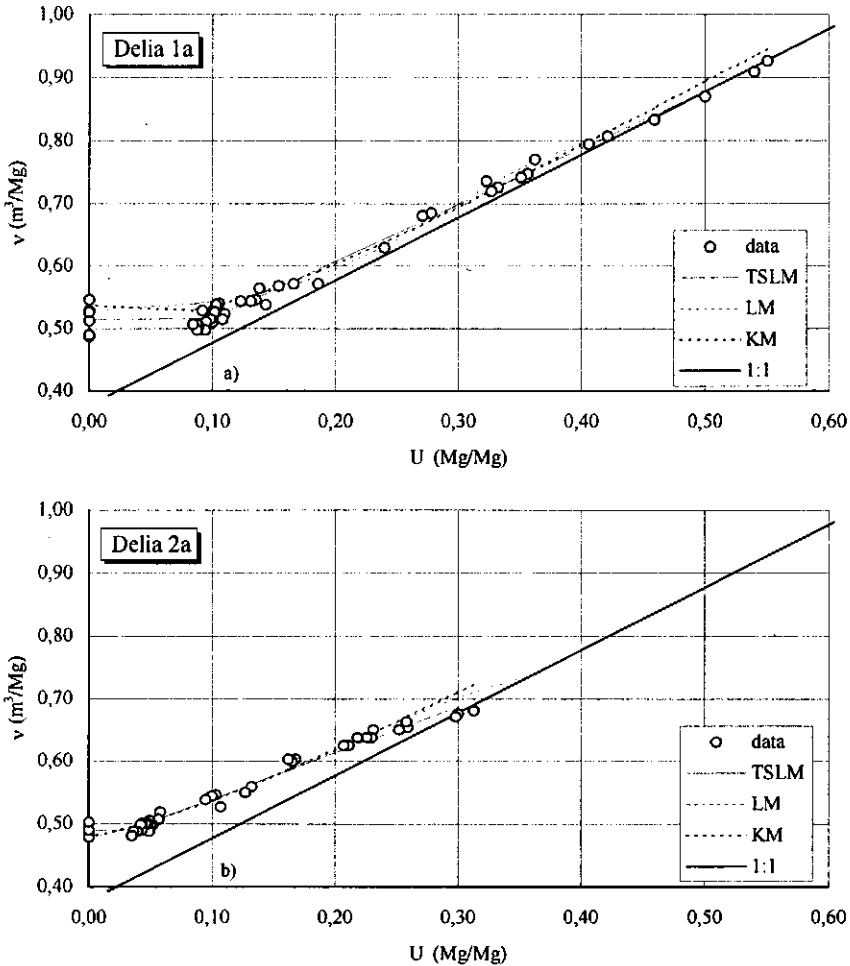
No structural shrinkage was observed in the SSCCs measured either in clods or in cores, with the consequence that the structural inflexion point (U_B) was coincident with the saturated water content (U_S), and that the TSLM reduced to a two-line model (2-L).

Figure 4 illustrates some comparisons between the (U,v) values measured on clods and cores. Larger v values, indicating less shrinkage, were found in the confined cores, except for U close to the saturated water content (U_S).

Table 4 reports the parameters obtained by fitting the TSLM to the (U,v) values measured on the clods. Table 5 reports the parameters obtained by fitting the TSLM to the (U,v) values measured on the cores, together with the geometry factors, with values generally lower than 3, indicating anisotropy in the shrinkage process.

Fig. 3 (a,b). Three-Straight-Lines-Model (TSLM), Logistic Model (LM) and model proposed by Kim (KM) fitted to the (U,v) values measured on cores.
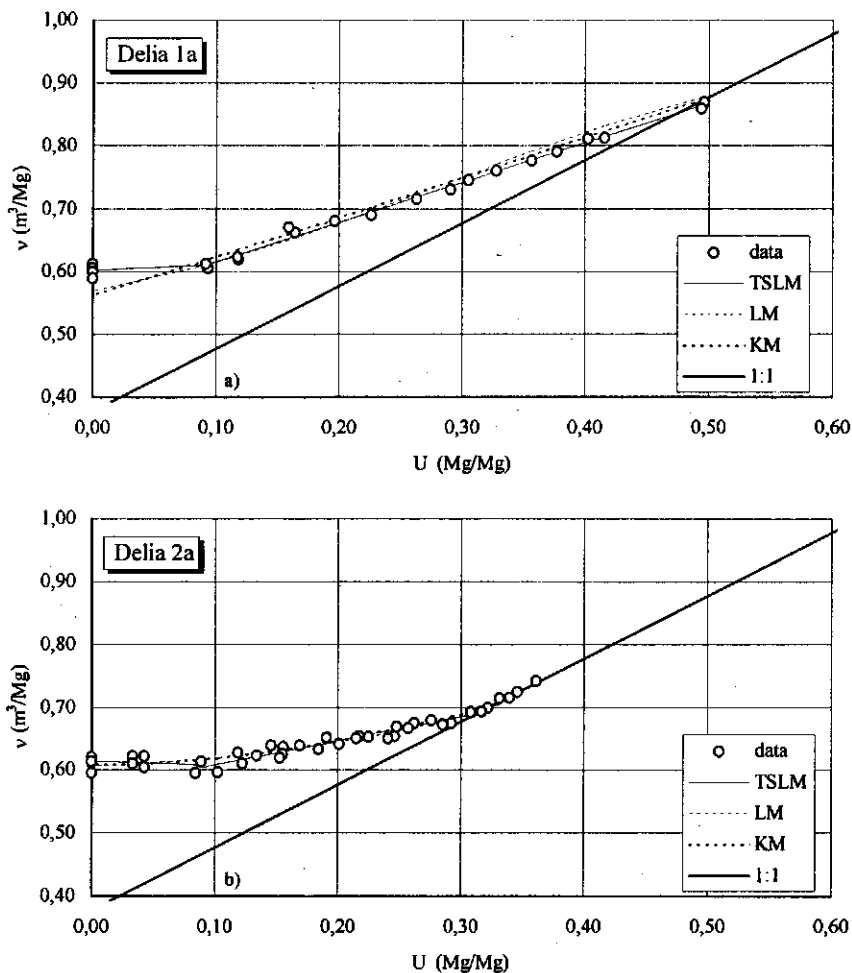
ANOVA and mean separation (Tukey test, P=0.05) performed on the TSLM parameters showed the existence of significant differences in the n (slope of the basic shrinkage line) and α (v value at U=0) obtained on clods and cores. No significant differences were found between the remaining TSLM parameters obtained for clods and cores.

The systematically lower n and larger α found for the confined cores indicate that the confined cores shrank less than the clods.

33

Table 4. Parameters obtained by fitting the Three-Straight-Lines-Model (TSLM) to the U,v values measured on the clods

Soil	TSLM model				
	α	r	n	U_A	$U_b = U_S$
	$m^3\,Mg^{-1}$	$m^3\,Mg^{-1}$	$m^3\,Mg^{-1}$	$m^3\,Mg^{-1}$	$m^3\,Mg^{-1}$
DELIA 1 a	0,51	0,02	0,90	0,099	0,500
DELIA 1 b	0,49	0,17	0,83	0,044	0,435
DELIA 2 a	0,49	0,05	0,74	0,033	0,313
DELIA 2 b	0,50	0,00	0,77	0,066	0,284
DELIA 3	0,52	0,18	0,58	0,014	0,318
DELIA 4	0,52	0,01	0,64	0,045	0,304
DELIA 5	0,49	0,06	0,79	0,057	0,321
DELIA 6	0,51	0,17	0,78	0,061	0,360
GELA 1 a	0,51	0,02	0,84	0,081	0,349
GELA 1 b	0,54	0,01	0,93	0,093	0,308
GELA 2	0,53	0,09	0,65	0,058	0,346
GELA 3	0,56	0,04	0,93	0,117	0,327
GELA 4	0,51	0,00	0,76	0,057	0,332
GELA 5	0,55	0,02	0,91	0,109	0,461
GELA 6	0,54	0,17	0,71	0,051	0,405
GELA 7	0,55	0,21	0,71	0,085	0,391
GIBBESI 14	0,55	0,17	0,88	0,122	0,480
GIBBESI 15	0,53	0,18	0,76	0,041	0,487
GORGO 1	0,51	0,02	0,76	0,053	0,305
GORGO 1	0,49	0,43	0,69	0,018	0,305
GORGO 2	0,51	0,18	0,48	0,023	0,247
MISILMERI	0,51	0,11	0,92	0,116	0,359
TIMETO 8	0,51	0,13	0,96	0,090	0,349
TIMETO A3	0,50	0,13	0,74	0,079	0,299
ZAFFERANA 1 a	0,53	0,11	0,82	0,078	0,395
ZAFFERANA 1 b	0,49	0,08	0,82	0,061	0,405

The different behavior of clods and cores could have been caused by the action of the inflexible ring upon sampling and later during saturation. Both clods and cores were sampled at a water content lower than the saturated water content (U_S). The confining action of the constrained boundary, along the undeformable steel ring, could have determined unidimensional rather than isotropic swelling, causing anisotripc shrinkage in the confined cores.

This hypothesis is supported by the geometry factors (r_s) measured at the end of the shrinkage process. These were generally lower than 3, indicating that the height deformation in the cores was greater than the diameter deformation.

However, the n and α values obtained by fitting the TSLM model to the (U, v) values obtained by assuming r_s equal to 3, were still significantly different from those determined on the clods, indicating that anisotropic shrinkage was not the unique reason for the different shrinkage behavior observed in the clods and in the confined cores.
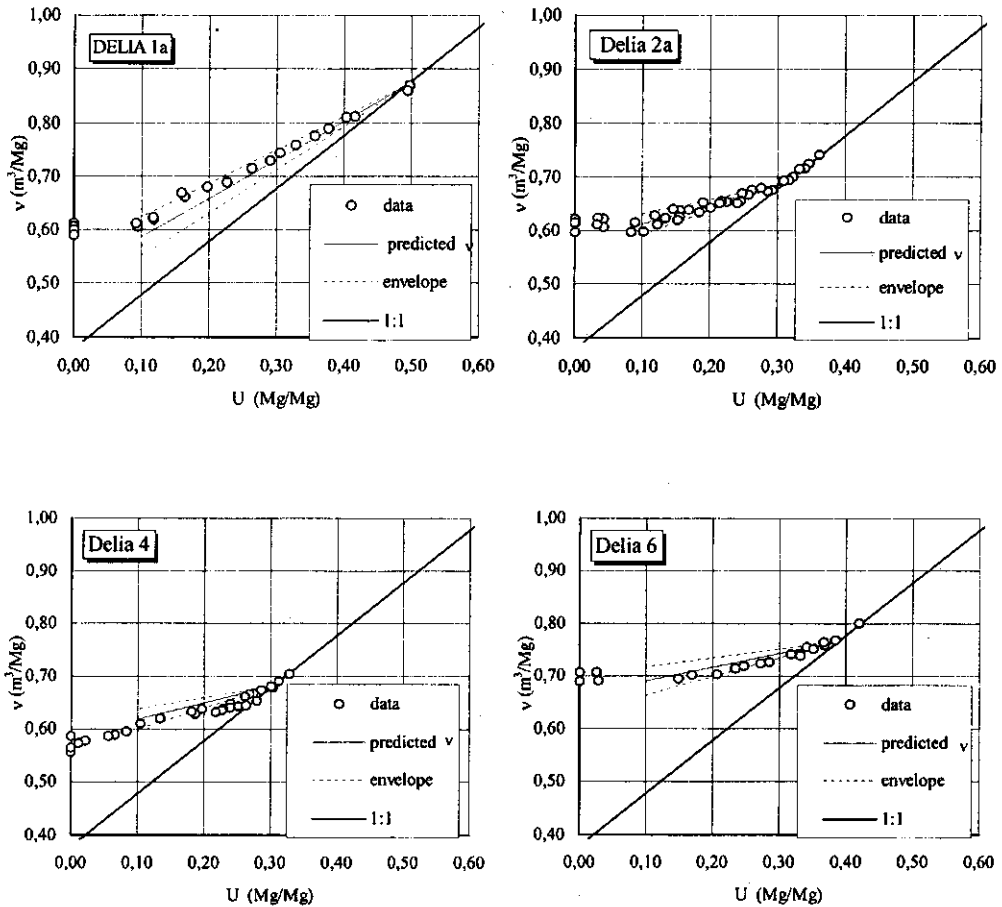
Fig.4. Comparisons between (U, v) values measured on clods and confined cores.

Another possible explanation for the lower shrinkage of the confined cores could be a different structural arrangement and porosity of the clods and cores. Natural aggregates represent elementary structural units, with inter-clod porosity which is likely to be absent or occasionally present. The confined cores represent an arrangement of various elementary units, with the inter-clod pores likely to be present, besides the intra-clod pores.

This explanation can be considered consistent with the findings of Mitchell and van Genuchten (1992), who attributed differences in shrinkage behavior of undisturbed cores extracted from cropped and fallow fields to differences in soil structure and porosity. They found less shrinkage in cores from the cropped field, which they attributed to stable voids caused by root anchoring, absent in cores from fallow fields.

Fig.5. Soil Shrinkage Characteristic Curve (SSCC) indirectly determined by eq.5b with the associated range of variability, and (U, v) values measured on confined cores.
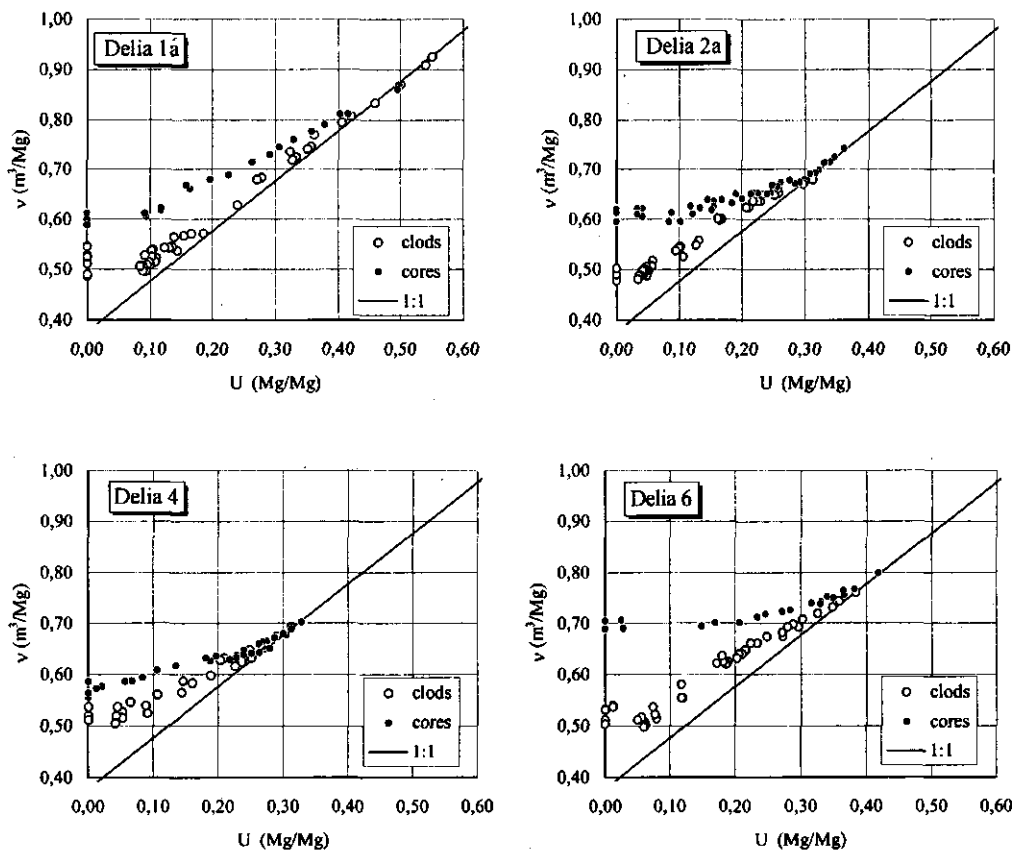
Another reason for the lower shrinkage of confined cores could be the re-orientation of clay particles caused by shear stresses along the sample walls and occurring during sampling. The re-orientation of clay particles could have been another factor preventing the confined cores from assuming the minimum possible configuration and volume.

With reference to the possibility of estimating the TSLM parameters indirectly from soil physical properties such as clay content (C), organic matter (OM) and cation exchange capacity (CEC), significant (P=0.001) linear regression equations predicting the slope (n) of the basic shrinkage line from (C) were found using measurements obtained on clods and on confined cores:

$$n = 0.5354 + 0.0062\ C \qquad\qquad \text{(clod data)} \qquad\qquad\qquad (5a)$$
$$r=0.78^{***} \qquad\qquad\qquad\qquad \text{SEE=0.0739} \quad\ \text{RMS=0.0054}$$

$$n = 0.0494 + 0.0116 \, C \quad r=0.90^{***} \qquad \text{(core data)} \qquad\qquad (5b)$$
$$\text{SEE}=0.0930 \quad \text{RMS}=0.0087$$

where r is the correlation coefficient, SEE the Standard Error of Estimate, and RMS the Residual Mean Square, accounting for the number of independent variables.

Table 5. Parameters obtained by fitting the Three-Straight-Lines-Model (TSLM) to the U,v values measured on the cores

Soil	TSLM model					
	α	r	n	U_A	$U_b=U_S$	r_s
	$m^3 \, Mg^{-1}$	$m^3 \, Mg^{-1}$	$m^3 \, Mg^{-1}$	$m^3 \, Mg^{-1}$	$m^3 \, Mg^{-1}$	
DELIA 1 a	0,60	0,09	0,63	0,091	0,497	2,91
DELIA 1 b	0,51	0,10	0,82	0,067	0,425	3,05
DELIA 2 a	0,61	0,03	0,34	0,086	0,322	2,67
DELIA 3	0,65	0,23	0,18	0,044	0,329	2,80
DELIA 4	0,56	0,44	0,34	0,089	0,304	2,88
DELIA 5	0,55	0,14	0,60	0,102	0,328	3,15
DELIA 6	0,70	0,00	0,28	0,125	0,390	2,49
GELA 6	0,66	0,05	0,43	0,074	0,436	2,59
GELA 7	0,62	0,22	0,57	0,136	0,482	3,06
ZAFFERANA 1 a	0,56	0,08	0,67	0,080	0,364	2,88

The possibility of improving n prediction was investigated by using CEC as an additional independent variable. The equation predicting n from C and CEC were:

$$n = 0.5017 + 0.0061 \, C + 0.0010 \, CEC \quad \text{(clod data)} \qquad\qquad (6a)$$
$$r=0.82^{***} \qquad\qquad \text{SEE}= 0.0749 \quad \text{RMS}=0.0056$$

$$n = -0.1165 + 0.0063 \, C + 0.0120 \, CEC \quad \text{(core data)} \qquad\qquad (6b)$$
$$r=0.92^{***} \qquad\qquad \text{SEE}= 0.0918 \quad \text{RMS}=0.0084$$

The obtained RMS indicated that eqs. (6a) and (6b) did not significantly improve the n prediction. No improvement was obtained by regressing n vs. C and OM, or by regressing n vs. C, OM and CEC.

Structural shrinkage being absent in the considered soils, the ability to predict n makes it possible to predict the basic shrinkage line. In this specific case the v value at $U=U_s$ is located on the 1:1 theoretical line, and can be calculated as:

$$v(\mathrm{U_s}) = U_s + \frac{1}{\rho_s} \qquad (7)$$

The $v(\mathrm{U})$ can be predicted by the following equation:

$$v(\mathrm{U}) = U_s + \frac{1}{\rho_s} + \mathrm{n}\left(\mathrm{U} - \mathrm{U_s}\right) \qquad (8)$$

Specific volume v at fixed U was calculated for all the soils by eq. (8), with n being calculated by eq.(5a) for the clod data set, and by eq.(5b) for the core data set.

Upper and lower envelope curves delimiting the range of variability of the predicted v values as a function of U were calculated accounting for the standard error of estimate (SEE) associated with the predicted n, i.e.:

$$v(\mathrm{U}) = U_s + \frac{1}{\rho_s} + (\mathrm{n} \pm \sigma)\left(\mathrm{U} - \mathrm{U_s}\right) \qquad (9)$$

Figure 5 illustrates for some soils the measured (U, v) values, and the v predicted by eq. (8) together with the envelope curves calculated by eq. (9).

ANOVA performed for all the soils showed that the predicted v values at fixed U were not significantly different from those measured. These results indicated that the accuracy associated with the predicted v was comparable to the variability associated with the measured v, proving the satisfactory performance of the predictive approach for an indirect determination of the SSCC.

Conclusions

This study showed significantly different SSCCs measured on small natural aggregates and on cylindrical confined cores having dimensions close to those of samples used for the determination of soil HC by routine laboratory techniques.

Less shrinkage was observed on the confined cores compared to clods. These results suggest that SSCC determined on cylindrical confined cores should be used for incorporating shrinkage behavior of clay soils in laboratory determined soil HC.

Furthermore, the investigation proved the good fitting of a two-line model to the measured (U, v) values and the possibility of indirectly estimating accurately the parameters of the basic shrinkage line. Predicting n from clay makes it possible to indirectly estimate the SSCC in confined cores, the measurement of which is time-consuming compared to that performed on resin-coated clods.

Further investigation will be performed in order to validate the predictive regression equations by using independently determined SSCC. The reasons for the different

shrinkage behavior of clods and confined cores need further investigation, also in order to establish whether SSCC measured on clods or on confined cores influence dynamic and practically relevant hydrological properties such as field cracking and preferential flow.

Chapter 3

Parameter estimation by inverse method based on one-step and multi-step outflow experiments

Hydraulic characterization of swelling/shrinking soils by a combination of laboratory and optimization techniques

Parameter estimation by inverse method based on one-step and multi-step outflow experiments

G. Crescimanno and M. Iovino
Università di Palermo, Dipartimento ITAF, Sezione Idraulica. Palermo, Italy

Abstract

The applicability of the inverse method for determining the soil water characteristic $\theta(h)$ and the hydraulic conductivity/water content $K(\theta)$ functions was investigated on two Typic Haploxerert characteristic of the Sicilian environment.

Shrinkage behaviour of the two soils was analysed in order to verify if significant changes in soil volume occurred during the outflow process.

One-step outflow experiments were performed, with comparisons between different procedures analysed not only in terms of estimated average functions, but also from the point of view of the uncertainty in the predictions, evaluated by a first-order analysis.

Multi-step outflow experiments were then performed and compared to results obtained by the one-step method. The results showed that the $\theta(h)$ and $K(\theta)$ functions deduced by performing optimization on the outflow volume V vs. time t obtained from multi-step experiments supplemented with three equilibrium $\theta(h)$ values were more reliable than the $\theta(h)$ and $K(\theta)$ functions determined by performing optimization on the V(t) obtained from one-step experiments supplemented with independently determined $\theta(h)$ values.

Introduction

Models simulating transport of water and solutes in unsaturated soil require the knowledge of soil hydraulic properties, i.e. the soil moisture characteristic curve $\theta(h)$ and the hydraulic conductivity function $K(\theta)$. A large number of field and laboratory techniques (Klute and Dirksen, 1986) have been developed to determine soil hydraulic properties.

Laboratory methods are often preferred to in-situ techniques as they permit measurements to be made simultaneously on many samples in a controlled environment, although the small size of soil samples used may alter the effects that soil macropores or structural units may have on hydraulic conductivity (Bouma, 1991).

The one-step outflow method (Passioura, 1976; Valiantzas et al., 1988; Mu'azu et al., 1990) represents an attractive and routinely used laboratory measurement technique. Validation of this method has been performed by comparisons with results obtained by other laboratory and field measurement techniques, such as the evaporation method and the crust method (Jaynes and Tyler, 1980; Borcher et al.,1986; Stolte et al., 1994).

Kool et al. (1985a; 1987) applied the inverse method (Zachmann et al., 1982; Hornung, 1983; Yeh, 1986) to determine simultaneously the $\theta(h)$ and $K(\theta)$ functions by minimizing deviations between predicted and measured outflow volumes V obtained from a one-step

outflow experiment supplemented with the soil moisture θ at the final equilibrium pressure. They validated the method on four soils with texture from sandy to clay (Kool et al., 1985b). Further investigations with the inverse method evidenced the need for additional $\theta(h)$ data (Hudson et al., 1991; van Dam et al., 1992; Bohne et al., 1993) or tensiometric measurements inside the sample (Toorman et al., 1992; Eching and Hopmans, 1993) to overcome the problem of non-uniqueness of the solution.

Yates et al. (1992) found that measured $\theta(h)$ and $K(\theta)$ functions obtained on a large number of different textured soils corresponded well to the hydraulic functions determined with the inverse method by a simultaneous estimation of five or six parameters.

van Dam et al. (1990) proposed multi-step outflow experiments as a valid alternative to one-step. They concluded that the problem of non-uniqueness does not occur in multi-step if the periods between each pressure increase are such as to reach equilibrium with suction in the ceramic plate.

Mous (1993) analysed the identifiability of Richards' equation and Mualem-van Genuchten's equations with reference to one-step and multi-step experiments. He concluded that the one-step model is numerically non-identifiable, while the multi-step function is identifiable if no more than five parameters are simultaneously estimated.

Eching and Hopmans (1993) performed one-step and multi-step experiments on soils from silty to loamy. They found that one-step and multi-step provided equally good results if in both cases optimization was performed on outflow volumes supplemented with simultaneously measured soil water pressure head data.

van Dam et al. (1994) compared the one-step and the multi-step approaches and concluded, for a loam soil, that the outflow data of multi-step experiments contain sufficient information for unique estimates of soil hydraulic functions.

Despite the many investigations and validations performed on the inverse method based on one-step outflow experiments (Kool and Parker, 1988; Mishra and Parker, 1989; Hopmans et al., 1992; van Dam et al., 1992; Eching et al., 1994), there are still some uncertainties about the feasibility of performing one-step or multi-step experiments and about the need or not of additional measurements when multi-step experiments are performed. Furthermore, the published comparisons between one-step and multi-step (Eching and Hopmans, 1993; van Dam et al., 1994) rely on accuracy of predictions rather than on evaluation of the reliability of the estimated hydraulic functions.

In addition, a few results concern clay soils, whose hydraulic characterization involves some specific problems connected to the presence of macropores (Beven and German, 1982), preferential flow (Bouma and Dekker, 1978) and changes in volume due to swelling-shrinkage processes (Bronswijk and Evers-Vermeer, 1990).

Bouma (1983) emphasized the importance of selecting the proper measurement technique as a function of soil texture and soil-structure, stressing the fact that in clay soils preferential flow and swelling-shrinkage processes may severely affect the reliability of the determined hydraulic properties.

Bronswijk (1988) quantified the effects of swelling and shrinkage on water transport in clay soils, concluding that shrinkage cannot be neglected when clay soils are considered.

Kim et al. (1992) proposed to incorporate the changes in volume, determined by the

shrinkage characteristic, in the hydraulic properties predicted by the evaporation method (Boels et al., 1978).

They compared the proposed method with the one-step outflow method and concluded that, accepting the hypothesis that changes in concentration of pore solution during evaporation were negligible, the results provided by the two methods were very similar when the moisture content was determined by incorporating the volume changes.

The advantage of the outflow method over the evaporation method is that no changes in concentration are connected to the transient outflow experiments, this making the technique suitable also for the hydraulic characterization of saline-sodic soils (Crescimanno and Iovino, 1995).

This paper investigates the applicability of the inverse method based on outflow one-step and multi-step experiments to determine the hydraulic functions of two Typic Haploxerert characteristic of the Sicilian environment.

The specific purpose is to define a procedure leading to accurate and reliable estimation of the unsaturated hydraulic functions, under the assumption that these can be adequately represented by the van Genuchten model (Russo, 1988).

Because of the high clay content of both soils, the shrinkage behaviour is investigated in order to verify both whether changes in volume of soil samples occur during the outflow process and whether any loss of contact between soil sample and porous plate, affecting the outflow measurements, may have occurred.

Starting from one-step experiments and independently determined soil water retention values, some analyses are carried out in order to find an optimization procedure leading to accurate predictions of the $\theta(h)$ function with the minimum number of independently determined $\theta(h)$ values.

Multi-step experiments are then carried out and optimization is performed both with additional $\theta(h)$ values and without.

Evaluation of the results provided by one-step and multi-step experiments is then carried out not only by comparing the accuracy in the predicted $\theta(h)$ values, but also by considering the uncertainty in the estimated parameters.

First-order analysis (Benjamin and Cornell, 1970) is used to compare the reliability of the $\theta(h)$ and $K(\theta)$ functions predicted by one-step and multi-step experiments. This analysis entails considerably less computational effort than Monte Carlo simulations for problems with a limited number of parameters, providing results of comparable accuracy for relatively simple flow problems (Mishra and Parker, 1989).

Background

Model for unsaturated flow

The governing equation for the one-dimensional vertical transient water flow is the Richards equation:

$$C(h)\frac{\partial h}{\partial t} = \frac{\partial}{\partial x}\left[K(h)\left(\frac{\partial h}{\partial x} - 1\right)\right] \tag{1}$$

where h is the pressure head [L], x is depth [L], t is time [T], $C=d\theta/dh$ is the water capacity [L^{-1}], θ is the volumetric water content [L^3/L^3] and K is the hydraulic conductivity [LT^{-1}].

The one-step experimental procedure involves the measurement of cumulative outflow V with time t from a soil core at a high initial water content, subjected to an instantaneous increment in pneumatic pressure at the top with a saturated porous plate at the bottom.

The appropriate initial and boundary conditions are:

h=h$_0$(x)	t=0	0≤x≤L	(2a)
$\partial h/\partial x$=1	t>0	x=0	(2b)
h=h$_L$-h^a	t>0	x=L	(2c)

where x=0 is taken at the top of the core, x=L is the bottom of the porous plate, h$_L$ is the pressure head at the bottom of the porous plate, h^a is the gauge gas pressure applied to the core, and h$_0$(x) is the initial distribution of the pressure head.

The hydraulic properties of soil are assumed to be represented by the van Genuchten model (1980) (Mualem, 1976):

$$\Theta = \begin{cases} \left[\dfrac{1}{1 + (\alpha|h|)^n}\right]^m & h < 0 \\ 1 & h \geq 0 \end{cases} \tag{3}$$

$$K(\Theta) = K_s\Theta^\gamma\left[1 - \left(1 - \Theta^{1/m}\right)^m\right]^2 \tag{4}$$

where $\Theta=\dfrac{\theta-\theta_r}{\theta_s-\theta_r}$; θ_s is the saturated water content; θ_r is the "residual" water content; K_s is the saturated hydraulic conductivity; α, n, m and γ are empirical parameters, with m=1-1/n.

Parameter estimation procedure

The inverse problem is formulated as a non-linear optimization problem, i.e. parameters in eqs. (3) and (4) are estimated by minimizing a suitable objective function which expresses the discrepancy between observed and predicted system response.

The experimental procedure results in a set of cumulative outflow measurements V at specific times t$_i$. These V(t$_i$) are employed as input data for the numerical inversion of equation (1).

Let $\hat{V}$ (t$_i$,b) be the numerically calculated values of outflow corresponding to a trial vector

b of parameter values; the problem is to find an optimum combination **b** of parameters of eqs. (3) and (4) minimizing the objective function:

$$O(b) = \sum_{i=1}^{N} \left\{ w_i \left[V(t_i) - \hat{V}(t_i, b) \right] \right\}^2 \tag{5}$$

If some measured $\theta(h_i)$ values are associated with the experimental $V(t_i)$, then the objective function becomes:

$$O(b) = \sum_{i=1}^{N_1} \left\{ w_i \left[V(t_i) - \hat{V}(t_i, b) \right] \right\}^2 +$$

$$+ \sum_{i=1}^{N_2} \left\{ W_1 v_i \left[\theta(h_i) - \hat{\theta}(h_i, b) \right] \right\}^2 \tag{6}$$

In this case w_i and v_i are weighing factors for the individual measurements $V(t_i)$ and $\theta(h_i)$; N_1 and N_2 are the number of $V(t_i)$ and $\theta(h_i)$ values respectively; $\hat{V}(t_i, b)$ and $\hat{\theta}(h_i, b)$ are the numerical calculated values and W_1 is a normalizing factor calculated as the ratio between the mean value of the measured $V(t_i)$ and the mean of the $\theta(h_i)$ values.

Material and methods

The soils considered in this investigation were taken from two irrigated areas of Sicily.

Table 1. Main characteristics of the two soils

	Soil 1	Soil 2
Site	Delia	Gela
Classification [†]	Typic Haploxerert	Typic Haploxerert
Horizon	Ap (0-30 cm)	Ap (0-27 cm)
Sand (2÷0.02 mm)[%]	8	19
Silt (0.02÷0.002 mm) [%]	35	27
Clay (<0.002 mm) [%]	57	54
Texture (ISSS)	C	C
Clay Mineralogy [%]		
Kaolinite	34.2	24.1
Chlorite	11.1	15.2
Illite	43.3	46.2
Smectite	11.5	14.5
EC (1:5) [dS/m]	0.87	0.30
CEC [cmol/kg]	40.6	34.6
ESP [%]	2.11	2.17
Organic matter [%]	3.55	3.47

[†] Soil Taxonomy (Soil Survey Staff, 1992)

Table 1 reports classification and some physico-chemical characteristics of the two soils; it can be noticed that both soils contain high swelling minerals (chlorite, illite and smectite).

Undisturbed soil cores were sampled using a thin wall hydraulic sampler ($\emptyset$=8.5 cm, h=5 cm). The saturated hydraulic conductivity K_S was measured by the constant-head method (Klute and Dirksen, 1986) using a 0.005 M $CaCl_2$ solution in order to minimize swelling and dispersion of clay particles.

Independent gravimetric water content/matric potential $U(h_i)$ values were determined by the Stakman apparatus (Stakman et al., 1969) (h = -1, -4, -7, -20 kPa) and by the pressure plate method (h = -80, -300, and -1500 kPa).

Shrinkage characteristics (Haines, 1923) of the two soils were determined, i.e. relationships between void ratio e and moisture ratio u, with e and u defined as:

$$e = V_p/V_s \tag{7}$$
$$u = V_w/V_s \tag{8}$$

with V_p (cm³) volume of pores, V_s (cm³) volume of solids, and V_w (cm³) volume of water.

The e(u) relationships were determined (Crescimanno and Provenzano, 1995) for each soil on three natural aggregates immersed in SARAN F-310 resin (Brasher et al., 1966) obtained from undisturbed large clods previously saturated in the Stakman apparatus at the matric potential of -0.2 kPa.

Weight and volume were determined by repeating weighing and weighing under-water. When weight losses became negligible,the SARAN-coated clods were oven-dried in order to determine final dry volume and dry weight (Bronswijk and Evers-Vermeer, 1990).

Once the e(u) relationship was determined, the relationship between the bulk density ρ and u was also known (e=ρ_S/ρ-1), with ρ_S density of the solid phase (g/cm³) and ρ dry bulk density (g/cm³).

The actual volumetric water content θ was then determined:

$$\theta = u/(1+e) \tag{9}$$

rather than the fictitious water content (Kim et al., 1992):

$$\theta_f = u/(1+e_0) \tag{10}$$

with e_0 void ratio at or near saturation. Consequently the water retention curve was expressed as $\theta(h)$ rather than as $\theta_f(h)$, thus incorporating changes in volume.

One-step outflow experiments were performed in pressure cells on soil samples ($\emptyset$=8.5 cm, h=5 cm) previously equilibrated with a small pneumatic pressure (1 kPa) in order to realize initial unsaturated conditions (Hopmans et al., 1992). A final pneumatic pressure equal to 80 kPa was then imposed.

Cumulative outflow volumes $V(t_i)$ were determined by weighing and automatic recording. The final water content was determined gravimetrically after reaching equilibrium at the pneumatic pressure of 80 kPa.

In order to verify if any loss of contact between soil sample and porous plate occurred during the outflow process, because of shrinkage, the water content θ at -1 kPa calculated

by adding the measured total outflow volume to the water content determined at -80 kPa was compared with the θ at -1 kPa independently determined in the Stakman apparatus. If contact between soil and porous plate during the outflow process is constantly maintained, the two θ values should approximately correspond.

The multi-step experiments were conducted by performing three successive steps with pneumatic pressure ranges 1÷4 kPa, 4÷7 kPa, and 7÷80 kPa.

The water content θ corresponding to the h values of -1, -4 and -7 kPa was calculated by adding the outflow volumes recorded during the three pressure steps to the θ determined at -80 kPa.

Hydraulic conductivity of the porous ceramic plate (K_p) was determined at the end of each outflow experiment by flushing the plate at the pneumatic head of 20 kPa.

The parameter estimation procedure was performed using the FLOFIT code (Kool and Parker, 1987). The mean value b_j and the standard deviation $\sigma(b_j)$ of each optimized parameter represent the output of the estimation procedure together with the correlation matrix R $[b_j b_k]$.

The accuracy of the optimization procedure was evaluated by statistics such as the standard error of estimate calculated on the $V(t_i)$ and on the $\theta(h_i)$ values, named SEE_V and SEE_θ respectively, the coefficient of determination R^2 and the Akaike Information Criterion AIC (Akaike, 1974); the lower the AIC, the better the result of the optimization procedure.

The reliability of each estimated parameter b_j was evaluated by the $\sigma(b_j)$ associated to the mean value.

In order to evaluate the reliability of the predicted $\theta(h)$ and $K(\theta)$ functions, a procedure keeping into account both $\sigma(b_j)$ and the correlation matrix R $[b_j b_k]$ was used.

At this purpose, a first-order Taylor expansion around the mean values of the parameters was used, as this procedure proved to furnish results of comparable accuracy of the Montecarlo technique (Mishra and Parker, 1989).

Given the expression of the variance of a parametric function f(**b**):

$$Var[f(\mathbf{b})] = \sigma^2 = E[(f(\mathbf{b}) - E[f(\mathbf{b})]^2] \tag{11}$$

Assuming small parameter perturbations around the mean value and negligible higher order terms, f(**b**) and E[f(**b**)] can be approximated by:

$$f(b) \approx f(\hat{b}) + \sum_j \frac{\partial f}{\partial b_j}(b_j - \hat{b}_j) \tag{12}$$

$$E[f(b)] \approx f(\hat{b}) + \sum_j \frac{\partial f}{\partial b_j} E(b_j - \hat{b}_j) \approx f(\hat{b}) \tag{13}$$

thus giving:

$$Var[f(b)] \approx \sum_j \sum_k \frac{\partial f}{\partial b_j} \frac{\partial f}{\partial b_k} E[(b_j - \hat{b}_j)(b_k - \hat{b}_k)] \tag{14}$$

Since:

$$E[(b_j - \hat{b}_j)(b_k - \hat{b}_k)] = Cov[b_j b_k] \qquad (15)$$

we obtain:

$$Var[f(b)] \approx \sum_j \sum_k \frac{\partial f}{\partial b_j} \frac{\partial f}{\partial b_k} Cov[b_j b_k] \qquad (16)$$

The covariance matrix of the estimated parameters, Cov[$b_j b_k$] in eq.(8), can be obtained from the correlation matrix R[$b_j b_k$] and from the standard deviation $\sigma(b_j)$ of the estimated parameters according to the expression:

$$(17)$$

$$Cov[b_j b_k] = R[b_j b_k]\ \sigma^2(b_j)\ \sigma^2(b_k)$$

After calculating Var[$\theta(h)$] and Var[$K(\theta)$] by eq. (16) in correspondence with some h and θ values, the one-standard deviation intervals (OSDI) associated with the $\theta(h)$ and $K(\theta)$ functions were calculated for each set of estimated parameters.

Results and discussion

Shrinkage behaviour and outflow process

Figures 1a,b illustrate the relationships between void ratio e and moisture ratio u obtained for soils 1 and 2. Although a considerable range of variability resulted to be associated with the bulk density ρ in the whole range of variability of U, going from saturation to the oven-dry condition, itwas found that ρ ranged from 1.24 to 1.29 for soil 1, and from 1.33 to 1.37 for soil 2, in the h range from -1 to -80 kPa.

This variability in ρ means that the difference $(\theta-\theta_f)/\theta_f$ increases at decreasing matric potential h, with values of 1.04%, 1.44% and 4.17% for soil 1, and of 0.6%, 0.9% and 2.46% for soil 2, at the h of -4, -7 and -80 kPa.

These $(\theta-\theta_f)/\theta_f$ values can be considered comparable with the differences usually found between replicated θ measurements for h=-4 and h=-7 kPa, while they could indicate that non negligible shrinkage occurred at h=-80 kPa.

Nonetheless, the good agreement between the θ value at -1 kPa, determined by adding the total outflow volume to the θ measured at -80 kPa, and the independently determined θ at -1 kPa proved maintenance of contact between soil sample and porous plate.

As a consequence it was concluded that the magnitude of shrinkage was not so great that it severely affected the outflow process in the h range from -1 to -80 kPa.
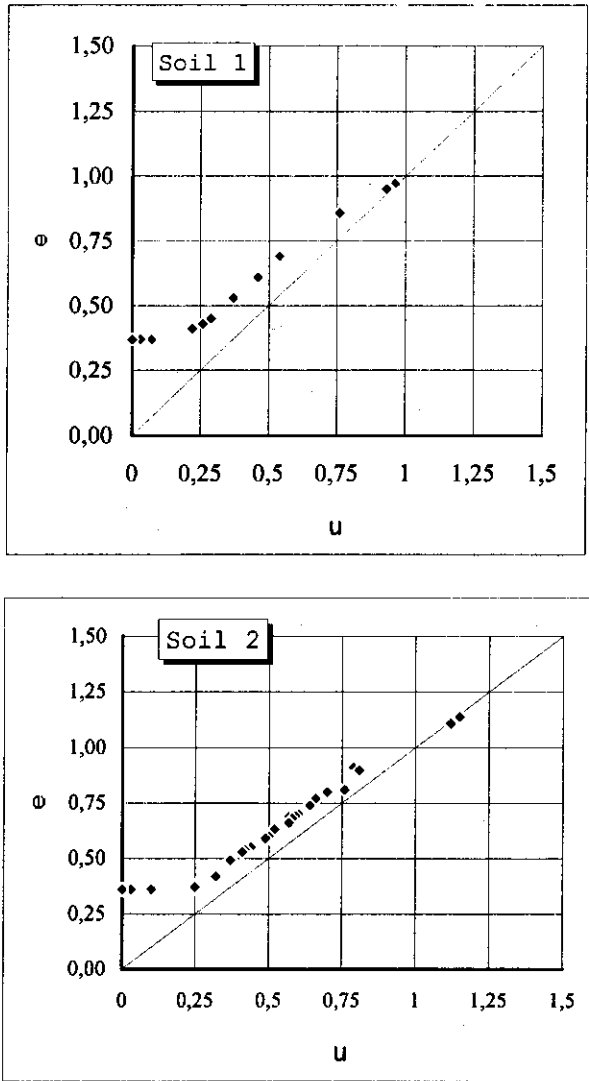
Fig.1 Relationship between void ratio e and moisture ratio u, represen-
ting the shrinkage characteristic for soil 1 (a) and soil 2 (b)

Parameter estimation: one-step outflow experiments

Optimization procedure

Analysis started from one-step experiments. By considering as input the $V(t_i)$ and the K_s values obtained as the mean of three replicates, six different sets of parameters were tested. Table 2 reports these sets as well as the ranges of variability selected for the optimized parameters.

Results of optimization performed on $V(t_i)$ only (Table 2), showed considerable variability in the estimated parameters, due to non-uniqueness of the solution. Furthermore, none of the optimized sets led to an accurate prediction of the $\theta(h)$ values.

A further step was then carried out by performing optimization on the $V(t_i)$ supplemented with all the independently measured $\theta(h_i)$ values with the objective of finding the set of optimized parameters leading to the lowest deviations between measured and predicted $\theta(h_i)$ values.

Analysis was carried out with the following constraints: (i) it is not possible to estimate θ_s and θ_r simultaneously (Mous, 1993); (ii) no fixed K_s was considered, but a wide range of possible variation around the measured value was established because of the generally recognized great variability connected to its measurement (Lauren et al.,1988; Mohanty et al., 1991); (iii) no fixed γ was considered, as a variable γ accounts for the correlation between pores and for flow path tortuosity (Russo, 1988).

The parameter sets 4, 5 and 6, reported in Table 2, were then tested.

In options 4 and 5, the fixed residual water content θ_r was the asymptotic value determined by pre-fitting the van Genuchten model to the $\theta(h)$ measured data.

The lowest SEE_θ was obtained with set 5, a similar result was obtained with set 4, while worsening was linked with set 6.

As a consequence further analysis focused on the parameter set 5, which involves optimizing α, n, θ_s, K_s, and γ, and fixing θ_r (procedure 5/1 in Table 3).

Weighing factors of the measured $V(t_i)$ and $\theta(h_i)$ values

Weighing factors w_i and v_i in eq. (6) incorporate data errors representing combined effects of measurement error and soil non-homogeneity which are not included in the model (Kool and Parker, 1988).

The real advantage of using equal or different values of w_i and v_i on results of optimization was investigated.

By considering sets of $V(t_i)$ and of $\theta(h_i)$ values obtained as the mean of three replicates, the standard deviation of each measured $V(t_i)$ and of each measured $\theta(h_i)$ was calculated. Mean σ_V and σ_θ values were assumed, and weighing factors w_i and v_i, inversely proportional to σ_θ and σ_V respectively, were calculated and attributed to the $V(t_i)$ and $\theta(h_i)$ measured values. The calculated ratio v_i/w_i was approximately equal to 1.15 for soil 1 and to 1.26 for soil 2.

The parameters obtained with this procedure (5/2, Table 3) led to a lower SEE_V for soil 1 and to a lower SEE_θ for soil 2, with simultaneously higher R^2 values and lower AIC than the R^2 and AIC obtained with procedure 5/1.

Table 2. Estimated parameter values

SET [†]	1	2	3	4	5	6
α	var	var	var	var	var	var
n	var	var	var	var	var	var
θ_s	fix	var	fix	fix	var	fix
θ_r	fix	fix	var	fix	fix	var
K_s	var	var	var	var	var	var
γ	fix	fix	fix	var	var	var
Soil 1						
α	0.0250	0.0295	0.0300	0.0240	0.0294	0.0288
n	1.1990	1.1838	1.1786	1.1992	1.1903	1.1787
θ_s	0.490	0.509	0.490	0.490	0.506	0.490
θ_r	0.300	0.300	0.271	0.300	0.300	0.263
K_s	0.080	0.098	0.097	0.085	0.099	0.096
γ	0.500	0.500	0.500	0.893	0.876	1.012
SEE_V	7.19E-03	6.97E-03	6.89E-03	7.51E-03	7.23E-03	7.07E-03
R^2	0.992	0.993	0.993	0.991	0.992	0.992
AIC	40.92	42.92	42.92	42.92	44.92	44.92
Soil 2						
α	0.0428	0.0252	0.0464	0.0309	0.0305	0.0246
n	1.1372	1.2176	1.3000	1.1658	1.2787	1.2964
θ_s	0.500	0.450	0.366	0.500	0.474	0.500
θ_r	0.280	0.280	0.280	0.280	0.280	0.363
K_s	5.000	1.196	2.173	4.755	3.189	0.958
γ	0.500	0.500	0.500	4.252	6.470	0.802
SEE_V	0.0175	0.0175	0.0146	0.0125	0.0113	0.0157
R^2	0.974	0.974	0.982	0.987	0.989	0.979
AIC	38.93	40.93	40.92	42.92	44.92	44.92

[†] fix = parameter fixed at the following values:
θ_s =measured; K_s=measured; γ=0.5.
var = parameter estimated into the following ranges:
$0.01 \leq \alpha \leq 0.5$; $n \geq 1.1$; $\theta_s - 0.03 \leq \theta_s \leq \theta_s + 0.03$; $0.5 K_s \leq K_s \leq 2 K_s$

Furthermore, the standard deviation associated with each optimized parameter was lower than that previously obtained, which indicated a greater parameter identifiability of procedure 5/2.

These results show the advantage of using w_i and v_i calculated as described above to

improve both accuracy and identifiability of the estimates.

Figures 2a,b illustrate the $\theta(h)$ functions obtained with procedure 5/2 together with the measured $\theta(h_i)$ values for soils 1 and 2, showing the good agreement between the estimated and measured values.

Table 3. Parameter values obtained by procedures 5/1, 5/2 and 5/3

Procedure	5/1		5/2		5/3	
Soil 1	Mean	St. Dev.	Mean	St. Dev.	Mean	St. Dev.
α	0.0341	0.0218	0.0233	0.0121	0.0225	0.0279
n	1.1681	0.0205	1.1810	0.0176	1.2091	0.1485
θ_s	0.497	0.010	0.492	0.007	0.492	0.010
θ_r	0.300		0.300		0.300	
K_s	0.160	0.155	0.089	0.069	0.055	0.157
γ	0.012	0.899	0.0001	bound	0.138	2.680
SEE_V	7.45E-3		7.35E-3		6.76E-3	
R^2	0.998		0.999		0.999	
AIC	57.79		54.81		50	
SEE_θ	2.91E-3		3.18E-3		8.80E-3	
Soil 2	Mean	St. Dev.	Mean	St. Dev.	Mean	St. Dev.
α	0.0119	0.0065	0.0122	0.0054	0.0191	0.0266
n	1.2393	0.0418	1.2341	0.0359	1.2348	0.2272
θ_s	0.502	0.010	0.501	0.008	0.503	0.013
θ_r	0.280		0.280		0.280	
K_s	1.098	0.798	1.187	0.734	1.917	5.922
γ	7.261	1.344	7.185	1.309	7.584	4.801
SEE_V	9.82E-3		0.010		9.60E-3	
R^2	0.994		0.996		0.997	
AIC	57.59		56.17		49.74	
SEE_θ	0.0105		0.0103		0.015	

Minimum number of required $\theta(h_i)$ values

The possibility of reducing the number of experimental $\theta(h_i)$ values to be combined with the $V(t_j)$ values was investigated by coupling to the $V(t_j)$ different combinations of $\theta(h_i)$ until a minimum of three was reached, then by selecting the combination giving both the

lowest SEE_V and the lowest SEE_θ.

Combining the $V(t_i)$ with the θ determined at the matric potential h equal to -1, -4, -7 kPa, the estimated $\theta(h)$ and $K(\theta)$ functions best approached those obtained with procedure 5/2. The results of this new procedure, 5/3, are reported in Table 3.

In procedure 5/3, the θ or the θ_f values may be equally used because of the small differences between θ and θ_f found at the h of -4 and of -7 kPa.

The experimental outflow volumes $V(t_i)$ and the estimated values (t_i) obtained by means of procedure 5/3 are represented, for the two soils, in Figure 3, with a satisfactory fitting for both soils, as testified by the low SEE_V values.

Figures 2a,b illustrate the $\theta(h)$ functions obtained by procedure 5/3. The good agreement between these average $\theta(h)$ functions and those obtained by procedure 5/2 is evident, but in this case a larger standard deviation appears to be associated with each estimated parameter.
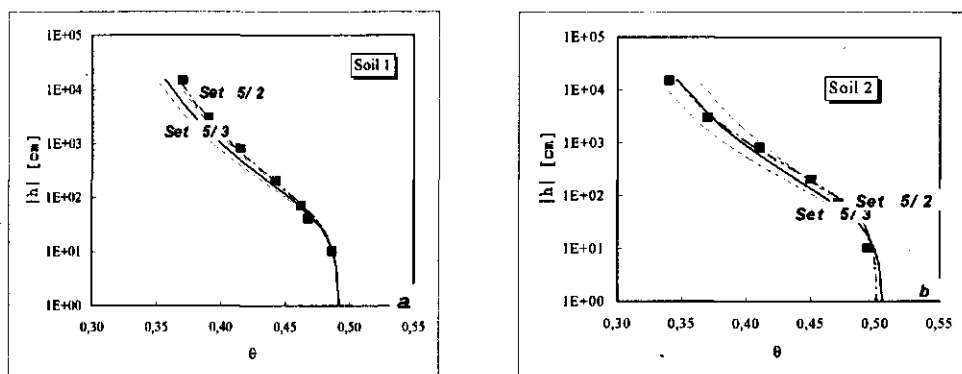

Fig 2. Soil moisture characteristic curves predicted by procedures 5/2 and 5/3 and measured $\theta(h)$ values. The one-standard deviation intervals (OSDI) obtained with procedure 8/3) are also represented by a dashed line.

First-order analysis is then used to make a comparison between the one-standard deviation intervals (OSDI) associated with these predicted $\theta(h)$ functions and the OSDI associated with those predicted by procedure 5/2. Figures 2a and 2b illustrate this comparison.

Although the OSDI associated with the $\theta(h)$ functions predicted by procedure 5/2 are practically indistinguishable (mean value of the standard deviation σ_θ equal to 4.3×10^{-5} for soil 1 and to 1.2×10^{-4} for soil 2 in the h range from -1 to -80 kPa), and larger OSDI are associated with those predicted by procedure 5/3 (σ_θ=0.0019 for soil 1, σ_θ=0.0045 for soil 2), deviation of the predicted function around the mean value can be considered acceptable.

Figures 4a,b illustrate the $K(\theta)$ functions obtained by procedure 5/3 together with the associated OSDI.

The large OSDI obtained especially for soil 2 (mean value of the standard deviation of log $K(\theta)$, σ_K equal to 0.328 for soil 1 and to 1.65 for soil 2) is a consequence of the poor ability of this procedure to identify the estimated K_s.
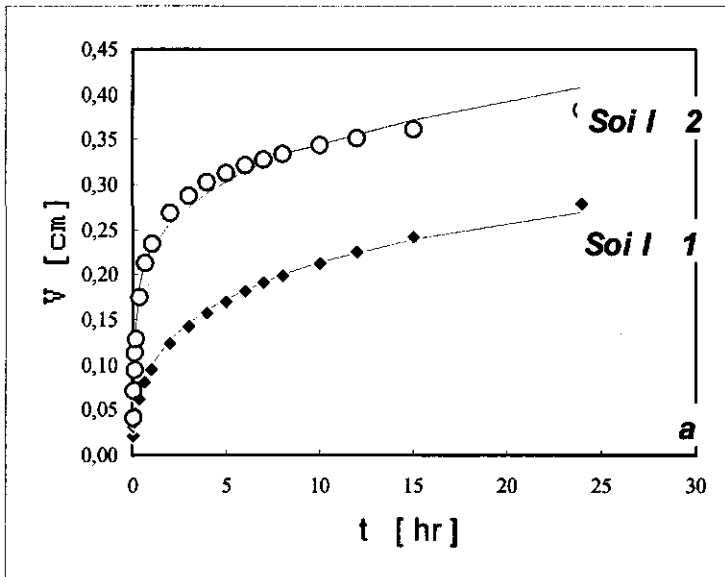
Fig.3. Measured outflow volumes obtained from one-step experiment and estimated volumes obtained with procedure 5/3 for soil 1 and soil 2.

Problems of non-identifiability of K_s have been evidenced by previous analyses (Kool and Parker, 1987; van Dam et al., 1992; Durner, 1994). Toorman et al. (1992) attributed this problem to the positive high correlation between α and K_S occurring when α and K_S are simultaneously estimated.

In our case, inspection of the correlation matrix of the optimized parameters revealead a high correlation between the estimated α and K_s for both soils, but despite this high correlation the estimated K_s of soil 1 appeared less affected by an identifiability problem.

Furthermore, although narrower OSDI were obtained for soil 1, comparable correlation coefficients between the remaining estimated parameters were obtained for both soils. No clear explanation was found for the larger OSDI obtained for soil 2.

An attempt to improve parameter identifiability was made by fixing θ_s, and estimating α ,n, K_s and γ only (procedure 4/3).

No significant improvement was obtained with procedure 4/3, but results comparable with those obtained with procedure 5/3 were found both in terms of accuracy and of reliability of the estimated parameters/functions.

The need for an approach leading to more reliable $K(\theta)$ predicted functions was then explored by performing multi-step experiments.
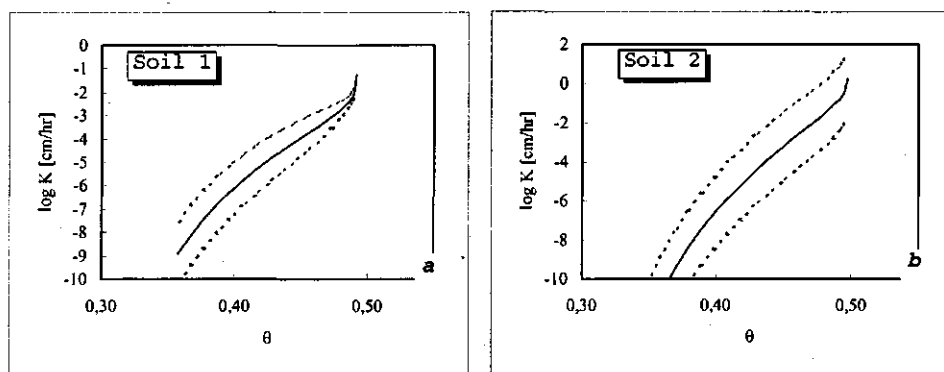
Fig. 4. Unsatured hydraulic conductivity K vs. volumetric water content θ predicted by procedure 5/3 and associated one-standard deviation intervals (OSDI). (a) Soil 1, (b) Soil 2.

Multistep outflow experiments and comparisons with results from one-step experiments

Optimization was carried out on the outflow volumes recorded during the three pressure steps supplemented with the θ corresponding to the matric potential of -1, -4, and -7 kPa. (procedure M/1, Table 4).

Weighing factors were calculated according to the procedure described in par. 4.2.2, although in this case closer values of w_i and v_i were found.

The experimental $V(t_i)$ and the estimated (t_i) obtained by procedure M/1 are represented for the two soils (Fig. 5) with a satisfactory fit obtained for both.

Comparison between the parameters obtained by procedure M/1 and those previously obtained by procedure 5/3 indicates differences in the estimated parameters especially for soil 1. It is difficult to state whether these differences are due to the different experimental procedures or to the unavoidable variability of the different soil samples used for one-step and multi-step experiments.

The statistics (SEE_v, R^2, AIC, SEE_θ) reported in Tables 3 and 4 indicate that a generally higher accuracy is linked to one-step experiments.

However, it is interesting to note that the standard error of the estimated parameters obtained with procedure M/1 is generally lower than that obtained with procedure 5/3. This is especially evident with reference to K_s of soil 2, indicating an improvement in the identifiability of this parameter. Furthermore, inspection of the correlation matrix of the optimized parameters reveals lower correlation coefficients R obtained with procedure M/1

57

in comparisons with those obtained with procedure 5/3.

Table 4: Parameter values obtained by multistep experiments.

Procedure		*M/1*		*M/2*	
Soil 1		Mean	St. Dev.	Mean	St. Dev.
	α	0.0258	0.0046	0.0288	0.0086
	n	1.2855	0.0353	1.3287	0.0667
	θ_s	0.504	0.006	0.480	bound
	θ_r	0.300		0.300	
	K_s	0.654	0.5678	0.699	1.274
	γ	5.566	2.267	4.382	3.359
	SEE_V	0.0111		0.0177	
	R^2	0.993		0.970	
	AIC	86.53		89.04	
	SEE_θ	0.0155		0.0290	
Soil 2		Mean	St. Dev.	Mean	St. Dev.
	α	0.0290	0.0090	0.0233	0.0028
	n	1.1761	0.0337	1.1817	0.0232
	θ_s	0.504	0.007	0.541	0.038
	θ_r	0.280		0.280	
	K_s	0.271	0.182	0.050	bound
	γ	2.096	2.711	0.129	1.054
	SEE_V	0.0115		0.0177	
	R^2	0.992		0.994	
	AIC	92.71		85.19	
	SEE_θ	2.25E-3		0.0330	

The $\theta(h)$ functions obtained with procedure M/1 are reported for the two soils in Figures 6a,b together with the OSDI associated with the predicted functions (σ_θ= 0.00031 for soil 1, σ_θ= 0.00039 for soil 2).

The obtained OSDI are not distinguishable, which indicates a high reliability of the predicted $\theta(h)$ functions even at the lowest θ values.

Figures 7a,b illustrate the $K(\theta)$ functions and their OSDI for the two soils. Narrower OSDI have been obtained with procedure M/1 (σ_K=0.593 for soil 1 and σ_K=0.873 for soil 2) than with 5/3. These results clearly indicate that despite the greater accuracy of procedure 5/3, the reliability associated with the hydraulic functions predicted by multi-step experiments is greater than that of one-step experiments.

This aspect is evidenced by first-order analysis which takes into account both the standard

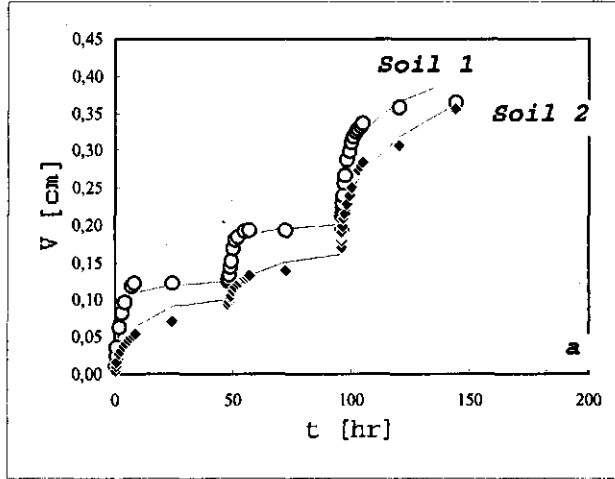deviation associated with each estimated parameter and the correlation between the estimated parameters.

Fig 5. Measured outflow volumes obtained fron multi-step experiments and estimated volumes obtained with procedure M/1 for soil 1 and soil 2.

The narrower OSDI associated with the hydraulic functions predicted by multi-step may be explained by the lower fluxes involving a better conformity to the Darcy law (van Dam et al., 1990), by the larger number of outflow measurements collected during multi-step experiments, and by considerations concerning model identifiability (Mous, 1993).
Optimization was also performed on the $V(t_i)$ obtained by multi-step but without additional $\theta(h_i)$ values (procedure M/2, Table 4).
Figures 6a,b illustrate the comparison between the $\theta(h)$ functions obtained with procedures M/1 and M/2. Procedure M/2 does not allow us to predict the $\theta(h)$ function accurately. This indicates that additional $\theta(h_i)$ values are necessary in order to obtain reliable results also when multi-step experiments are performed.
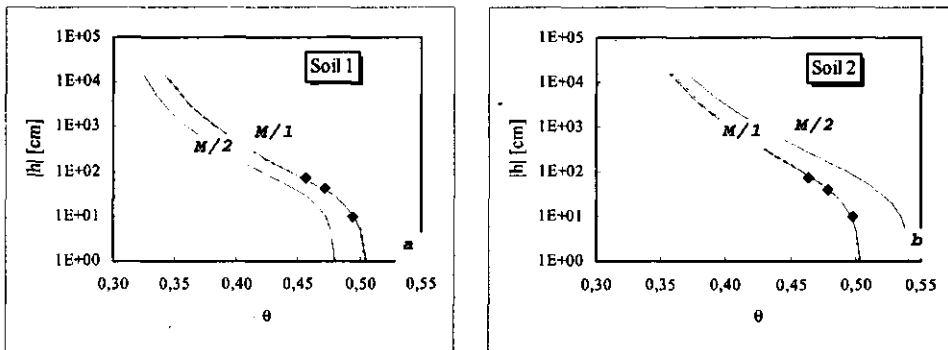

Fig 6. $\theta(h_i)$ functions predicted with procedure M/1 and associated (undistinguashable) one-standard deviation intervals. The $\theta(h_i)$ functions predicted with procedure M/2 are also represented. (a) Soil 1, (b) soil 2.

Conclusions

This paper illustrates some results obtained by means of the parameter estimation method based on one-step and multi-step experiments on two Sicilian Typic Haploxerert.
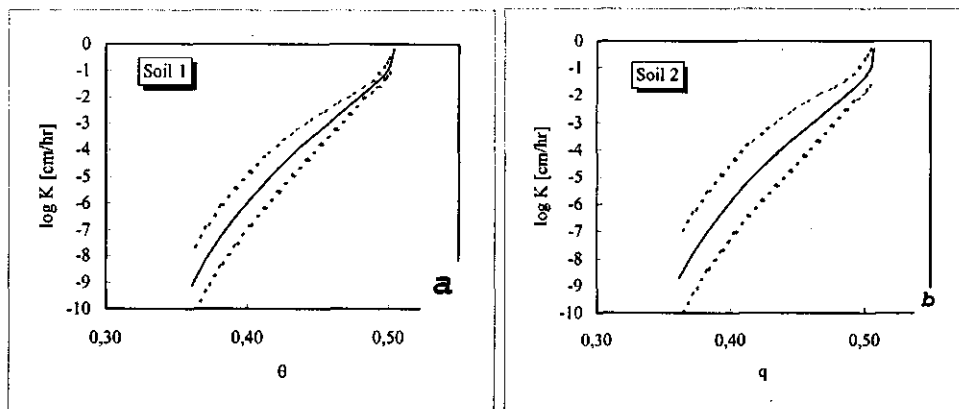

Fig. 7. Unsatured hydraulic conductivity K vs. volumetric water content θ predicted with procedure M/1 and associated one-standard deviation intervals (OSDI). (a) Soil 1, (b) Soil 2.

The shrinkage behaviour of the two soils was analysed, and the changes in the soil samples volume that occurred in the pressure range explored in the outflow experiments were found not to affect the outflow process.

With reference to one-step outflow experiments, a procedure is presented which allows accurate hydraulic functions to be obtained by optimization performed on outflow volumes supplemented with three independently determined $\theta(h)$ values.

The reliability of the predicted $\theta(h)$ functions, assessed by first-order analysis, can be considered satisfactory, while large one-standard deviation intervals, due to the poor identifiability of the estimated K_s and γ parameters, are associated with the predicted $K(\theta)$ functions.

With reference to multi-step outflow experiments, optimization performed only on outflow volumes did not allow the soil water retention curve to be accurately predicted, indicating the need for additional $\theta(h)$ data.

Comparisons between results provided by one-step and multi-step outflow experiments lead to the conclusion that although a greater accuracy is generally linked to the hydraulic functions obtained from the one-step approach greater reliability is associated with the hydraulic functions provided by multi-step experiments.

The narrower one standard deviation intervals associated with both the $\theta(h)$ function and the $K(\theta)$ function obtained from multi-step indicate that the performance of this approach is better than that of the one-step.

Due to the lack of validation of the predicted $K(\theta)$ functions with independently measured values, the conclusions of this paper rely on the hypothesis that the van Genuchten model

accurately predicts the $\theta(h)$ and $K(\theta)$ functions.

Validation of the predicted $K(\theta)$ functions is under way, as well as evaluation of results of simulations of the transport processes of water in unsaturated soil performed by using the hydraulic functions predicted by one-step and multi-step outflow experiments.

Hydraulic characterization of swelling/shrinking soils by a combination of laboratory and optimization techniques

G. Crescimanno and G. Baiamonte
Università di Palermo, Dipartimento ITAF, Sezione Idraulica. Palermo, Italy

Abstract

The multistep outflow method (MSTEP) with inverse modeling is widely used to determine the soil hydraulic properties. Previous investigation performed with the inverse method based on MSTEP experiments showed a poor identifiability of the estimated hydraulic conductivity in the near-saturation zone. Validation of the proposed optimization procedure through comparison with independently determined hydraulic conductivity measurements was considered necessary to assess the accuracy of the estimated hydraulic conductivity function.

This paper investigated an optimization procedure based on measurements obtained from MSTEP outflow experiments and on hydraulic conductivity values, K(h), obtained by the suction crust infiltrometer method (SCIM).

The results showed the need for using an optimization procedure in which the saturated hydraulic conductivity (K_s) was fixed at the value measured with the SCIM rather than considered a fitting parameter, with the K(h) values determined by the SCIM also enclosed in the optimization procedure.

In addition, the results showed that use of the hydraulic conductivity equation proposed by Gardner instead of that proposed by van Genuchten makes it possible to estimate hydraulic functions in close agreement with the independently determined K(h) values. This aspect can be relevant for hydraulic characterization of soils with macropores and/or susceptible to swelling and shrinkage.

Keywords: inverse method, hydraulic conductivity, multi-step method, suction crust infiltrometer method.

Introduction

In spite of continuous efforts for several decades, modeling water flow and solute transport in soils with macropores or cracks remains a very challenging endeavour. The most important approaches to model water flow in unsaturated soils are based on the Richards equation.

To solve this equation, a proper knowledge of the soil hydraulic properties, namely, the moisture content-pressure head curve, θ(h), and the hydraulic conductivity function, K(θ), is necessary.

Kool *et al.* (1985; 1987) applied the inverse method (Zachmann *et al.*, 1982; Yeh, 1986) to simultaneously determine the θ(h) and K(θ) functions by minimizing deviations between

predicted and measured outflow volumes (V) obtained from a one-step (OSTEP) outflow experiment supplemented with the soil moisture (θ) at the final equilibrium pressure. Further investigation with the inverse method evidenced the need for additional $\theta(h)$ data (Hudson *et al.*, 1991) or tensiometric measurements inside the sample (Toorman *et al.*, 1992) to overcome the problem of non-uniqueness of the solution. van Dam *et al.* (1990) proposed multi-step (MSTEP) outflow experiments as a valid alternative to OSTEP. Mous (1993) analyzed the identifiability of Richards' equation and Mualem-van Genuchten's equations with reference to OSTEP and MSTEP experiments. He concluded that the OSTEP model is numerically non-identifiable, while the MSTEP function is identifiable if no more than five parameters are simultaneously determined.

Crescimanno & Iovino (1995) investigated the applicability of the inverse method based on OSTEP and MSTEP experiments to determine the hydraulic functions of two Typic Haploxererts characteristic of the Sicilian environment. Based on the knowledge of the soil shrinkage characteristic curve (SSCC), the changes in volume were incorporated in the predicted hydraulic parameters. Using a first-order analysis, the reliability of the $\theta(h)$ and $K(\theta)$ functions predicted by OSTEP and MSTEP was compared, and the performance of the MSTEP approach was found to be better than that of the OSTEP. However, large one-standard deviation intervals, due to the poor identifiability of the estimated saturated hydraulic conductivity (Ks), were found to be associated with the $K(\theta)$ functions predicted from MSTEP experiments.

The increasing awareness of the role that macropores and cracks may have on water flow and solute transport in the vadose zone evidences the need for measuring the hydraulic conductivity of structured soils by measurement techniques suitable to represent macropore patterns, by using soil samples having a Representative Elementary Volume, (Bouma, 1983). Booltink *et al.* (1991) proposed the suction crust infiltrometer method (SCIM) (modified crust test) to determine the hydraulic conducitivity, K(h), of structured soils in the near-saturation range.

The objective of this paper is to explore a combination of laboratory and optimization techniques leading to accurate estimation of soil hydraulic parameters/functions in soils with macropores or cracks. The analysis is based on measurement of the saturated/unsaturated hydraulic conductivity performed by the SCIM on large soil cores ($\varnothing$=20 cm, h=20 cm) and on MSTEP outflow experiments performed in pressure cells on soil cores ($\varnothing$=8.5 cm, h=5 cm) sampled inside those used for the SCIM. Soil shrinkage characteristic curves determined on soil samples having the same geometry as those used for MSTEP experiments (Crescimanno & Provenzano, 1999), are used in order to incorporate soil shrinkage in the estimated hydraulic parameters/functions.

Parameter estimation is performed by using the measurements collected during the MSTEP experiments only, or supplementing this information with the K(h) values obtained by the SCIM. Different optimization options are analyzed and compared, with the influence of the analytical functions used to represent the hydraulic functions (Gardner, 1958; Brutsaert, 1966; Mualem, 1976; van Genuchten, 1980) also explored.

Materials and methods

Five soils with a considerable susceptibility to swelling and shrinkage were considered. Table 1 reports the main characteristics of these soils.

Table 1. Characteristics of the soils considered.

Soil	Classification[1]	Depth (cm)	Sand (2-0.02 mm)	Silt (0.02-0.002 mm)	Clay (<0.002 mm)
A1	Typic Haploxerert	0 - 30	32	24	44
A2	Typic Haploxerert	0 - 30	33	31	36
B1	Typic Haploxerert	0 - 30	33	23	44
B2	Typic Haploxerert	0 - 30	31	31	38
D2	Typic Haploxerert	0 - 30	33	23	44

[1] Soil Taxonomy (Soil Survey Staff, 1992)

Measurement of the saturated/unsaturated hydraulic conductivity was performed by the suction crust infiltrometer method, SCIM (Booltink *et al.* 1991) using large soil cores (ø=20 cm, h=20 cm) previously saturated and placed on a funnel. After measuring the saturated hydraulic conductivity, Ks, the soil samples were placed on 50 cm long PVC cylinders with the same diameter and filled with medium textured sand.

Two tensiometers were installed at 6 and 10 cm below the soil surface and connected with a pressure transducer. Crusts were made of mixtures of sand and quick setting hydraulic cement, and the mixture was applied on the soil and compressed on the soil surface to ensure good contact between crust and surface.

After hardening, a perxpex cap was glued on top of the cylinder and water was put immediately on top of the crust. Hydraulic pressure was applied on top of the crust by manipulating the changing level of a Mariotte tube. When a unit hydraulic gradient was established, fluxes and pressures (h) were measured, and hydraulic conductivity values (K) were determined.

Undisturbed soil cores (ø=8.5 cm, h=5 cm) were sampled inside the larger cores used for the SCIM measurements. MSTEP experiments were performed in pressure cells on the soil samples previously equilibrated with a small pneumatic pressure (1 kPa). Three successive steps with pneumatic pressure ranging from 1 to 4 kPa, from 4 to 7 kPa, and from 7 to 80 kPa were performed. Cumulative outflow volumes V(t) were determined by weighing and automatic recording.

Soil shrinkage characteristic curves determined on soil samples having the same geometry as those used for MSTEP experiments (Crescimanno & Provenzano, 1999), made it possible to incorporate soil shrinkage in the estimated hydraulic parameters/functions.

Parameter estimation was performed by considering as starting point the procedure proposed by Crescimanno and Iovino (1995) *(option 1)*, in which the saturated hydraulic conductivity (Ks) was an optimized parameter, and the θ(h) and K(θ) functions were

represented by the van Genuchten model (van Genuchten, 1980; Mualem, 1976):

$$\frac{\theta - \theta_r}{\theta_s - \theta_r} = \Theta = \left[1 + \alpha |h|^n\right]^{-m} \tag{1}$$

$$K(\theta) = K_s \cdot \Theta^\gamma \left[1 - \left(1 - \Theta^{1/m}\right)^m\right]^2 \tag{2}$$

where θ is the volumetric water content, θ_s is the saturated water content, θ_r is the residual water content, h is the pressure head , α, n and m are empirical parameters (m = 1 - 1/n), and K_s is the saturated hydraulic conductivity.

Revision of the proposed procedure, based on the comparison between the estimated K(h) function and the K(h) values determined by the SCIM, was considered:

(i) by fixing the saturated Ks at the value measured by the SCIM *(option 2)*;

(ii) by optimization performed on the V(t) values supplemented not only with some θ(h) values but also with the K(h) values measured by the SCIM, using the van Genuchten model *(option 3):*

(iii) by optimization performed on the V(t) values supplemented with some θ(h) values and with the K(h) measured by the SCIM, using the model proposed by Gardner (1958) for the hydraulic conductivity function and a modified form of the equation proposed by van Genuchten for the water retention curve (Brutsaert, 1966) *(option 4):*

$$\frac{\theta - \theta_r}{\theta_s - \theta_r} = \Theta = \left[1 + \alpha |h|^n\right]^{-1} . \tag{3}$$

$$K(\theta) = \frac{K_s}{1 + |\beta \cdot h|^\lambda} \tag{4}$$

with β and λ shape parameters.

Results and discussion

Table 2 reports the hydraulic parameters obtained for the five considered soils by using the described four options.

As can be seen in Table 2, the results obtained with *option 1* (Ks, θ_r, α and n optimized parameters) showed large deviations between the optimized and the measured Ks, except for soil D2. In addition, large standard deviation values (Std), indicating a poor identifiability of the estimated Ks, were found to be associated with this parameter.

Figures 1a, 2a and 3a illustrate the water retention curves, θ(h), obtained with *option 1* together with the standard errors of the estimate (SEEθ) calculated on the θ(h) values. In figures 1b, 2b and 3b the comparison between the optimized K(h) functions and the K(h) values measured by the SCIM is reported, together with the standard error of estimate

(SEEk) calculated on the K(h) values.

Although a good agreement between the estimated and the measured V(t), as well as between the estimated and the measured θ, was found, large deviations between the estimated and the measured K(h) were observed. Only for soil B2 optimization performed with *option 1* provided an estimated K(h) function showing a satisfactory agreement with the measured K(h).

Further analysis was carried out by performing optimization with *option 2*, in which the Ks was fixed at the value measured by the SCIM. Table 2 reports the parameters obtained with *option 2*. Figures 1a, 2a and 3a, and 1b, 2b and 3b illustrate the optimized θ(h) and K(h) obtained with *option 2*.

Larger SEEV values were obtained with *option 2* compared to results of *option 1*, but the predicted V(t) was satisfactory.

The SEEθ obtained for soils A2 and B1 were larger than those obtained with *option 1*, but accuracy of the predicted θ(h) values was satisfactory.

Considerable reductions in the SEEK values were observed only for soils A1 and A2, while large SEEK were still evident for soils B1, B2 and D2. It is interesting to notice that the K values determined by the SCIM were generally higher than those obtained by the inverse method based on MSTEP, which cannot account for the soil structural porosity because of the small volume of the soil samples used.

The results obtained with *option 2* indicated the need for further analysis, which was carried out by including in the optimization procedure the K(h) measurements obtained by the SCIM. Figures 1c, 2c and 3c illustrate the results obtained by *option 3* (optimization performed on the V(t) values supplemented with the θ(h) values and with the K(h) measured by the SCIM, using the van Genuchten-Mualem model).

As can be seen in the Figures, inclusion of the independently measured K(h) values in the optimization process generally led to a better agreement between estimated and measured k values, with considerable reductions in the SEEK values compared to those obtained with *option 2*. However, for soils B2 and D2 the performance of *option 3* was not satisfactory.

Table 2. Parameter values and standard deviations obtained by multi step-experiments with options 1, 2, 3 and 4.

|	Parameter	Option 1		Option 2		Option 3		Option 4	
		Mean	Std	Mean	Std	Mean	Std	Mean	Std
A1	α	0.0292	0.0058	0.0180	0.0082	0.0139	0.0048	0.0045	0.0052
	n	1.2575	0.0396	1.3418	0.1293	1.8455	0.1313	1.0971	0.4216
	θ_s	0.452		0.452		0.452		0.452	
	θ_r	0.385	0.005	0.387	0.031	0.400	0.024	0.3829	0.0496
	K_s	0.0035	0.0008	4.6964		4.6964		4.6964	
	γ	-4.350	1.590	10.000	9.800	10.000	9.700		
	β							0.0793	0.0049
	λ							4.7642	0.3163
	SEEv	0.2166		0.6704		0.7770		0.5389	
A2	α	0.0159	0.0034	0.0235	0.0104	0.0116	0.0070	0.0070	0.0039
	n	1.2567	0.1090	1.1644	0.0713	1.5371	0.1337	1.3462	0.3619
	θ_s	0.490		0.490		0.490		0.490	
	θ_r	0.3363	0.0678	0.3492	0.0512	0.3758	0.088	0.4082	0.0327
	K_s	0.0101	0.0056	7.40		7.40		7.40	
	γ	-0.659	1.8619	10.000	8.065	10.000	15.406		
	β							0.1300	0.0086
	λ							3.9436	0.2193
	SEEv	0.4029		0.9385		2.0223		0.7463	
B1	α	0.0196	0.0055	0.0235	0.0046	0.0122	0.0039	0.0005	0.0031
	n	1.1692	0.1203	1.1481	0.0375	0.4611	0.0850	0.4509	0.3518
	θ_s	0.450		0.450		0.450		0.450	
	θ_r	0.3537	0.0664	0.3617	0.0154	0.3873	0.0218	0.3414	0.1976
	K_s	0.2032	0.2927	3.026		3.026		3.026	
	γ	6.991	10.609	10.000	3.4607	10.000	7.2253		
	β							0.0925	0.0063
	λ							3.8177	0.2372
	SEEv	0.2603		0.3257		0.8213		0.3609	
B2	α	0.1008	0.0815	0.0728	0.0257	0.0685	0.0220	0.0389	0.0382
	n	1.4021	0.1681	1.5263	0.0723	1.5332	0.0701	0.4056	0.0919
	θ_s	0.510		0.510		0.510		0.570	
	θ_r	0.4022	0.0263	0.4166	0.0070	0.4172	0.0066	0.3696	0.0445
	K_s	0.2825	0.4772	0.0828		0.0828		0.0828	
	γ	-1.8987	0.8744	-2.0708	0.770	-1.9691	0.7354		
	β							0.1356	0.0414
	λ							2.3199	0.3041
	SEEv	0.8964		1.0038		1.0014		0.8501	
D2	α	0.2732	0.0402	0.2845	0.0274	0.2766	0.0567	0.0313	0.0118
	n	1.3634	0.0188	1.3584	0.0098	1.3603	0.0211	0.6163	0.0883
	θ_s	0.580		0.580		0.580		0.580	
	θ_r	0.3760	0.0089	0.3733	0.0045	0.3749	0.0094	0.3656	0.0302
	K_s	2.3571	0.9389	2.671		2.671		2.671	
	γ	-2.0753	0.2060	-2.0540	0.1768	-2.0102	0.3873		
	β							0.0682	0.0105
	λ							4.2311	0.4044
	SEEv	0.8964		1.0038		1.0014		0.8501	
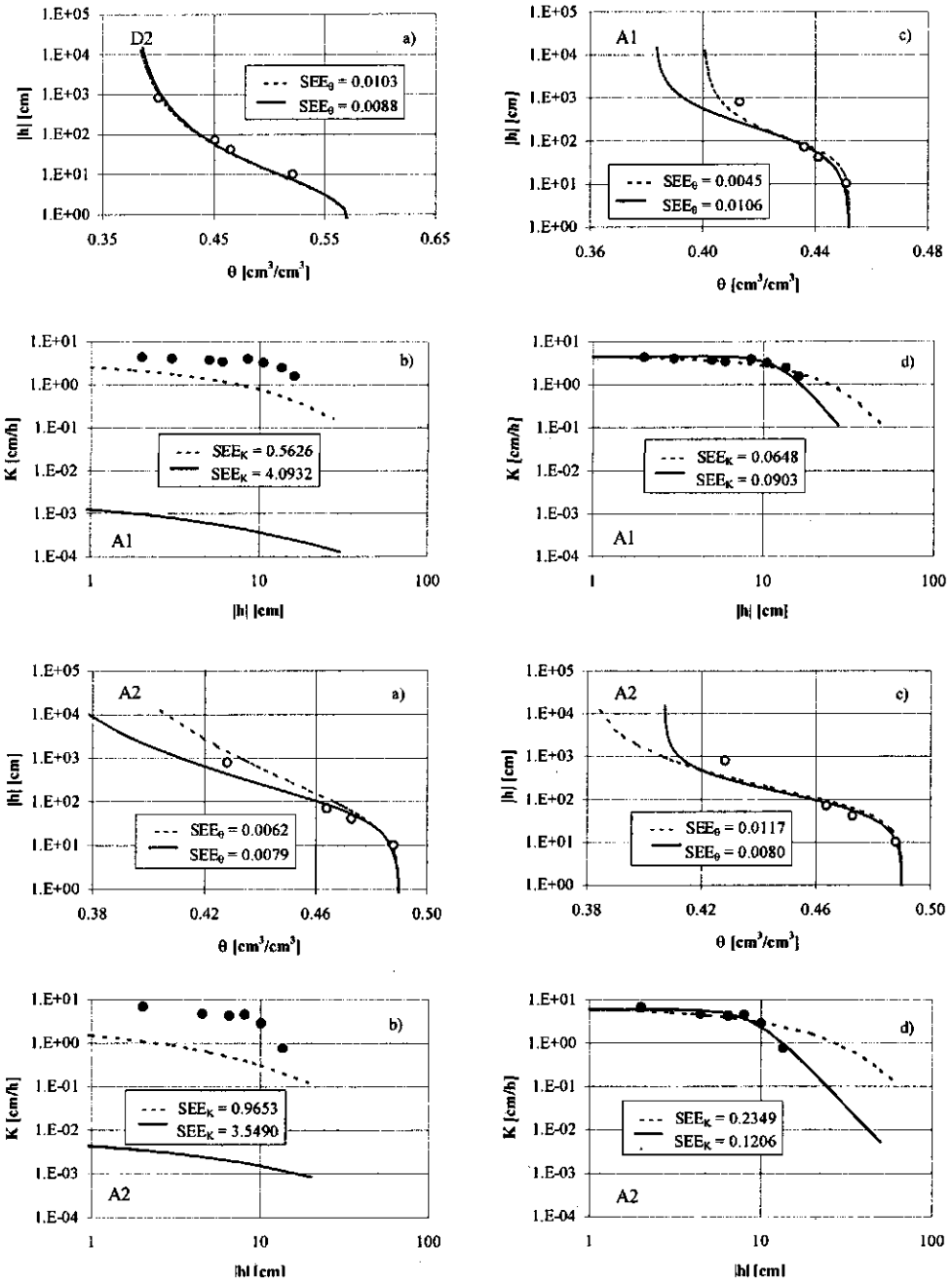
Figure 1. Water retention and hydraulic conductivity functions obtained for soils A1 and A2 with option 1 (a, b, ——), option 2 (a, b, - - -), option 3 (c, d, - - -) and option 4 (c, d, ——). The black circles indicate the hydraulic conductivity values obtained with the SCIM.
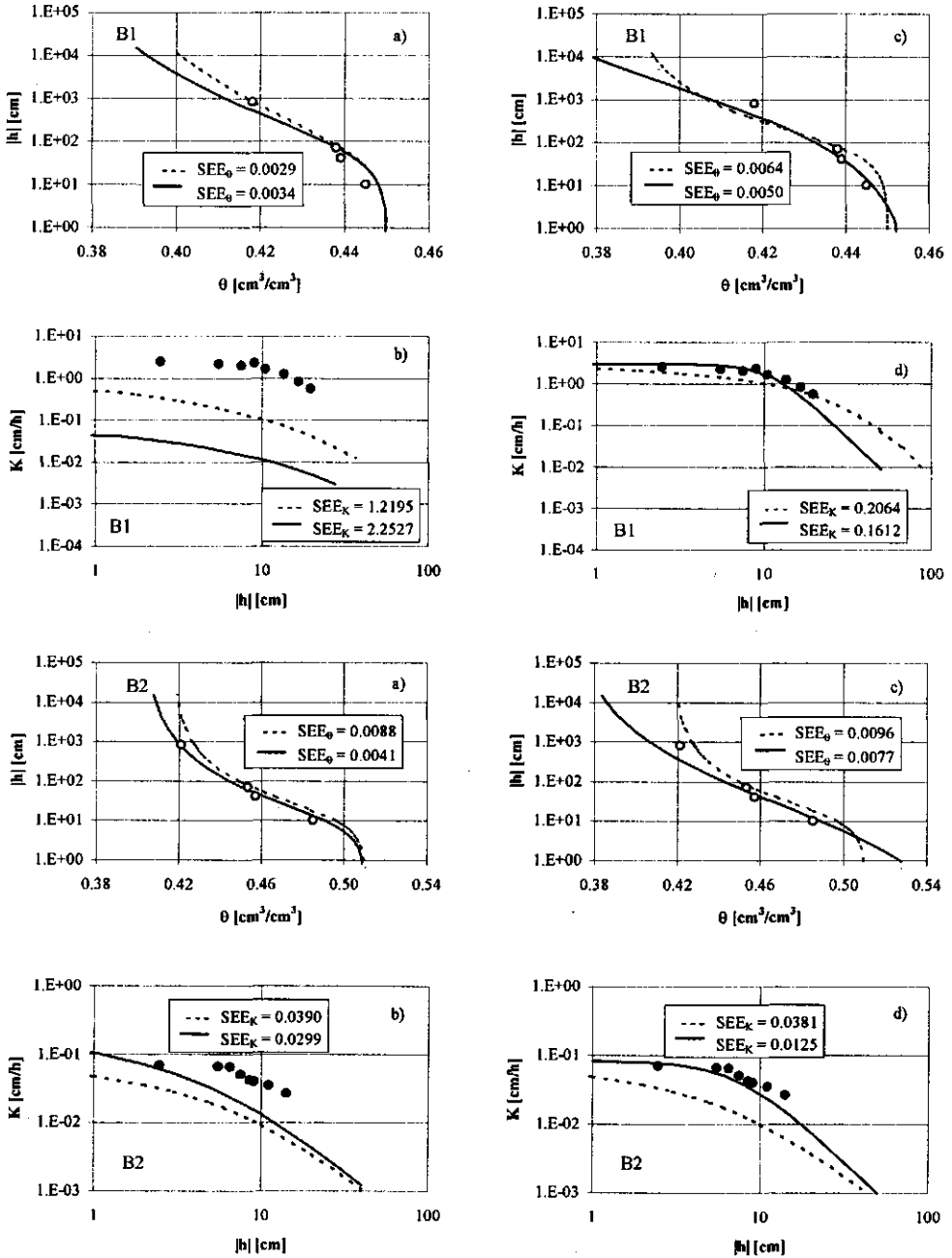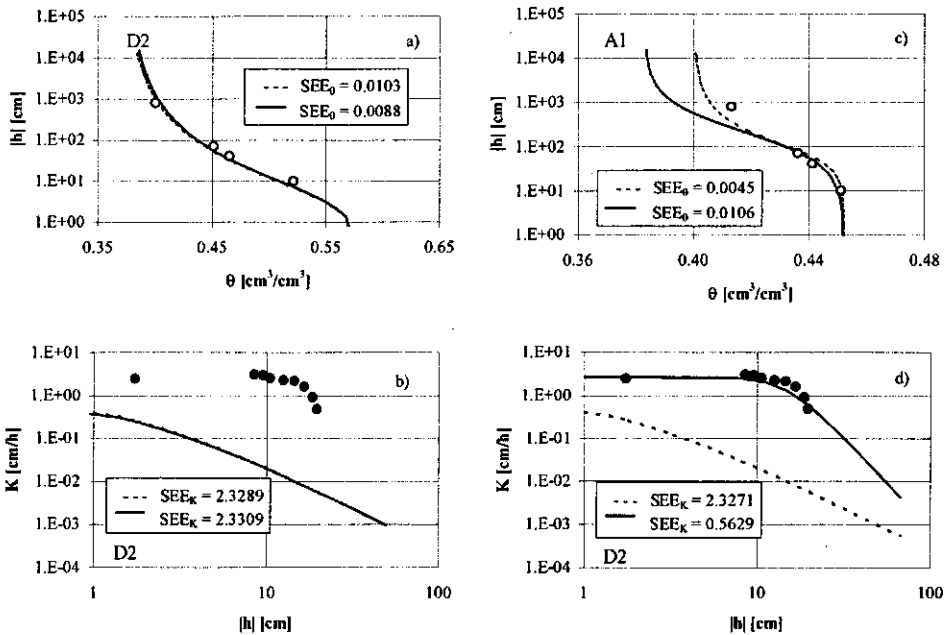
Figure 2. Water retention and hydraulic conductivity functions obtained for soils B1 and B2 with option 1 (a, b, ——), option 2 (a, b, - - -), option 3 (c, d, - - -) and option 4 (c, d, ——). Theblack circles indicate the hydraulic conductivity values obtained with the SCIM.

Figure 3. Water retention and hydraulic conductivity functions obtained for soil D2 with option 1 (a, b, —), option 2 (a, b, - - -), option 3 (c, d, - - -) and option 4 (c, d, —). The black circles indicate the hydraulic conductivity values obtained with the SCIM.

This result was attributed to the shape of the van Genuchten hydraulic conductivity function in the near-saturation zone compared to that of the measured K(h).

Further investigation was carried out with *option 4*, in which optimization was performed on the V(t) values supplemented with some θ(h) values and with the K(h) measured by the SCIM, with use of the hydraulic conductivity function proposed by Gardner instead of that proposed by van Genuchten.

Results provided by optimization performed with *option 4* are illustrated in Figures 1c, 2c and 3c, and 1d, 2d and 3d. The close agreement between the estimated and the measured K(h) is evident, and proved by the lower SEEK obtained for all the soils compared to those obtained with *option 3*. Only for soil A1 optimization performed with *option 4* did not determine any improvement in the agreement between estimated and measured K(h) values. With reference to the θ(h) function, the SEEθ obtained with *option 4* were lower than those obtained with *option 3* for all the soils except for soil A1.

The results obtained with *option 4* proved that optimization based on the modified van Genuchten equation for the water retention curve, and on the equation proposed by Gardner for the hydraulic conductivity curve (Vereecken *et al.*, 1990; Droogers and Bouma, 1996), led to estimated hydraulic parameters/functions in close agreement with the independently

71

determined hydraulic conductivity values.

Conclusions

The investigation showed that the hydraulic conductivity functions obtained by optimization performed on measurements collected during MSTEP experiments only showed large deviations from the hydraulic conductivity values K(h) determined by the suction crust infiltrometer method (SCIM).

Instead, inclusion of the K(h) values in the optimization procedure made it possible to determine hydraulic conductivity functions in close agreement with the independently determined K(h) values. The need for fixing the saturated hydraulic conductivity at the value measured by the SCIM rather than considering Ks as a fitting parameter was also evident.

The results also showed that use of the Gardner model for the hydraulic conductivity curve instead of equation proposed by van Genuchten made it possible to improve the overall performance of the optimization procedure, leading to estimated hydraulic parameters/functions accounting for the soil structural porosity.

Further investigation is under way on a larger number of soil samples with a considerable susceptibility to swelling and shrinkage.

Chapter 4

Influence of salinity and sodicity on soil structural and hydraulic characteristics

Influence of salinity and sodicity on soil structural and hydraulic characteristics

G. Crescimanno, M. Iovino and G. Provenzano

Università di Palermo, Dipartimento ITAF, Sezione Idraulica. Palermo, Italy

Abstract

An exchangeable sodium percentage (ESP) greater than 15 is traditionally considered to affect soil structural and hydraulic characteristics. Recent investigations show that both this critical value and the concept of critical threshold need reconsideration, because soil degradation often takes place even at lower ESP in dilute solutions, and soil behaviour at increasing ESP appears to be a continuum.

This study was carried out to analyze the response of two Sicilian Typic Haploxererts to ESP values up to 15, at a low cationic concentration. The investigation was carried out on aggregate stability, rating of soil shrink-swell potential and on both saturated and unsaturated hydraulic conductivity.

The specific purpose was to verify if a critical ESP threshold exists, or if the hypothesis of a continuum behaviour is more appropriate.

The High Energy Moisture Characteristic technique was used for determining aggregate stability, and Brasher's method for the shrinkage characteristic. The constant-head method was used for determining saturated hydraulic conductivity, and the parameter estimation method based on one-step outflow experiments for unsaturated hydraulic conductivity.

Almost linear relationships between the investigated soil properties and ESP, indicating no critical ESP threshold, were found; furthermore the results obtained indicate that an effective hazard of soil quality degradation can be forecast even in a 2 to 5 ESP range at a low cationic concentration.

This is a basic indication for irrigation management aimed to combat and prevent degradation of soil quality.

Introduction

Many arid and semi-arid regions of the world are affected by soil salinization and alkalization. An exchangeable sodium percentage (ESP) greater than 15 (US Salinity Laboratory, 1954) generally affects the structural and hydraulic characteristics of soil. Some investigations suggested that this threshold may need reconsideration because soil degradation can take place even at low ESP in dilute solutions (Quirk and Schoefield, 1955; Shainberg et al., 1981). McIntyre (1979) proposed an ESP>5 to define a sodic soil, Northcote and Skene (1972) an ESP>6 for Australian soils; similar values were indicated by Rengasamy et al.(1984) and Agassi et al. (1985). Sumner (1993) explained that the reason for these apparently contrasting findings lay in the different values of solution concentration (C) used in the various investigations. According to him, the establishment of a critical ESP threshold may be very arbitrary because the properties exhibited by the so-

called classic sodic soils are simply the upper end of a continuum of behaviour which extends over the full range of Na saturations, being increasingly dependent on reduced C.

Sodium in the exchange complex may negatively affect soil structure, and *aggregate stability* (Abu-Sharar et al., 1987a). Sodium causes *swelling* and/or *dispersion* of clay particles, and slaking of unstable aggregates. Clay swelling and dispersion increase at increasing ESP and at decreasing cationic concentration of pore solution (Cass and Sumner, 1982).

The assessment of volume change associated with a change in soil moisture, expressed by the *shrinkage characteristic* (Bronswijk and Evers-Vermeer, 1990), is also a fundamental feature of soil structural quality. The magnitude of shrinkage processes, with the subsequent changes in bulk density and in potential cracking, is also dependent on ESP (Murray and Quirk, 1980). Aggregate stability and rate of swelling-shrinkage are interrelated (Coughlan et al., 1991); soils with good aggregation shrink less than structureless soils, being less susceptible to cracks under field conditions (Mitchell and Van Genuchten, 1992).

Soil structure is linked to hydraulic conductivity (Abu-Sharar et al., 1987b); slaking of aggregates and/or an increase in bulk density may cause reductions in hydraulic conductivity (So and Aylmore, 1993). Interactions between structural and hydraulic characteristics are complex (Creswell et al., 1992) and still need systematic studies with a view to formulating quantitative relationships between them (Kirby and Blunden, 1991) and establishing their links with salinity and sodicity (Fitzpatrick et al., 1994).

Assessing the influence of salinity and sodicity on structural and hydraulic characteristics, which has been the subject of much research (Shainberg et al., 1981; Cass and Sumner, 1982; Lima et al., 1990; Rengasamy and Olsson, 1991), can help to prevent irreversible deterioration of soil quality.

Sicilian soils generally exhibit ESP lower than 15, but the high salinity levels characterizing irrigation waters used in many areas make leaching necessary to keep salinity under levels tolerated by crops. Since leaching, as well as rainfall, interacts closely with soil-physical properties (Oster,1994), great attention is focused on deterioration of soil structural and hydraulic characteristics in the Sicilian environment.

This paper assesses the influence of ESP, at a low cationic concentration, on aggregate stability, rate of swelling-shrinkage, and on both saturated and unsaturated hydraulic conductivity, for two Typic Haploxererts. The specific objective is to analyze the relationships between the investigated soil properties and ESP, in order to verify if a critical ESP threshold can be found.

Materials and methods

Two soils, characteristic of the Sicilian environment, belonging to areas irrigated with saline-sodic waters, were considered. Table 1 reports classification and some physico-chemical characteristics of the two soils; it can be noticed that both soils are clayey and contain variably swelling minerals.

Re-packed soil samples were used in order to prepare soil samples that were as homogeneous as possible. Air-dried soil samples, crushed to pass a 2-mm sieve, were packed at the bulk density value determined on the undisturbed soil cores into cylinders of diameter 8.5 cm and height 10 cm. They were saturated under suction with NaCl-CaCl$_2$ solutions of variable SAR (SAR = 0, 10, 20 and 30) and concentration C = 100 mol/m^3 and then leached with solutions of the same SAR and gradually decreasing concentration C (C = 100, 20, 10, 5 and 1 mol/m^3) in constant-head permeameters (Klute and Dirksen, 1986).

Table 1: Classification and main physico-chemical characteristics of the soils studied.

	Soil n. 1	Soil n. 2
Site	Delia	Gela
Classification [†]	Typic Haploxerert	Typic Haploxerert
Horizon	Ap (0-27 cm)	Ap (0-30 cm)
Sand (2÷0.02 mm)(%)	8	19
Silt (0.02÷0.002 mm) (%)	35	27
Clay (<0.002 mm) (%)	57	54
Texture (ISSS)	C	C
Clay Mineralogy (%)		
Kaolinite	34.2	24.1
Chlorite	11.1	15.2
Illite	43.3	46.2
Smectite	11.5	14.5
EC (1:5) (dS/m)	0.87	0.30
CEC (cmol/kg)	40.6	34.6
ESP (%)	2.11	2.17
Organic matter (%)	3.55	3.47

([†]) Soil Taxonomy (Soil Survey Staff, 1992)

Saturated hydraulic conductivity, K_s, corresponding to each combination of SAR and C was determined on two replicated soil samples when the electrical conductivity of the effluent solution was approximately equal to the concentration of the incoming solution. Relative K_r values were defined as the ratio between the K_s measured at the different values of SAR and C and the K_s determined at SAR = 0 and C = 100 mol/m^3.

At the end of the pre-treatments chemical analyses were performed in order to determine the ESP and the final C; the ESP values were about 2, 5, 10 and 15 and the concentration C, evaluated on the 1:5 saturated extract, was about 2.5 mol/m^3.

The pre-treated soil, air-dried and crushed to pass a 2-mm sieve again, was used for preparing samples for subsequent investigations on aggregate stability and unsaturated hydraulic conductivity.

The moisture characteristic at high energy (HEMC) technique (Collis-George and Figueroa, 1984) was used to investigate soil aggregate stability due to its suitability for detecting even small differences in aggregate stability (Pierson and Mulla, 1989). The experimental technique consists of preparing beds of sieved aggregates and determining the relationship between matric head h (cm) and gravimetric water content U (g g^{-1}). A structural index SI (g g^{-1} cm^{-1}) is defined as the ratio: (1)

$$SI = \frac{\Delta U_g}{|\tau_d|} \qquad (1)$$

in which ΔU_g is the volume of drainable pores and τ_d (cm) is the modal suction. The volume of drainable pores is defined as the area under the water capacity curve dU/dh (cm^{-1}), which is the change in water content U per unit change of matric head h, and above the dashed base-line representing the rate of water loss due to aggregate shrinkage rather than pore emptying (Fig. 1); the modal suction corresponds to the suction of the peak of the water capacity curve (Collis-George and Figueroa, 1984) (Fig. 1).
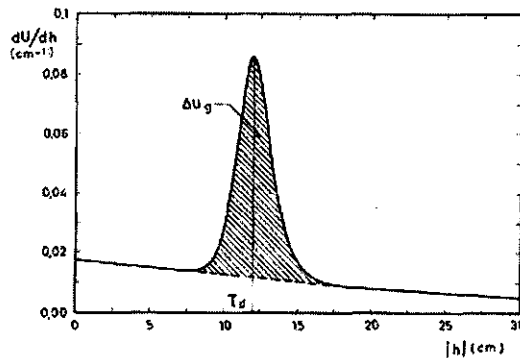
Figure 1. Water capacity dU/dh vs. matric head h; the shaded area represents the volume of drainable pores ΔU_g, and τ_d is the modal suction.

Three aggregate size fractions (0.25-0.5; 0.5-1; 1-2 mm) were considered for determining SI (Collis-George and Figueroa, 1984); two replicated samples (5 cm diameter, 1 cm height) were prepared by mixing percentages of the three fractions corresponding to their frequence in the aggregate size distribution obtained by dry-sieving. The samples were put in sintered funnels connected to a hanging water column which can be adjusted in height to control the matric suction difference between the center of the aggregate bed and the free water level in a pipette at the end of the column. Wetting of aggregates takes place via upward water flow through the sintered glass funnel (Stolte and Veerman, 1991).
A very slow saturation was realized by a 45-minute treatment in which matric head values h

of -10, -5, -2 and 0 cm were imposed with an equilibration period of 15 minutes at each setting; thirteen U values corresponding to h ranging from -2 to -100 cm were determined. The van Genuchten equation (1980) was fitted to the U, h values in order to determine the modal suction τ_d corresponding to the peak of the dU/dh function (Pierson and Mulla, 1989); the procedure proposed by Collis-George and Figueroa (1984) was adopted in order to determine the ΔU_g values.

A stability ratio SR was defined as the ratio between the structural index obtained at increasing ESP (ESP = 5, 10 and 15) and the structural index obtained at the lowest ESP (ESP = 2).

Shrinkage characteristic curves (Bronswijk and Evers-Veermer, 1990) of the two soils were determined on clods obtained from pre-treated (ESP = 2 and ESP = 10) undisturbed soil samples (8.5 cm diameter, 10 cm height). Shrinkage characteristic is usually represented as void ratio e vs. moisture ratio u, with e and u defined as:

$$e = \frac{V_p}{V_s} \tag{2}$$

$$u = \frac{V_w}{V_s} \tag{3}$$

with V_p (cm^3) volume of pores, V_S (cm^3) volume of solids and V_w (cm^3) volume of water. Clods (volume 20-30 cm^3) were immersed in SARAN F-310 resin (resin to solvent ratio 1:5 in weight) (Brasher et al., 1966) after performing saturation in the Stakman apparatus (Stakman et al., 1969). The applied SARAN-coating is very elastic, impermeable to water and permeable to water vapor; as the clods dry and shrink, the elastic coating remains tightly fitted around the clods. By repeating weighing and weighing under-water, both the weight and volume of the clod were determined at different stages of shrinkage, in a non-destructive way; when weight losses became negligible, the SARAN-coated clods were oven-dried in order to determine final dry volume and dry weight. Measurements were carried out on three clods at each ESP. The coefficient of linear extensibility COLE (cm^{3}cm^{-3}) (Grossman et Al., 1968) was calculated:

$$COLE = \left(\frac{V_{wet}}{V_{dry}}\right)^{\frac{1}{3}} - 1 \tag{4}$$

Changes in void ratio e, derived from shrinkage characteristic, were converted into change in volume of soil aggregates by the expression (Bronswijk and Evers-Vermeer, 1990):

$$\frac{V_1}{V_2} = \frac{1+e_2}{1+e_1} \tag{5}$$

in which V_2, V_1 and e_2, e_1 represent volume and void ratio at two different values of moisture content respectively; the volume of cracks was calculated by (5) in the range between saturation and oven-dry in order to determine the maximum predictable potential value.
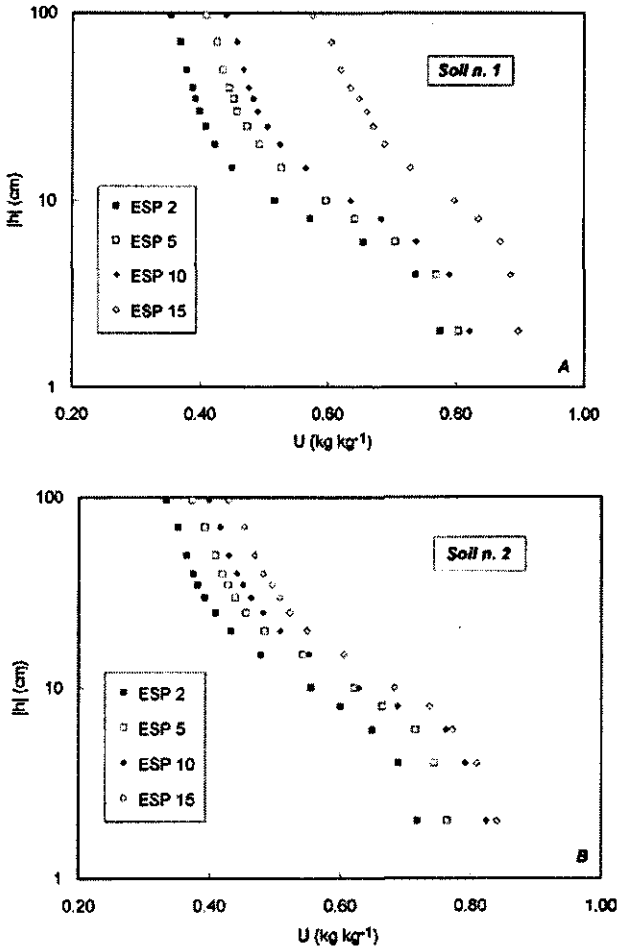
Figure 2.
Matric head h vs. gravimetric water content U obtained on soil aggregates at ESP = 2, 5, 10 and 15 and cationic concentration C = 1 mol m^{-3}. The figure shows the increase in U at increasing ESP, at equal h: (A) soil n.1, (B) soil n.2.

Soil samples (5 cm diameter, 5 cm height) were prepared for one-step outflow experiments (Kool and Parker, 1985a, b); an air pressure head equal to 816 cm was applied to the soil samples previously equilibrated at an air pressure head of 10 cm into volumetric pressure plate extractor (Soilmoisture, Santa Barbara, California). The outflow volume V at the different times t_i was determined by weighing and automatically recorded. The volumetric water content θ (cm^3 cm^{-3}) corresponding to the matric head h of -10, -40 and -70 cm was determined by the Stakman apparatus (Stakman et al., 1969) on separate samples (5 cm diameter, 5 cm height); the residual water content θ_r, i.e. the value corresponding to a matric head h of -15300 cm, was determined by the pressure plate method (Klute, 1986) on different samples (5 cm diameter, 1 cm height). Both one-step outflow experiments and measurement of θ(h) values were performed on three replicated samples. Table 2: Structural index SI and stability ratio SR at ESP = 2, 5, 10 and 15, and cationic concentration C=1 mol m^{-3}.

Table 2.

	ΔU_g (kg kg^{-1})	$|\tau_d|$ (cm)	SI (kg kg^{-1}cm^{-1})	SR (-)
Soil n. 1				
ESP 2	0.293	5	0.0586 a[†]	1.00
ESP 5	0.244	5.5	0.0444 b	0.76
ESP 10	0.218	6	0.0363 b	0.62
ESP 15	0.128	8.5	0.0151 c	0.26
Soil n. 2				
ESP 2	0.245	6.5	0.0376 a	1.00
ESP 5	0.218	8	0.0273 b	0.73
ESP 10	0.207	9	0.0230 c	0.61
ESP 15	0.152	10	0.0152 d	0.40

([†]) Row values followed by different letters are significantly different at the 0.05 probability level

The parameter estimation method (Kool and Parker, 1985 a,b) was applied to determine the water retention $\Theta(h)$ and the hydraulic conductivity $K(\Theta)$ functions, represented by the equations (van Genuchten, 1980; Mualem, 1976):

$$\Theta = \begin{cases} \left[1 + |\alpha h|^n\right]^{-m} & h < 0 \\ 1 & h \geq 0 \end{cases}$$ (6)

$$K(\Theta) = K_s \Theta^\gamma [1-(1-\Theta^{1/m})^m]^2$$ (7)

where $\Theta=(\theta-\theta_r)/(\theta_s-\theta_r)$; θ_s is the saturated water content; θ_r is the residual water content; K_s is the saturated hydraulic conductivity (cm hr^{-1}); α, n, m and γ are empirical parameters, with m=1-1/n. Optimization was performed according to a procedure that provided accurate predictions of the $\theta(h)$ and $K(\theta)$ functions (Crescimanno and Iovino, 1994).
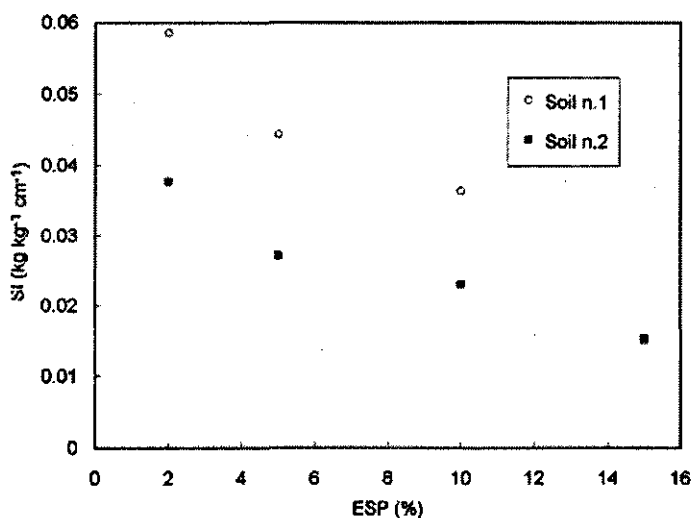
Figure 3. Structural index SI vs. ESP at cationic concentration $C = 1$ mol m^{-3}. The figure shows the decrease in SI at increasing ESP from 2 to 15; a linear trend, indicating no critical ESP threshold, is also evident.

The significance of the differences between the replicated measurements and between the measurements at the different ESP was investigated by analysis of variance (ANOVA) according to a randomized complete block design where the blocks were represented by the replicated measurements at the same ESP and treatments by the measurements at the different ESP values on the same soil sample. Mean separation was performed according to Duncan's multiple-range test (Little and Hills, 1978). A 0.05 probability level was chosen for all tests.

Results and discussion

Table 2 reports the structural indices SI obtained for soil n.1 and n.2; these values represent the average of the two replicated measurements.

Table 3: COLE values, shrink-swell potential and crack volume at ESP = 2 and 10.

	V_{wet}/V_{dry} [†] $(m^3\ m^{-3})$	COLE [‡] (-)	Shrink-swell potential §	Crack volume [¶] [%]
Soil n. 1				
ESP 2	1.60	0.103 a#	Very high	36
ESP 10	1.83	0.151 b	Very high	44
Soil n. 2				
ESP 2	1.44	0.071 a	High	29
ESP 10	1.69	0.122 b	Very high	41

([†]) V_{wet} = V at saturation; V_{dry} = oven-dry volume
([‡])   COLE values calculated in the range h=-33 kPa to oven-dry
([§])   Parker et Al., 1977
([¶])   Calculated in the range between saturation and oven-dry
([#])   Row values followed by different letters are significantly different at the 0.05 probability level
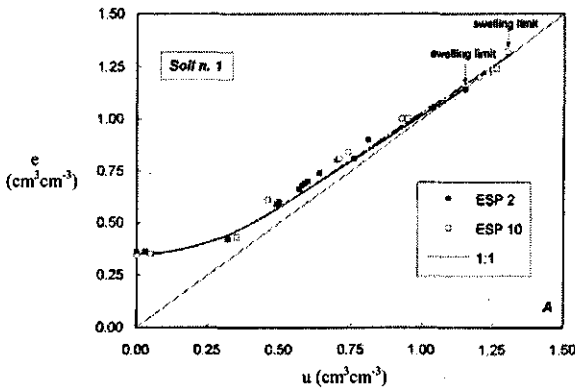
Figure 4.
Void ratio e vs. moisture ratio u, representing the shrinkage characteristic, obtained on clods at ESP = 2, 10 and cationic concentration C = 1 mol m^{-3} T. The relationship e(u) obtained at ESP = 10 shows a higher swelling limit (indicated by the arrow) than the relationship at ESP = 2: (A) soil n.1, (B) soil n.2.
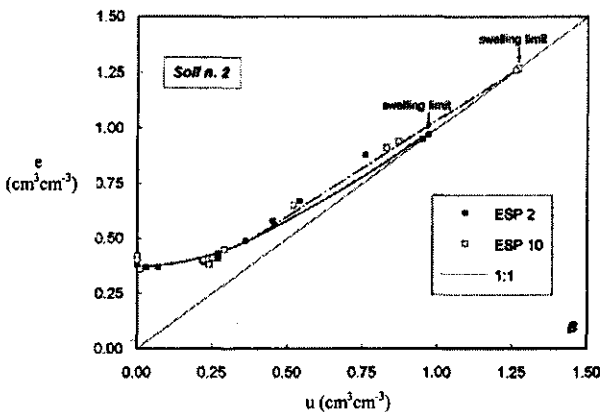
83

ANOVA showed that differences between the blocks were not significant, while differences between the treatments were; the results of Duncan's test are reported in Table 2.

Figures 2 a, b illustrate the average HEMC curves obtained at the different ESP for the two soils. The values of ΔU_g and $|\tau_d|$ deduced from these curves are reported in Table 2; at increasing ESP, ΔU_g decreases and the modal suction $|\tau_d|$ increases, indicating that slaking of aggregates has taken place. Consequently, the SI values and the stability ratio SR, also reported in Table 2, significantly decrease.
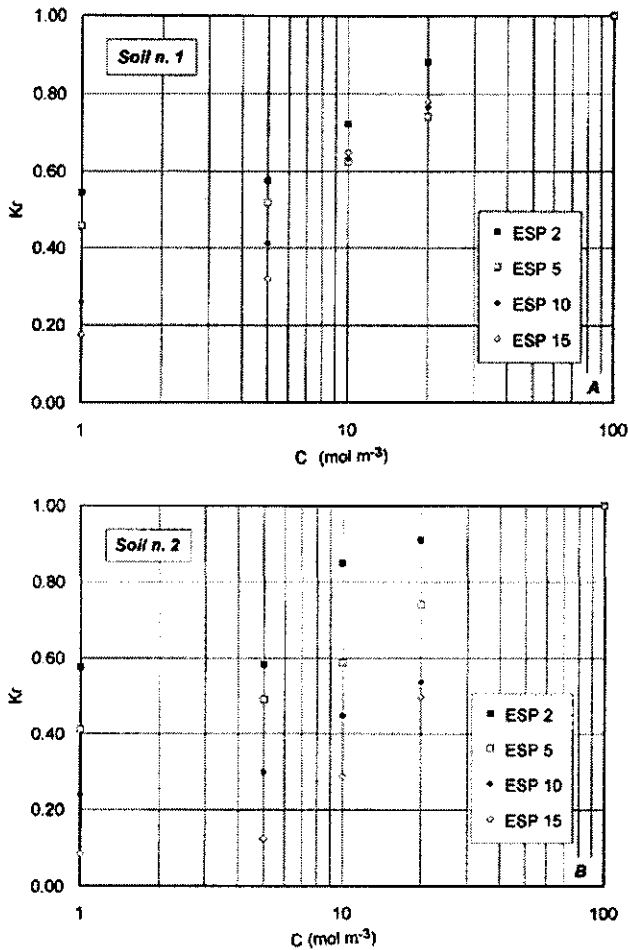
Figure 5. Relative hydraulic conductivity at saturation K_r vs. cationic concentration C (mol m^{-3}) at ESP = 2, 5, 10 and 15. The figure shows the decrease in K_r at increasing ESP and decreasing C: (A) soil n.1, (B) soil n.2.

The SI values as a function of ESP are represented in Figure 3. No critical ESP threshold is detectable in the figure, but a linear trend, indicating a continuous behaviour, is evident.

Table 3 reports the COLE values representing the average of the measurements obtained on the three clods considered; ANOVA showed that differences between the blocks were not significant, while differences between the treatments were.

The average shrinkage characteristic curves are represented in Figures 4 a, b for soil n.1 and n.2 respectively. As can be seen, the normal, residual and zero shrinkage phases are clearly distinguishable (Bronswijk and Evers-Veermer, 1990); the three phases have a similar trend except for the higher swelling limit of soil clods having ESP = 10.

Table 3 reports the ratio V_{wet}/V_{dry} together with the rating of shrink-swell potential based upon COLE values (Parker et al., 1977). Table 3 also reports the maximum potential values of crack volume calculated at the two ESPs considered; for both soils crack volume increases by about 10% when ESP increases from about 2, which represents the soil ESP in natural conditions, to 10. On a macroscopic level the potential occurrence of cracks may be significantly influenced by ESP.

With reference to the saturated hydraulic conductivity K_s, ANOVA showed that, at each combination of SAR and C, the differences between the blocks were not significant. In Figures 5 a, b, the average K_r is represented for each combination of ESP and C. The K_r values decrease at increasing ESP and at decreasing C (Shainberg et al., 1981). The differences between the treatments are significant at every C $(C<100 \text{ mol/m}^3)$ for soil n.2, while for soil n.1 they are significant only at the lowest C values $(C \leq 10 \text{ mol/m}^3)$.

Since a high cationic concentration counterbalances the deleterious effect of high ESP on hydraulic conductivity (Quirk and Schoefield, 1955), this result means that soil n.2 is more susceptible to ESP even at higher C concentrations.

Table 4. Saturated hydraulic conductivity K_s (cm hr^{-1}) measured at ESP = 2, 5, 10 and 15 and cationic concentration C=1 mol m^{-3}.

	Soil n.1	Soil n.2
ESP 2	0.0450 a[†]	0.0764 a
ESP 5	0.0378 a	0.0548 a
ESP 10	0.0214 b	0.0288 b
ESP 15	0.0145 b	0.0114 c

([†])   Row values followed by different letters are significantly different at the 0.05 probability level

In order to verify if any ESP threshold exists at C = 1, the K_s obtained at the different ESPs, whose values are reported in Table 4, are represented in Figure 6. As was already found for aggregate stability, an almost linear relationship between K_s and ESP is evident (So and Aylmore, 1993).

With reference to the one-step experiments, Figure 7 reports the $V(t_j)$ values obtained for soil n.1 at ESP = 2 and C = 100, and at ESP = 5, 10 and C = 1. ANOVA showed that the differences between the outflow volumes V at some t_j ($t_j > 1$ hr) measured on the three replicated soil samples at the same ESP and C (blocks) were not significant, while the differences between the $V(t_j)$ at the different ESP and C (treatments) were significant.

The estimated parameters α, n, θ_s, K_s and γ are reported in Table 5. No clear trend was observed in the α, n and γ values at increasing ESP and decreasing C, while an evident increase in θ_s with a simultaneous decrease in K_s, reflecting swelling and/or dispersion, was evident.
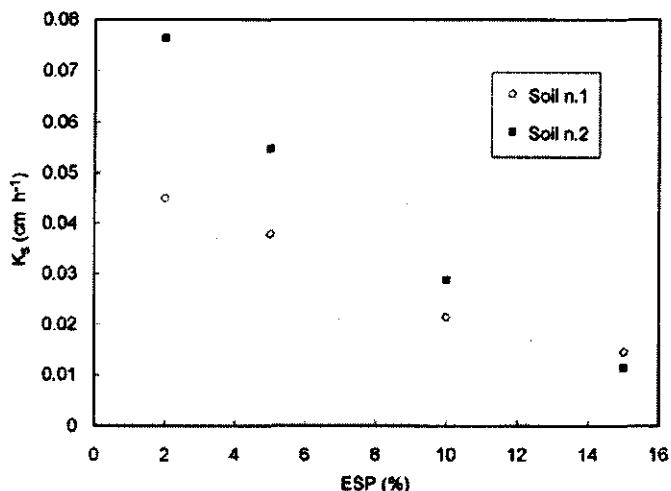
Figure 6. Saturated hydraulic conductivity K_s determined at C = 1 mol m^{-3} vs. ESP. The figure shows the decrease in K_s at increasing ESP; an almost linear trend indicating no critical ESP threshold is evident in the figure.

Figures 8 a, b illustrate the predicted hydraulic conductivity functions $K(\theta)$ for soil n.1 and n.2 respectively. The $K(\theta)$ values show decreases of about one order of magnitude when ESP increases from 2 to 5, and of about two orders of magnitude when ESP increases from 2 to 10. Similar reductions in unsaturated hydraulic conductivity have been previously published (Lima et al.,1990).

In order to compare the investigated soils with other soils in terms of their sensitivity to ESP, some reductions of 25% in K_S calculated at different ESP and C have been represented in Figure 9. Reductions of 25% in K_S are considered as a reference in order to evaluate soil susceptibility to the combined effects of Na and C (McNeal and Coleman, 1966; Cass and Sumner,1982), although the threshold concentration curve TC originally proposed by Quirk and Schoefield (1955) (Fig. 9) was determined by considering as critical the C value causing a 10-15 % decrease in K_S.

As can be seen, the presented values, which are consistent with previous results obtained on

a similar, montmorillonitic soil (McNeal and Coleman, 1966), show reductions of 25% at very low ESP (ESP=2) when C is lower than about 10 mol/m^3; this indicates a great susceptibility of the examined soils even at very low ESP.
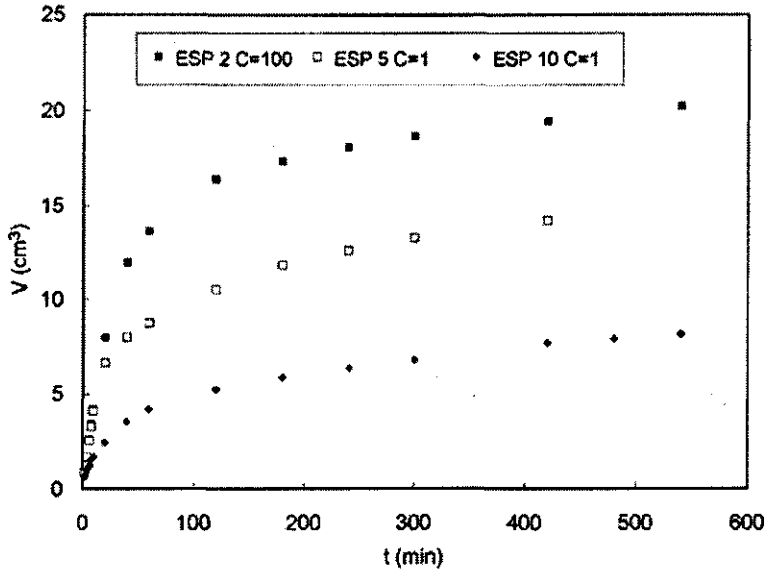

Figure 7. Cumulative outflow volume V vs. time t obtained for soil n. 1 from one-step experiments carried out on soil samples at ESP 2 and C = 100 mol m^{-3}, and at ESP = 5, 10 and C = 1 mol m^{-3}. The figure shows the decrease in $V(t_i)$ at increasing ESP.

In Figure 10 some reductions in K_S, expressed as ΔK ($\Delta K=1-K_r$) obtained from the data of Quirk and Schoefield (1955) at ESP=9 are represented as a function of C together with ΔK values obtained on our soils at ESP=10.

Table 5. The van Genuchten-Mualem parameters α, n, θ_s, K_s and γ obtained by the parameter estimation method within the indicated ranges of variability.

	α (cm^{-1})	n[†] (-)	θ_s[†] (cm^3 cm^{-3})	K_s (cm/hr)	γ[†] (-)
Soil n. 1					
ESP 2	0.0128	1.4764	0.62	0.953	1.50
ESP 5	0.0100	1.5100	0.65	0.380	1.50
ESP 10	0.0116	1.4636	0.66	0.011	0.88
Soil n. 2					
ESP 2	0.0212	1.5524	0.56	0.899	0.83
ESP 5	0.0197	1.4965	0.56	0.200	1.50
ESP 10	0.0150	1.6000	0.59	0.031	1.50

([†]) Ranges of variability: $0.01 \leq \alpha \leq 0.1$; $n>1.1$; $\theta_S-0.03 \leq \theta_s \leq \theta_S+0.03$; $0.5K_S \leq K_S \leq 2K_S$; $-0.5 \leq \gamma \leq 1.5$

Figure 10 shows the greater susceptibility of our soils compared to those investigated by Quirk and Shoefield; furthermore, the shape of the Quirk and Shoefield curve clearly shows a threshold behaviour, while a linear trend indicating a continuous behaviour is evident in our relationships in the C range explored.
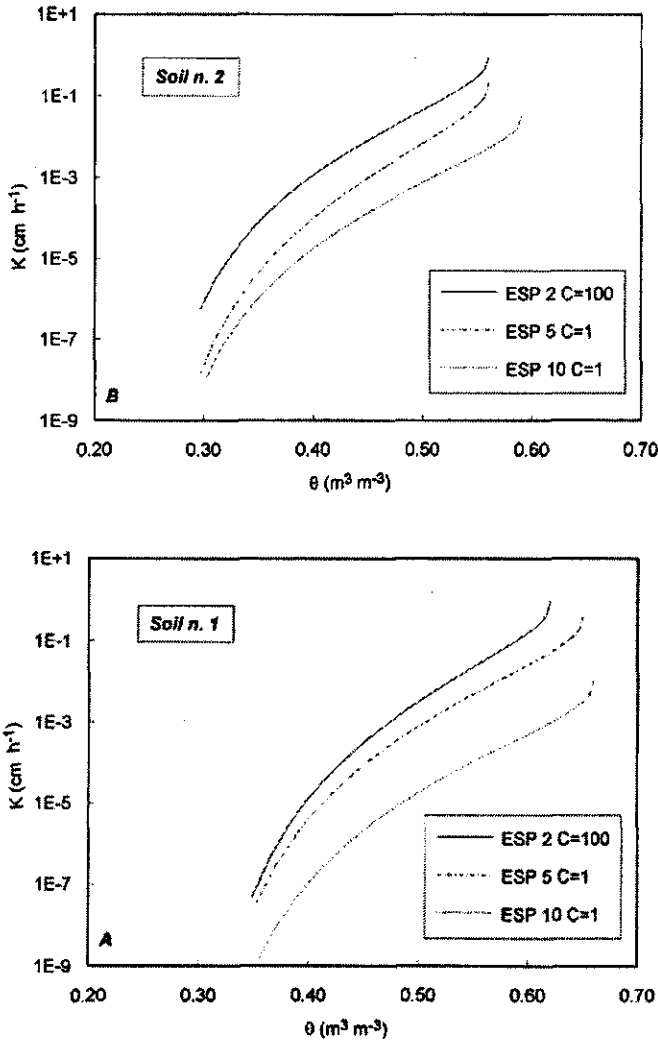

Figure 8.
Unsaturated hydraulic conductivity K vs. volumetric water content θ obtained by the parameter estimation method.
The van Genuchten-Mualem parameters used to draw the K(θ) functions at the different ESP and C are as reported in Table 5: (A) soil n.1, (B) soil n.2.

With reference to the interactions between structural and hydraulic characteristics, the results obtained appear consistent; in fact, for both soils at increasing ESP, aggregate stability decreases, susceptibility to cracks increases and both saturated K_S and unsaturated hydraulic conductivity K(θ) decrease. Reductions of about 25% in K_r take place at ESP= 2, while reductions of about 25% in SR take place at ESP = 5, and the maximum change in

crack volume is about 10% in ESP from 2 to 10. ESP evidently has a greater influence on
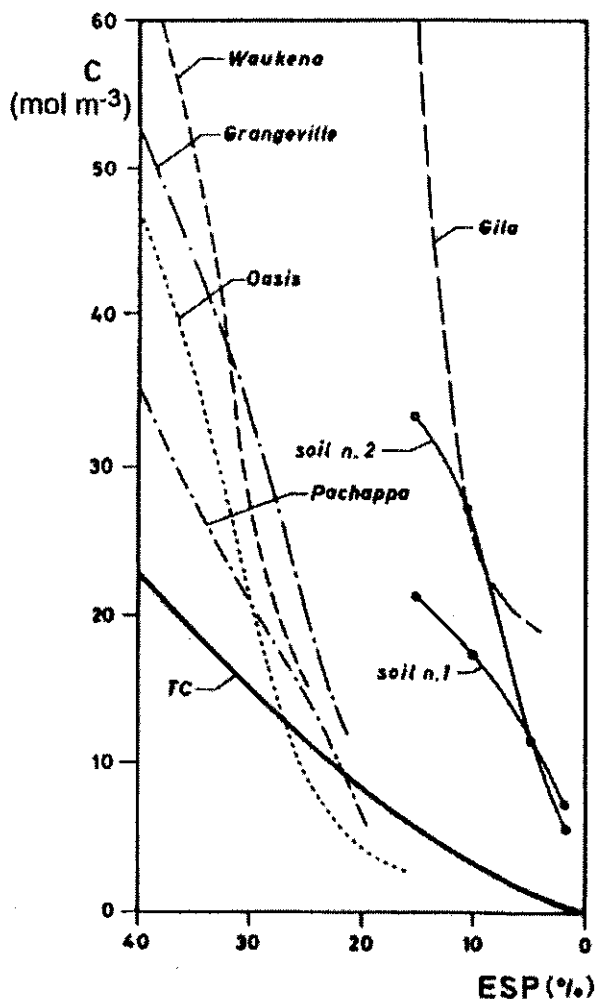

Figure 9
Combinations of cationic concentration C and ESP required to produce a 25% reduction in saturated hydraulic conductivity for selected soils (McNeal and Coleman, 1966). The threshold concentration curve TC (Quirk and Schoefield, 1955) is also represented.

hydraulic conductivity than on aggregate stability and susceptibility to shrinkage. This result may be explained in terms of the domain theory (Shainberg and Caiserman, 1971), according to which small increases in ESP result in dispersion of the aggregates into domains, which are small enough to be transported with water and block the larger pores, causing large reductions in hydraulic conductivity. Instead, it is only at very high ESP that macroscopic swelling takes place (So and Aylmore, 1993); this explains why aggregate stability and especially rating of shrinkage, which reflect swelling more than dispersion and pore occlusion, are less affected by ESP than hydraulic conductivity.

Conclusions

Our results show that no critical ESP threshold can be defined, since almost linear relationships between the investigated soil properties and ESP were found at a low cationic concentration.

Consistency has been observed among the different examined aspects, although a greater influence of ESP on hydraulic characteristics than on aggregate stability and susceptibility to swelling-shrinkage is evident. ESP values ranging from 2 to 5, associated with low C values, cause hydraulic conductivity to decrease by 25% or even more; similar reductions in aggregate stability occur at ESP ranging from 5 to 10, while rating of swelling-shrinkage appears less affected by ESP in the explored range.
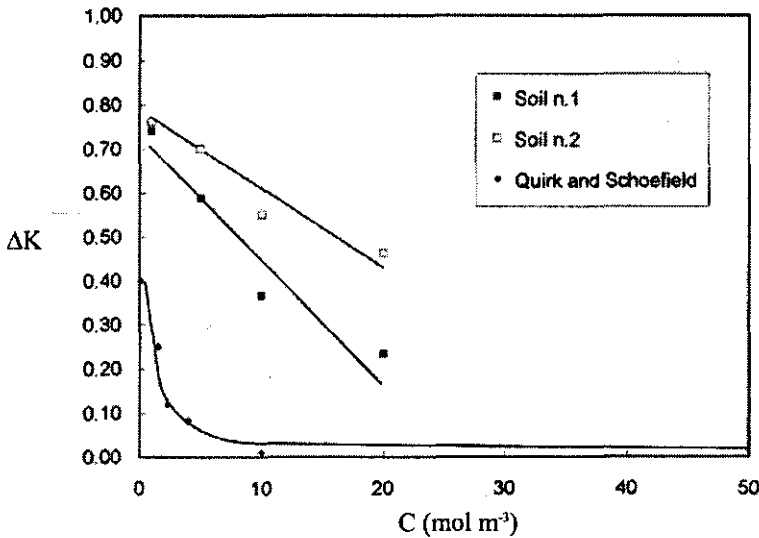

Figure 10. Reductions in saturated hydraulic conductivity ΔK ($\Delta K=1-K_r$) vs. cationic concentration C, calculated from the data of Quirk and Schoefield (1955) at ESP=9, and ΔK vs. C calculated for soils n.1 and n.2 at ESP=10. The figure shows the threshold behaviour of the Quirk and Schoefield curve compared to the almost linear trend of the ΔK, C relationships of soils n.1 and n.2.

These results show an effective hazard of soil quality degradation even at very low ESP levels when cationic concentration is low, providing a basic indication for irrigation management aimed to prevent and control deterioration of soil quality in the Sicilian environment.

Extension of similar investigations to some different soils may lead to the determination of quantitative relationships among the different aspects of soil behaviour, at different ESP values, to be used also for predictive purposes.

Chapter 5

Irrigation with saline/sodic waters in mediterranean regions: soil quality degradation and desertification

Irrigation with saline/sodic waters in mediterranean regions: soil quality degradation and desertification

G. Crescimanno
Università di Palermo, Dipartimento ITAF, Sezione Idraulica. Palermo, Italy

Abstract

This paper shows the relevent influence of changes in hydraulic characterictics due to salinity/sodicity on water flow in the soil-crop system. The paper also shows the possibility to use the LEACHM model to predict salinity and sodicity under field conditions, indicating the need for further investigation finalized to assess the relevance of bypass flow on water flow and solute transport under saline/sodic conditions.

Introduction

There is an increasing awareness of the importance of soil as a substantial part of the environment and irreplaceable basis for the production of food, fodder, and raw material. One of the main adverse effects of production on the environment is the salinization of waters and soils. Saline and sodic soils cover about 10% of the total arable lands and exist in over 100 countries, and although affecting mostly arid and semi-arid regions, are not limited to these regions; according to the estimates 10 million Ha of irrigated land are abandoned yearly as a consequence of the adverse effect of irrigation, mainly secondary salinization and sodication (Szabolcs, 1989).

Desertification has been defined as "degradation of land in arid, semi-arid and dry sub-humid areas resulting mainly from adverse human impact" (UNEP, 1991). Irrigation with saline/sodic waters, often consequence of intensive agricultural systems, is one of the main causes of groundwater salinization and reduced crop yield (Rhoades, 1989; Szabolcs, 1994).

Assessing the influence of salinity and sodicity on soil structural and hydraulic characteristics, which has been the subject of much research (Shainberg et al., 1981; Lima et al., 1990; Rengasamy, Olsson, 1991; Crescimanno and Iovino, 1995a), can help to prevent irreversible deterioration of soil quality and to find basic indication for irrigation management aimed to prevent and control extension of desertification (Crescimanno et al., 1995a).

Irrigation with saline-sodic waters is practiced in Sicily in many areas where these waters represent the only source of available water; clay soils with variably swelling/shrinking properties are widespread in these areas (Crescimanno and Provenzano, 1995). Great attention is focused in Sicily on the possible environmental adverse effects of irrigation such as secondary salinization and sodication (Crescimanno et al., 1995b; Baiamonte and Crescimanno, 1997).

The objectives of this paper are (i) to show the relevant influence that reductions in hydraulic conductivity due to increasing sodicity (ESP) play in water transport in the soil-

crop system and (ii) to show the possibility to use the LEACHM model (Wagenet and Hutson, 1992) for predicting the hazard of salinization/sodication due to irrigation with saline/sodic waters.

Materials and methods

A Typic Haploxerert belonging to a Sicilian area irrigated with saline-sodic waters was selected; Table 1 reports the main physico-chemical characteristics of the soil.

Table 1. Characteristics of the soil considered

Site	Delia
Classification (USDA, 1992)	Typic Haploxerert
Horizon	Ap (0-27 cm)
Sand (2÷0.02 mm)[%]	8
Silt (0.02÷0.002 mm) [%]	35
Clay (<0.002 mm) [%]	57
Texture (ISSS)	C
Clay Mineralogy [%]	
Kaolinite	34.2
Chlorite	11.1
Illite	43.3
Smectite	11.5
EC (1:5) [dS/m]	0.87
CEC [cmol/kg]	40.6
ESP [%]	2.11
Organic matter [%]	3.55

Six solutions of NaCl and $CaCl_2$ having fixed SAR (SAR=0, 10, 20) and values of concentration C equal to 300 and to 1 mol/m^3 respectively were used for the laboratory experiments. Undisturbed soil cores, sampled into cylinders having diameter equal to 8.5 cm and height equal to 5 cm, were leached with solutions having SAR=0, 10, 20 and cationic concentration C=300 in constant head permeameters; the total leaching volume was at least three times greater than the pore volume. When the electrical conductivity of the effluent reached a value equal to the one of the incoming solution, the solution having C=300 was substituted with the one having the same SAR and concentration C=1; the saturated hydraulic conductivity K_s was determined at this equilibrium condition. The final ESP values corresponding to SAR 0, 10 and 20 were approximately equal to 0, 5 and 10 respectively.

The parameter estimation method (Kool, et Al., 1987) was applied to determine the water retention curve $\theta(h)$ and the hydraulic conductivity function $K(\theta)$. Multi-step outflow experiments were performed in pressure cells by appying to the soil samples, previously equilibrated at the pneumatic potential of 1 kPa, the pneumatic potential values of 4, 7, and 80 kPa, and by performing the optimization on the outflow volumes $V(t_i)$ recorded during the three pressure steps supplemented with the three equilibrium $\theta(h_i)$ values (Crescimanno

and Iovino, 1995b). The $K(\theta)$ and $\theta(h)$ functions determined at ESP=0 and at ESP=10 were used as input in the LEACHW version of the LEACHM code in order to evaluate the influence of reductions in hydraulic characteristics caused by increasing ESP on soil water flow (Crescimanno and Iovino, 1995a).

The LEACHM model (Wagenet and Hutson, 1992) is a process-based numerical model of water and solute movement, plant uptake and chemical reactions in the unsaturated zone. It uses a one dimensional finite difference solution for the transient unsaturated flow equation together with the transient diffusive and convective solute transport equation. The model requires as input for the upper boundary condition the amount and rate of irrigation/precipitation and potential evapotranspiration, the chemical characteristics of irrigation water and the soil hydraulic characteristics. Possible lower boundary conditions include a fixed water table depth, a free-draining profile, zero water flux, or a lysimeter tank.

To evaluate possibility of using the LEACHM model to predict hazard of salinization/sodication, simulations were performed with the climatic data recorded from 26 July 1992 to 25 July 1994, with grape as a crop and with a freely draining profile as bottom boundary condition. A root depht of 0.60 m was assumed with a root distribution linearly decreasing at increasing depht. Initial equilibrium between soluble and exchangeable ions was assumed at the starting simulation date (26 July 1992). Table 2 reports the hydraulic parameters of the selected soil profile and Table 3 reports the amount of soluble and exchangeable ions determined in the soil profile at the starting date.

Table 2. The van Genuchten hydraulic parameters of the soil profile and the correspondent Campbell parameters.

| | van Genuchten | | | | | | Campbell | |
| | α | n | θ_s | θ_r | K_s | γ | a | B |
	cm^{-1}		$m^3 m^{-3}$	$m^3 m^{-3}$	$cm\ h^{-1}$		kPa	
Ap (0-30)	0.0258	1.2855	0.504	0.3	0.653	5.566	1.113	16.898
A1 (30-60)	0.0331	1.2144	0.518	0.3	0.911	3.181	1.01	19.001
A2 (60-100)	0.0124	1.1818	0.53	0.3	0.02	0.001	3.12	19.833

Table 3. Soluble and exchangeable ions at the starting simulation date.

| | Soluble ions | | | | | | | Exchangeable ions | | | |
| | Ca | Mg | Na | K | SO_4 | Cl | HCO_3 | Ca | Mg | Na | K |
	mmol l^{-1}							mmol kg^{-1}			
Ap (0-30)	0.77	0.36	5.14	0.14	3.28	0.86	0.13	196.00	12.50	8.60	4.40
A1 (30-60)	0.72	0.43	11.43	0.14	6.43	0.86	0.15	155.50	50.00	16.2	5.10

Results and discussion

Figure 1 illustrates the hydraulic conductivity K vs. water content θ as determined by the parameter estimation method at the different ESP values. The Figure shows the considerable decrease in K at fixed θ at ESP=10 compared to ESP=0.
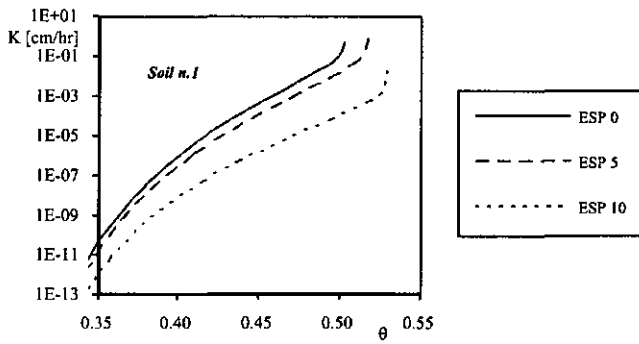
Figure 1. Hydraulic conductivity K vs. water content θ determined at the different ESPs.

Figure 2 (a, b, c and d) shows the effects of the decreased hydraulic conductivity $K(\theta)$ on water flow in the unsaturated zone. The considerable reductions in the predicted cumulative infiltration, evapotranspiration, and drainage obtained using the $K(\theta)$ and $\theta(h)$ functions determined at ESP=10 show the significant effects of high ESP and low C on water flow; the Figure shows that in a soil having ESP equal or greater than 10 water movement becomes extremely slow and as a consequence water available for crops sensibly decreases.
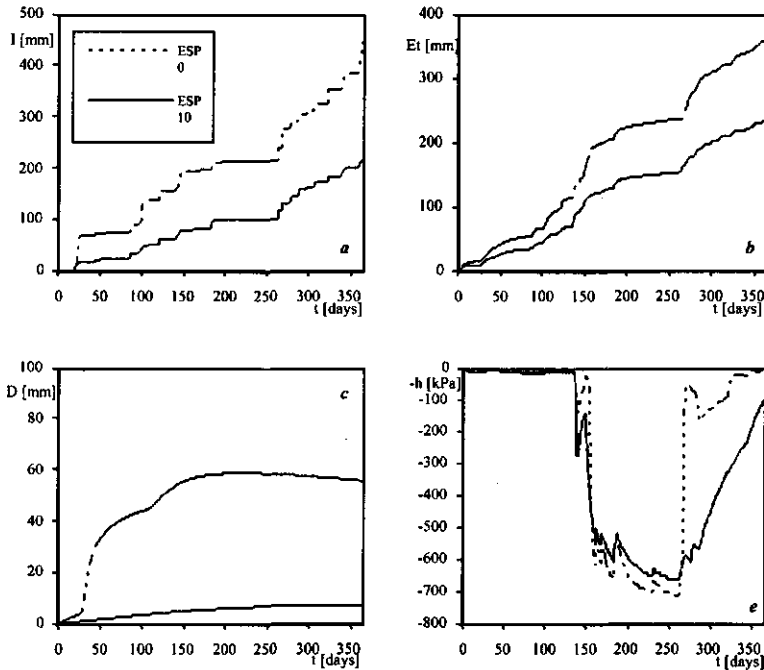
Figure 2. Cumulative infiltration (a), actual evapotranspiration (b), drainage (c) and matric potential (d) in the root zone predicted by LEACHW at ESP=0 and ESP=10

These results show the relevant role that the hydraulic characteristics play in water transport in the soil-plant system, indicating that great attention must be focused on management of soils irrigated with saline-sodic waters in order to find the techniques suitable to avoid irreversible changes in the hydraulic characteristics.

With reference to application of the LEACHM model for field prediction of salinity and sodicity, Figures 3 and 4 illustrate the average predicted electrical conductivity (EC) compared to that measured in the Ap and the A1 horizons.
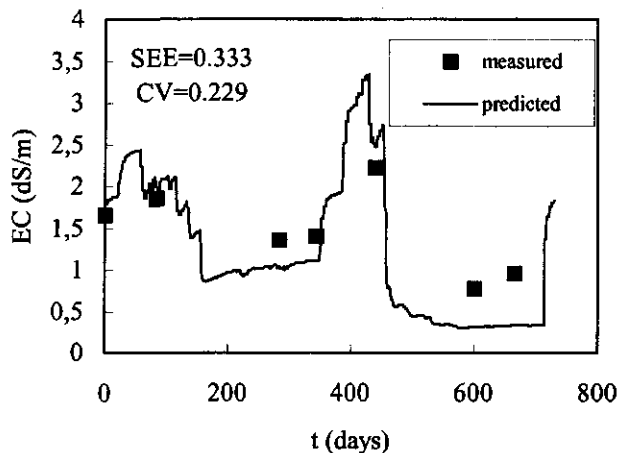
Figure 3. Measured and predicted electrical conductivity EC in the Ap horizon.
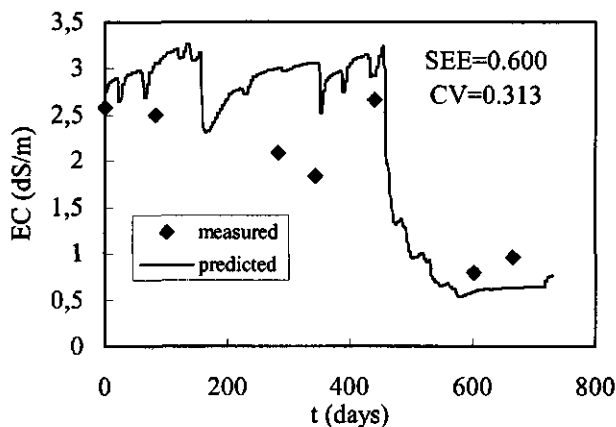

Figure 4. Measured and predicted electrical conductivity EC in the A1 horizon

In order to evaluate the predictive accuracy of the model, the standard error of estimate SEE and the coefficient of variation CV were calculated and are reported in the figures. According to the criterion for model acceptance set by the Predictive Exposure Assessement Workshop (Hedden, 1986), which recommends that a model should be able to replicate field data within a factor of 2 for site specific applications, the predictive accuracy is satisfactory for both horizons, although a best performance is evident for the Ap horizon.
The less satisfactory performance of the model in the A1 horizon could be attributed to the occurrence of bypass flow (Beven and German, 1982; Bouma, 1991) not accounted by the model. Tillage could have caused a lower heterogeneity and occurrence of preferential pathways in the Ap horizon than that existing in the untilled horizon (Yasuda et al., 1994). The considerable influence of bypass flow on the discrepancy between predicted and measured water content for a clay soil was also proved by Clemente et al. (1994).
With reference to prediction of ESP, Figures 5 and 6 illustrate the predicted and measured ESP for the Ap and A1 horizons.
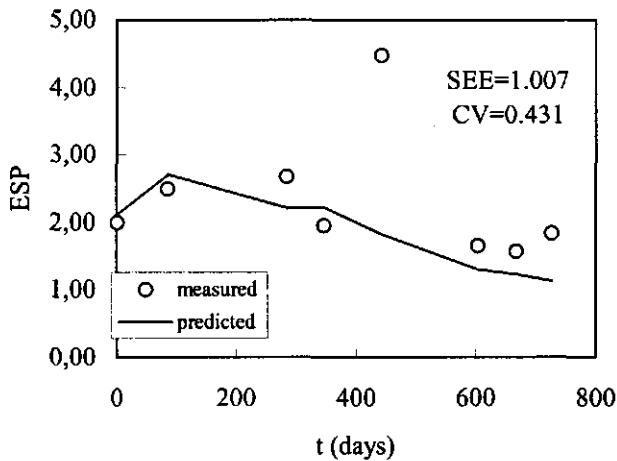

Fig. 5. Measured and predicted ESP in the Ap horizon

According to the criterion for model acceptance, the predictive accuracy of the model appears satisfactory, but a poor agreement between the trend observed in the predicted ESP and that observed in the measured ESP can be noticed.
This result questions the accuracy of the model to predict soil ESP. A possible explanation for the poor agreement between predicted and measured ESP could be the field occurrence of non equilibrium sorption processes that could adeguately be described only by models considering a wider range of sorption sites and physical heterogeneity (Hutson and Wagenet, 1995).
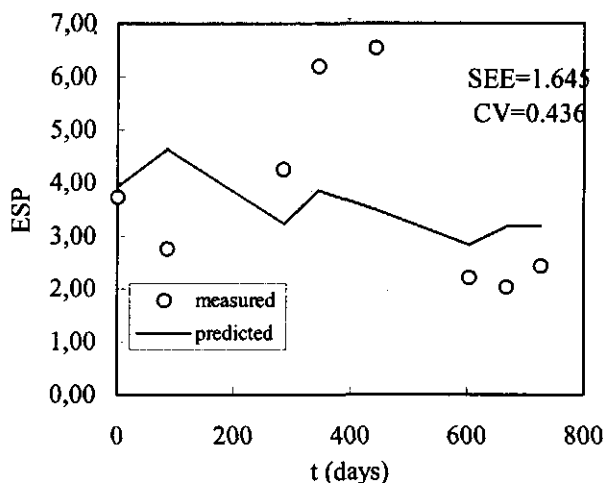
Figure 6. Measured and precticted ESP in the A1 horizon

Conclusions

This paper showed the fundamental role of hydraulic characteristics on water flow in the soil-crop system, proving the significant influence of salinity/sodicity conditions on water movement and crop transpiration. The paper also illustrated the possibility to use the LEACHM model to predict the hazard of salinization connected with use of saline/sodic waters, evidencing the need for improving the model performance with reference to prediction of ESP.

Model validation with a larger number of measurements and application to irrigated areas with different climate, soil, water composition, will be the object of further investigation. The possibility to test approaches accounting for bypass flow and non equilibrium soil and chemical processes represents a further objective to pursue in the attempt to obtain more accurate predictions in the saline-sodic environment.

Notation

C	cationic concentration (mol/m^3)
EC	electrical conductivity (dS/m)
CEC	cation exchange capacity (cmol/Kg)
D	cumulative drainage (mm)
ESP	exchangeable sodium percentage
Et	cumulative actual evapotranspiration (mm)
h	matric potential (kPa)
I	cumulative infiltration (mm)
K	unsaturated hydraulic conductivity (cm/hr)
K_s	saturated hydraulic conductivity (cm/hr)

n	parameter of the $\theta(h)$ equation
SAR	sodium adsorption ratio $(mol/m^3)^{1/2}$
V	cumulative outflow volume (cm^3/cm^2)
α	parameter of the $\theta(h)$ equation (cm^{-1})
γ	parameter of the $K(\theta)$ equation
θ_s	saturated water content (cm^3/cm^3)
θ	volumetric water content (cm^3/cm^3)
θ_r	residual water content (cm^3/cm^3)

Chapter 6

Hydrological processes affecting land degradation in the Mediterranean environment

Hydrological processes affecting land degradation in the Mediterranean environment

G. Crescimanno and G. Provenzano
Università di Palermo, Dipartimento ITAF, Sezione Idraulica. Palermo, Italy

Abstract

Swelling/shrinking clay soils change volume with changes in water content, and during dry periods extensive cracks will form in the field. Soil cracks alter the pore-size distribution through intermittent wetting, acting as significant pathways for water and salts and determining the occurrence of bypass flow.

Under climatic conditions such as those occurring in a Mediterranean region like Sicily, characterized by high values of the rainfall intensity, bypass flow may be a considerable percentage of the rainfall, representing a relevant term in the soil water balance. Occurrence of bypass flow reduces the amount of available water in the root zone, decreasing crop evapotranspiration, and enhancing the transport of water and/or solutes to the groundwater.

Results of this investigation proved that in cracking soils and in areas characterized by high values of the rainfall intensity, application of models not accounting for bypass flow may lead to a serious underestimation of the hazard of land degradation/desertification.

Key words: Desertification, Shrinkage, Bypass Flow.

Introduction

According to UNEP (1991), Desertification is "land degradation in arid, semi-arid and dry sub-humid areas resulting from climatic variations and human activities".

"Land degradation" involves the reduction of resources potential by one or various combined processes acting on soil. Combating desertification includes prevention (i) of land degradation, (ii) of deterioration of the physical, chemical and biological properties of the soil, (iii) of qualitative or quantitative degradation of aquifers.

Land degradation is a major problem in Mediterranean regions because of a combination of factors. These include the variability of climate, the nature of the soil and the land use.

Clay soils present hydrological and management problems different from those of non-swelling soils. Specifically, water content changes result in significant volume changes, and drying is associated with steep water content gradients and cracking.

The dynamic process of swelling and shrinkage in clay soils has significant practical consequences, such as the rapid transport of water and solutes via shrinkage-cracks to subsoil and to groundwater, i.e. the preferential flow, bypass flow or short-circuiting (Beven and Germann, 1982; Bouma, 1991).

The relevancy that the occurrence of bypass flow may have on water, solute or pesticide transport is becoming increasingly recognised (Ahuja et al., 1991; Steenhuis and Parlange, 1991). Bypass flow may determine water and nutrient shortage to crops (Belmans et al.,

1983) and/or pollution of the groundwater, e.g. when fertilisers or liquid manure are applied to a cracked clay soil (Dekker and Bouma, 1984).

In salt-affected soils, bypass flow may considerably affect the efficiency of salt-leaching during irrigation (Tanton et al., 1988), increasing the hazard of soil or groundwater contamination (Bouma and Dekker, 1978), and affecting water application uniformity and soil profile wetting (Van der Tak and Grismer, 1987).

The objective of this paper is to evaluate the impact that bypass flow may have on the hazard of land degradation in a Mediterranean region like Sicily, where the climatic conditions are characterized by a low amount of the total annual rainfall, by high values of the rainfall intensity, and by extremely high evapotranspiration rates during the dry season.

The investigation is performed by using a simulation model accounting for the occurrence of bypass flow (Oostindie and Bronswijk, 1992) in a Sicilian site where investigation aimed at preventing land degradation and desertification is underway (Crescimanno, 1998).

Materials and methods

A soil belonging to an area potentially affected by desertification was considered. Table 1 reports some physico-chemical characteristics of the soil.

Table 1 - Physico-chemical characteristics of the soil

Site	Delia
Soil Classification†	Typic Haploxerert
Horizon	Ap (0-27 cm)
Sand (2-0.02 mm), %	8
Silt (0.02-0.002 mm), %	35
Clay (<0.002 mm), %	57
Texture (ISSS)	C

† Soil Taxonomy (Soil Survey Staff, 1992)

The FLOCR model (Oostindie and Bronswijk, 1992) is based on the Richard equation, and considers the soil as divided into matrix and cracks. The soil shrinkage characteristic curve (SSCC) as a third function besides the water retentivity curve, $\Box(h)$, and the hydraulic conductivity function, $k(h)$, is required by the model to calculate the crack volume, and to partition the total infiltration (I) into matrix infiltration (I_m) and crack infiltration (I_{cr}), according to the following equations:

if $i<k_s$:

$$I_m = A_m\, i \qquad\qquad (1a)$$
$$I_{cr} = A_{cr}\, i \qquad\qquad (1b)$$

if $i> k_s$:

$$I_m = A_m\, k_s \qquad\qquad (2a)$$

$$I_{cr} = A_m (i - k_s) + A_{cr} i \qquad (2b)$$

in which i represents the rainfall intensity, k_s is the saturated hydraulic conductivity in the top layer, A_m and A_{cr} are the relative areas of the soil matrix and cracks, and I_{cr} is the amount of bypass flow (BF).

According to eqs. (1) and (2), the amount of water infiltrating into the cracks depends on the rainfall intensity, on the saturated hydraulic conductivity of the soil matrix (k_s) in the top layer and on the relative area of cracks. Most of the water flowing through the cracks accumulates at the bottom of the cracks. Horizontal infiltration into the crackwalls of the water rapidly running downwards along cracks is considered negligible (Hoogmoed and Bouma, 1980).

Water in the cracks and water in the matrix eventually reaches the groundwater; some of this water flows, via the subsoil, towards drains and ditches, and some will reach the aquifer.

The soil hydraulic characteristics used for the simulations, i.e. the $\theta(h)$ and the $k(\theta)$ functions, were determined by the parameter estimation method based on multi-step outflow experiments (Crescimanno and Iovino, 1995). The soil shrinkage characteristic curve (SSCC) was determined by measuring vertical and horizontal shrinkage in cylindrical soil cores (Crescimanno and Provenzano, 1999).

Simulations with FLOCR were performed using the climatic data recorded from 1/1/1992 to 31/12/1996, with the rainfall intensities as input data. A homogeneous soil profile having a depth of -300 cm, with a variable water table and absence of any drainage system, was considered.

In order to evaluate the influence of bypass flow on the hazard of land degradation, simulations were performed by considering the soil (1) as deformable (i.e. shrinkage and cracking) and (2) as undeformable (i.e. no shrinkage, no cracking).

Results and discussion

Figures 1 and 2 illustrate the soil hydraulic characteristics used for the simulations performed with the FLOCR model, i.e. the $\theta(h)$ and the $k(\theta)$ functions.

Figure 3 illustrates the soil shrinkage characteristic curve (SSCC), expressed as specific volume (v), which is the reciprocal of the bulk density (ρ), vs. the gravimetric water content (U). As can be seen in the figure, the soil shows a considerable susceptibility to shrinkage and cracking, with ρ values ranging from 1.31 g/cm^3 to 1.89 g/cm^3 in the U range between saturation and the oven-dry condition, and maximum cracking volumes equal to about 30% of the initial volume.

Figure 4 illustrates the course of rainfall intensity (i) and reference evapotranspiration (Eto) during the simulation period. The figure shows the considerable variability of i, which ranges from a minimum of 0.01 to a maximum of 10.6 cm/h, as well as the high values of the reference evapotranspiration, which were calculated using the Hargreaves formula (1983).

Figure 5 illustrates the cumulative frequency distribution of the rainfall intensity i, for the

considered years. The figure shows a probability ranging from 42% (in 1994) to 70% (in 1993) that i may exceed the saturated hydraulic conductivity k_s (k_s=0.172 cm/h), thus determining the occurrence of bypass flow.

Table 2 reports the results of the simulations performed for the years from 1992 to 1996 by considering the soil (1) as deformable (i.e. shrinkage and cracking) and (2) as undeformable (i.e. no shrinkage, no cracking).
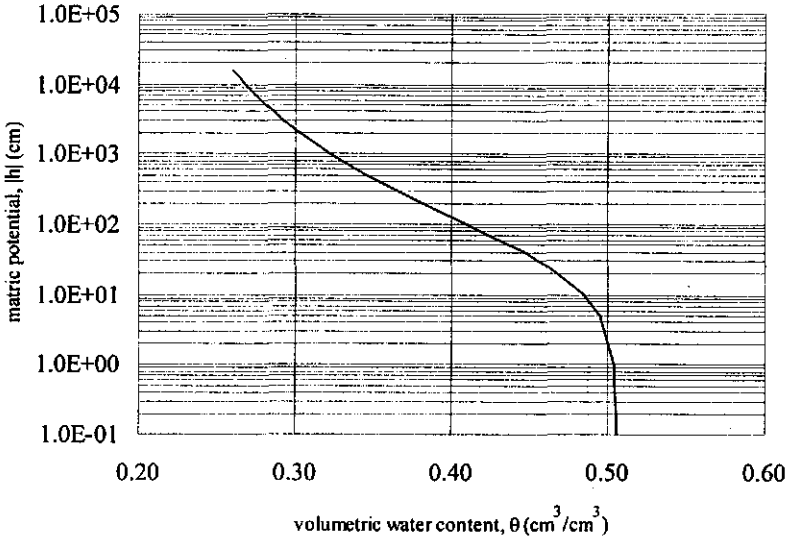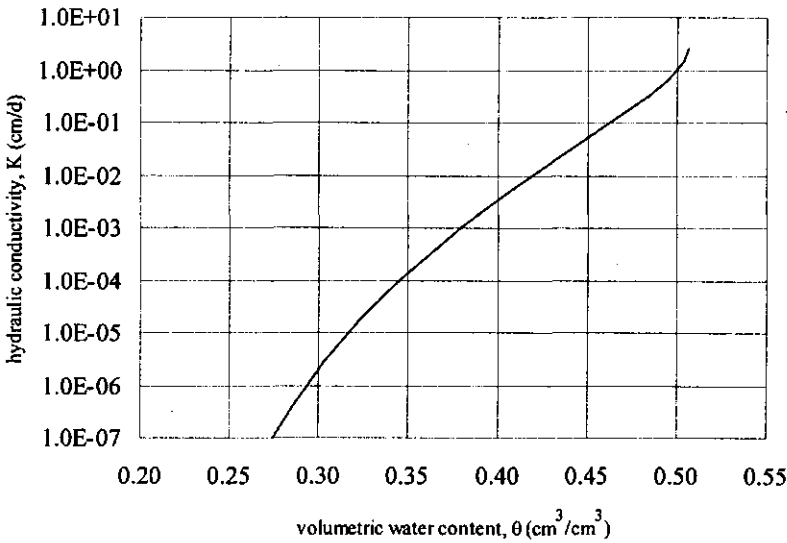

Fig. 1
Water retention curve
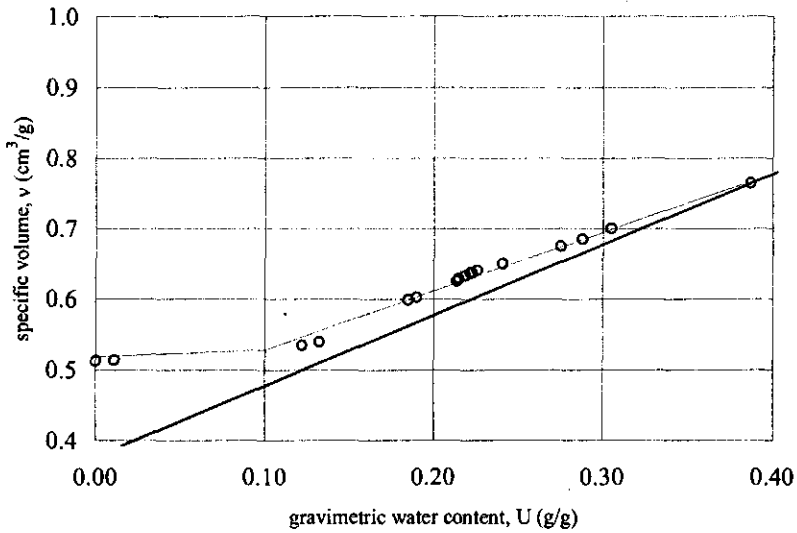

Fig. 2
Hydraulic conductivity curve

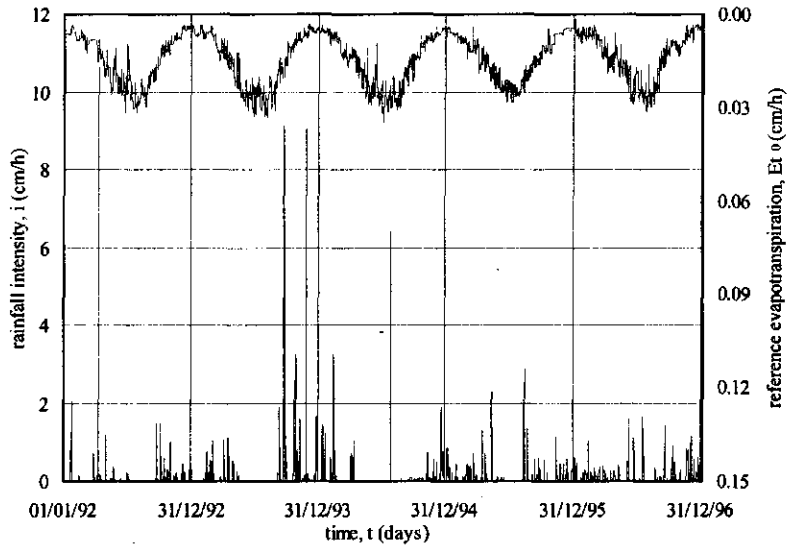**Fig. 3.** Soil shrinkage characteristic curve (SSCC)

Fig. 4. Rainfall intensity (i) and reference evapotranspiration (Eto) during the simulation period (1/1/92-31/12/96)
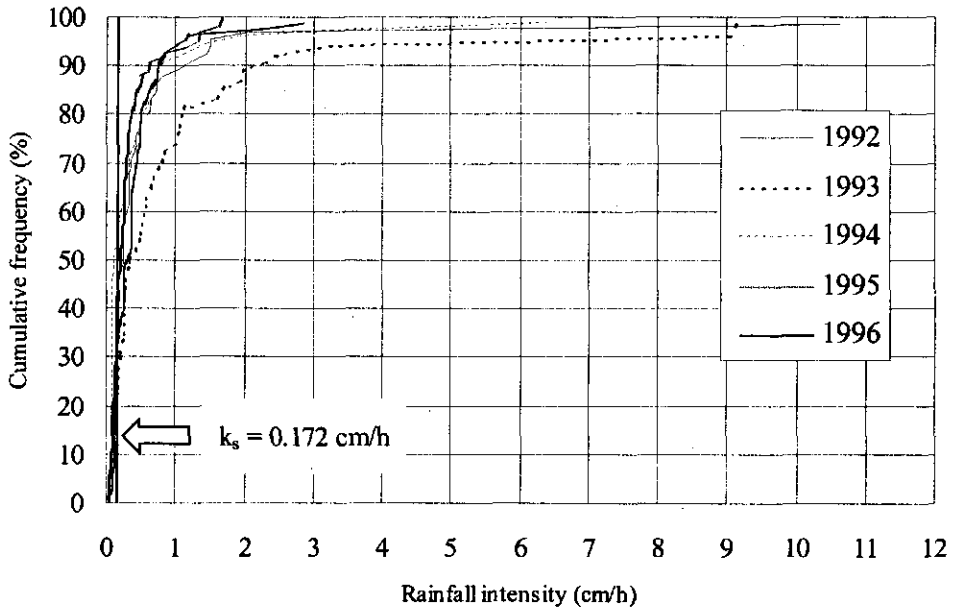
Fig. 5. Cumulative yearly frequency distribution of the rainfall intensity

Table 2. Yearly cumulative values of rainfall (R), reference evapotranspiration (Eto), actual evapotranspiration (Et), percolation flux (P_f), matrix infiltration (I_m), bypass flow (BF) and surface runoff (S_r)

year	R	Eto	Et		D	P_f		D	I_m		BF		S_r	
	(cm/yr)	(cm/yr)	(cm/yr)		(%)	(cm/yr)		(%)	(cm/yr)		(cm/yr)		(cm/yr)	
			(1)	(2)		(1)	(2)		(1)	(2)	(1)	(2)	(1)	(2)
1992	43.5	125.9	15.7	32.2	-104.5	30.3	20.5	32.4	11.3	38.9	32.2	0.0	0.0	4.5
1993	42.1	130.0	11.7	27.4	-133.6	25.1	15.4	38.6	11.5	41.8	30.7	0.0	0.0	0.3
1994	47.0	136.2	15.1	26.2	-72.9	27.5	15.9	42.3	13.8	44.1	33.2	0.0	0.0	2.9
1995	38.5	121.4	12.8	34.9	-172.2	23.7	6.0	74.7	11.3	38.5	27.2	0.0	0.0	0.0
1996	62.3	118.2	18.4	43.5	-136.3	39.9	15.1	62.2	17.7	62.1	44.6	0.0	0.0	0.2

(1) Deformable soil

(2) Undeformable soil

As can be seen in the Table, the water balance performed by accounting for shrinkage (1)

leads to cumulative yearly BF values ranging from 27.2 cm/yr to 44.6 cm/yr, which represent about the 70-74% of the cumulative yearly rainfall.

The Table also shows that the presence of cracks and bypass flow determines lower values of the actual evapotraspiration (Et), with differences ranging from 72.9 to 172% between the Et calculated by accounting for BF (1) and the Et calculated by considering the soil as undeformable (2). These considerable differences in the Et values depend on the fact that in the water balance part of the rainfall flows into the cracks rather than infiltrating into the soil matrix, and a lower amount of water remains available for crops compared to the amount of available water in the absence of cracks (2).

Analysis of Table 2 shows a larger amount of percolation water in the cracked soil compared to the case of undeformable soil, with differences ranging from 32.4% to 74.7% between the (1) and (2) percolation flux (P_f). This is the direct consequence of bypass flow, as the water infiltrating into the cracks rapidly reachs the groundwater, while in the case of underfomable soil a larger amount of water remains in the soil matrix.

These results show the relevancy that bypass flow may have on soil water balance when high rainfall intensities occur in clays soils with low values of the hydraulic conductivity and high susceptibility to shrinkage and cracking.

Comparison between the results of the (1) and (2) water balance shows that models not accounting for bypass flow may lead to a serious overprediction of crop evapotranspiration and to a serious underestimation of the hazard of land degradation and desertification.

The occurrence of bypass flow must be taken into account for selection of countermeasures leading to prevention of land degradation and desertification.

Chapter 7

The effect of alternating different water qualities on accumulation and leaching of solutes in a Mediterranean cracking soil

The effect of alternating different water qualities on accumulation and leaching of solutes in a Mediterranean cracking soil

G. Crescimanno[1], G. Provenzano[1] and H.W.G. Booltink[2]

[1] Università di Palermo, Dipartimento ITAF, Sezione Idraulica. Palermo, Italy
[2] Wageningen University, Laboratory of Soil Science and Geology, Wageningen, The Netherlands.

Abstract

The relevance of bypass flow on water flow, solute or pesticide transport is becoming increasingly recognized. Recent investigations proved that soil salinization may be influenced by bypass flow, i.e. the rapid transport of water and solutes via macropores and/or shrinkage-cracks to subsoil and groundwater.

This paper explored the role of bypass flow in the process of accumulation and leaching of solutes, as well as of Sodium, in a Mediterranean cracking soil irrigated with saline/sodic waters.

The results of bypass flow experiments performed on undisturbed soil cores showed that leaching of solutes occurred in concomitance with bypass fluxes when a low salinity solution was alternated to a high salinity solution. Exchange of solutes between the incoming solution and the soil matrix occurred during the bypass flow events at the contact surfaces (cracks' walls) between the solution and the soil matrix and where cracks terminated in the soil samples.

Concomitant exchanges of Sodium were indicated by measurements performed in the effluent solution during the bypass flow measurements. The amount of Sodium released from the soil during the bypass flow events, as well as that of the soluble salts leached from the soil, were found to depend on the degree of soil cracking.

These results indicated that (i) in management of irrigation in cracking soils, under the occurrence of bypass fluxes, alternating a low salinity/sodicity water to a high salinity/sodicity solution can be effective for preventing salinization and sodification, and that (ii) the higher efficiency of removal of Sodium/soluble salts can be obtained if application of the leaching solution is performed when the soil is at a considerable degree of cracking.

KEY WORDS: Cracking, Bypass flow, Salinization.

Introduction

The amount of water available for agriculture, and specifically for irrigation, is decreasing all over the world. In addition, the quality of irrigation water is decreasing.

Irrigation with saline/sodic waters, which is a current practice in many arid and semi-arid environments, carries a risk of soil degradation and desertification due to salinization and sodification (Szabolcs, 1992). If the internal drainage of the soil profile is inadequate to

drain salts brought by the irrigation water, a build-up of salts in the topsoil may occur due to the high evapotranspiration rates. If the quality of irrigation water is poor, this process is accelerated.

Clay soils change volume with changes in water content (Murray and Quirk, 1980), and during dry periods extensive cracks will form in the field (Bronswijk, 1989), which act as pathways for water and salts, determining the occurrence of bypass flow (Beven and Germann, 1982; Bouma, 1991).

The relevance of bypass flow on water flow, solute or pesticide transport is becoming increasingly recognized (Steenhuise and Parlange, 1991; Bouma, 1991; Oostindie and Bronswijk, 1995).

In structured soils, bypass flow is dominated by hydrological processes, such as rain intensity, initial conditions in the soil, surface storage of rain, and hydraulic conductivity of the soil matrix. Bypass flow occurs when, during a rain event, the rainfall intensity is higher than the infiltration capacity at the soil surface (Booltink and Bouma, 1991). Consequently, magnitude and intensity of bypass flow is controlled by external conditions, such as rainfall intensity, but also by internal conditions, e.g. soil texture and structure with different hydraulic characteristics (Jarvis and Leeds-Harrison, 1987).

Sodium (Na) in the exchange complex may negatively affect soil structure, causing swelling and/or dispersion of the clay particles, slaking of unstable aggregates and changes in the aggregate stability (Abu-Sharar et al., 1987).

Clay swelling and dispersion increase at high levels of the Exhangeable Sodium Percentage (ESP) and at decreasing cationic concentration (C) of the pore solution (Cass and Sumner, 1982).

Swelling and/or dispersion increase the soil susceptibility to cracking, causing concomitant decreases in the saturated and unsaturated hydraulic conductivity (Crescimanno et al., 1995). The enhanced susceptibility to cracking and the concomitant reduction in the hydraulic conductivity of the soil matrix may both concur to enhance soil cracking and bypass flow phenomena (Crescimanno and Provenzano, 1998a).

Conjunctive or alternated use of different quality irrigation waters can be a necessary practice to reduce salt-accumulation in the root zone through adequate leaching (Prendergast, 1995), and to keep the cationic concentration (C) of the pore solution at thresholds compatible with crops' tolerance (Maas, 1990).

However, in clay soils high velocity fluxes travelling through cracks may have less opportunity than slower moving water to leach salts from the root zone. In addition, the reduction in the soil hydraulic conductivity occurring at increasing ESP and at decreasing cationic concentration C (Cass and Sumner, 1982; Crescimanno et al., 1995) may contribute to decrease the degree of exchanges between the incoming solution and the soil matrix, reducing the efficiency of salt-leaching (Crescimanno and Provenzano, 1998b) and enhancing the hazard of salt-accumulation in the root zone.

Little work has been done to determine the extent at which bypass flow contributes to leaching of salts in the root zone (White, 1985). In order to simplify calculations of water loss below the root zone, some researchers assumed that bypass flow does not contribute to leaching (van der Molen, 1973; Thorburn and Rose, 1990). Yet in one field experiment on a

heavy clay soil, it was suggested that bypass flow provided the primary mechanism for leaching (McIntire et al., 1982a,b).

The objective of this paper is to investigate the role of bypass flow in the process of salt-accumulation and/or salt-leaching in a Mediterranean cracking soil where irrigation with saline-sodic waters is practised.

The specific objectives are to investigate (i) if the alternated application of high salinity and low salinity waters can be effective in reducing the hazard of salinization and/or sodification when bypass fluxes occur in a cracking soil and (ii) to explore the role of cracking in the process of solutes and Sodium release under the occurrence of bypass fluxes.

Materials and methods

Two undisturbed soil cores (200-mm diameter by 200-mm long) were sampled from the C1 horizon of a Sicilian field where investigation aimed at preventing land degradation is being conducted (Crescimanno, 1998).

The hydraulic conductivity of the soil matrix at saturation, K(sat), was determined by the suction crust infiltrometer method (Booltink et al., 1991). The van Genuchten-Mualem (1980) hydraulic parameters were determined by the parameter estimation method based on multi-step outflow experiments (Crescimanno and Baiamonte, 1999).

The soil shrinkage characteristic curve (SSCC) was determined by measuring vertical and horizontal shrinkage on confined soil cores (Crescimanno and Provenzano, 1999). Based on the water retentivity function ($\theta(h)$), and on the SSCC, the crack volume (ΔV_{cr}), as percentage of the soil volume at saturation (V), was calculated (Bronswijk, 1989) as a function of the matric potential (h).

In order to evaluate the soil susceptibility to cracking, the coefficient of linear extensibility, COLE, was calculated according to Grossman et al. (1968).

Two series of bypass flow measurements were performed. The first serie (S_1) was carried out through six consecutive sequences performed by alternating a solution of NaCl and CaCl$_2$, with electrical conductivity, EC, and sodium adsorption ratio, SAR, equal to that of the irrigation water (EC= 2 dS/m, SAR= 5 me$^{0.5}$/l$^{0.5}$), to distilled water (DW) (core n. 1).

The second serie (S_2) was carried out by alternating a solution of NaCl and CaCl$_2$, with same EC as that used in the S_1 and SAR=20 (SAR 20, EC 2), to distilled water (DW) (core n. 2).

Bypass flow measurements were performed by placing each soil core on a funnel connected to an outflow collector equipped with a pressure transducer. Two tensiometers were installed at -2 cm and -7 cm from the top of the samples. These tensiometers provided information on: (i) the initial pressure head in the soil; (ii) the time when water started to infiltrate in the macropores (top tensiometer) and (iii) the hydraulic conditions in the upper part of the soil column. All measurements were controlled by and stored in a computer. Figure 1 schematically shows the set-up used for the experiments (Booltink et al., 1993).

Rain showers with intensities (Ir) higher than the K(sat) measured on each soil and thus inducing bypass flow (Bouma, 1991) were applied on the top of the samples using a small rain simulator.

According to the K(sat) measured on each soil core, the Ir used during the S_1 serie was equal to 13.9 cm/h, and the Ir used during the S_2 was equal to 2.32 cm/h.

The applied water volume was constant in all the measurements and equal to 1400 cm³.

During the bypass flow measurements, the electrical conductivity (EC) of the outcoming solution was measured at fixed time intervals by a conductivimeter. During the S_2 serie, the Sodium (Na) was measured at the same time intervals by ion selective electrodes.
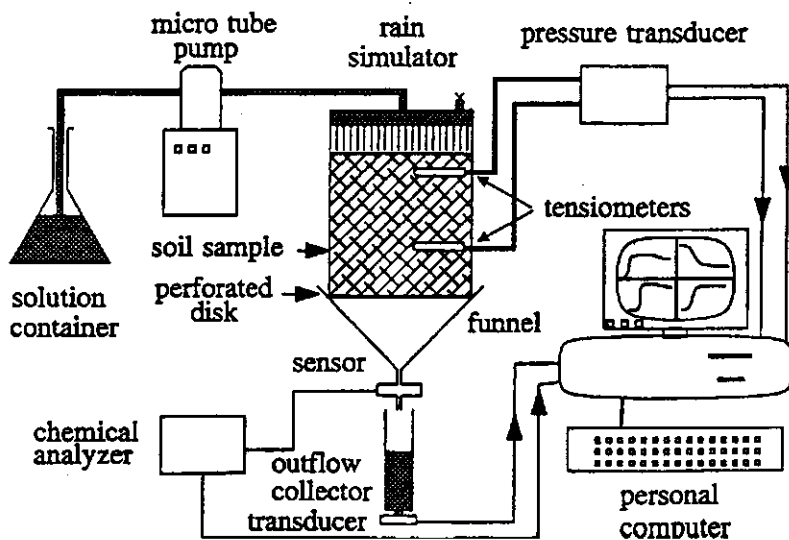

Figure 1. Schematic set-up of the device used for the bypass flow measurements (Booltink et al., 1993).

Results and discussion

Table 1 reports the textural information and the soil classification together with the K(sat) and the COLE values determined on the two soil cores. According to the classification proposed by Parker et al. (1977), the COLE values evidenced a high soil susceptibility to cracking.

116

Table 1. Classification and physical characteristics of the soil cores.

Site		Baglio	
Horizon	Ap (0-15 cm)	C1 (15-40 cm)	C2 (40-60 cm)
Sand (2-0.02 mm), %	36	44	44
Silt (0.02-0.002 mm), %	31	24	23
Clay (<0.002 mm), %	33	32	33
Texture (ISSS)	Clay loam	Clay	Clay
Classification †		Vertic Chromoxerert	
core n.1 K(sat) [cm/h]		2.67	
COLE*		0.105	
susceptibility to cracking**		high	
core n.2 K(sat) [cm/h]		0.51	
COLE*		0.099	
susceptibility to cracking**		high	

† Soil Taxonomy (Soil Survey Staff, 1992)

* Calculated between saturation and air-dry conditions

** Parker et al., 1977

Figure 2 illustrates the $\theta(h)$ function as well as the relationship between the crack volume $(\Delta V_{cr}/V)$, and the matric potential (h).
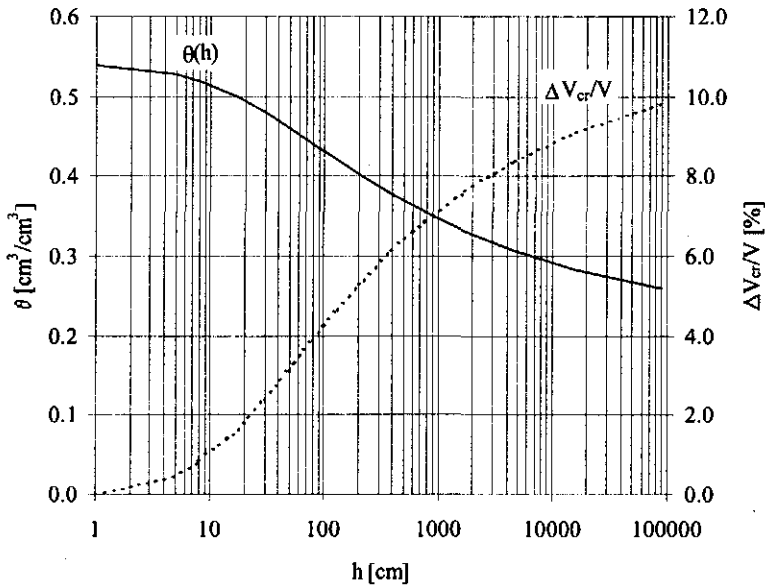

Figure 2. Retentivity curve $\theta(h)$ and relationship between the $\Delta V_{cr}/V$ and the matric potential (h).
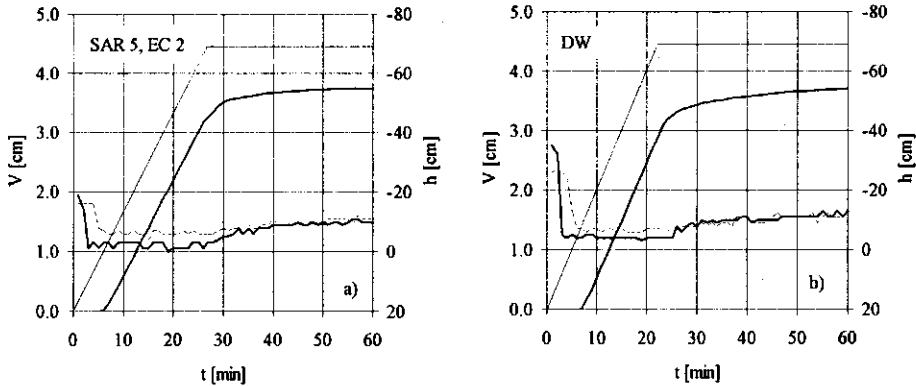
Figure 3 (a,b). Cumulative outflow vs. time during the
first sequence of bypass flow experiments (S_1 serie).

Figures 3a and 3b illustrate some results of the bypass flow measurements performed during the first sequence of the S_1 serie. The figures report the inflow and the outflow volume (V) as a function of the time (t), together with the matric potential, (h), recorded by the tensiometers during the measurements. The cumulative outflow curves determined during the six sequences of the S_1 serie all showed similar behaviour. After the time when outflow started, t_d, an exponential progression between the times t_d and t_{cs} (start of linear outflow) could be observed. Between t_{cs} and t_{ce} (end of linear outflow) there was a nearly linear outflow pattern, and after t_{ce} an exponential fade out pattern was evident. The linear outflow occurring between t_{cs} and t_e (i.e. the time derivative of outflow is constant) has been observed in earlier measurements (van Stiphout et al., 1987; Booltink et al., 1993).

Table 2 reports some parameters deduced from the inflow/outflow curves. The outflow rate during steady-state, Or, was almost equal to the application rate, Ir, indicating that water adsorption on the macropores/cracks walls was very low.

The Table also showed that in all the experiments the outflow from the core started after a certain time-lag from the start of water application. This time-lag is a function of internal catchment (storage of water in vertically non-continuous macropores) and of surface storage at the soil surface, which both depend on the initial matric potential (h_{in}).

Figure 4 illustrates the relationship between the total outflow, $V(t_e)$, which represents the bypass flow (Booltink et al., 1993), and the matric potential (h_{in}) at the start of each experiment, either for the SAR 5, EC 2 solution or for DW.

The figure shows that $V(t_e)$ decreases at decreasing h_{in} according to the amount of internal catchment and surface storage in the soil core, which both are larger when the soil is relatively dry at the beginning of the bypass flow measurements.

Being the $V(t_e)$ measured in the experiments performed with the saline solution comparable to that obtained by using distilled water, no effect of the water composition on the amount of bypass flow was evidenced by these measurements.

Figures 5a and 5b illustrate the cumulative outflow curves together with the EC of the effluent as measured during the first sequence of the S_1 serie.

Table 2. Relevant parameters deduced from the bypass flow experiments performed with the SAR 5, EC 2 solution and with distilled water (DW).

sequence	Applied solution	h_i [cm]	t_d [min]	t_{cs} [min]	t_e [min]	$V(t_{cs})$ [cm]	$V(t_e)$ [cm]	W_s [cm]	Or/Ir [-]
1	SAR 5, EC 2	-17.4	5.4	7.9	26.7	0.26	3.27	0.90	0.96
	DW	-30.2	6.6	8.0	22.2	0.16	2.90	1.33	0.96
2	SAR 5, EC 2	-18.9	5.2	8.5	21.8	0.34	3.18	1.05	0.99
	DW	-148.8	8.7	10.0	21.8	0.06	2.14	1.79	0.86
3	SAR 5, EC 2	-56.1	5.3	7.4	16.3	0.30	2.66	1.46	0.97
	DW	-23.9	4.8	6.0	17.0	0.16	2.94	1.26	0.96
4	SAR 5, EC 2	-40.8	5.6	6.5	17.0	0.12	2.83	1.47	0.98
	DW	-15.0	3.9	5.8	16.8	0.36	3.15	1.04	0.96
5	SAR 5, EC 2	-18.4	5.7	7.9	22.5	0.27	3.21	1.13	0.99
	DW	-14.5	3.8	5.6	18.3	0.21	3.31	0.93	0.99
6	SAR 5, EC 2	-120.7	6.8	8.6	-18.7	0.19	2.56	1.63	0.98
	DW	-18.4	4.2	5.2	17.5	0.17	3.17	1.06	0.96

h_i = Initial matric potential

t_d = Time-start of outflow

t_{cs} = Time-start of linear outflow

t_e = Time-stop of linear outflow

$V(t_{cs})$ = Cumulative outflow at the time t_{cs}

$V(t_e)$ = Cumulative outflow at the time t_e

W_s = Water stored in the soil

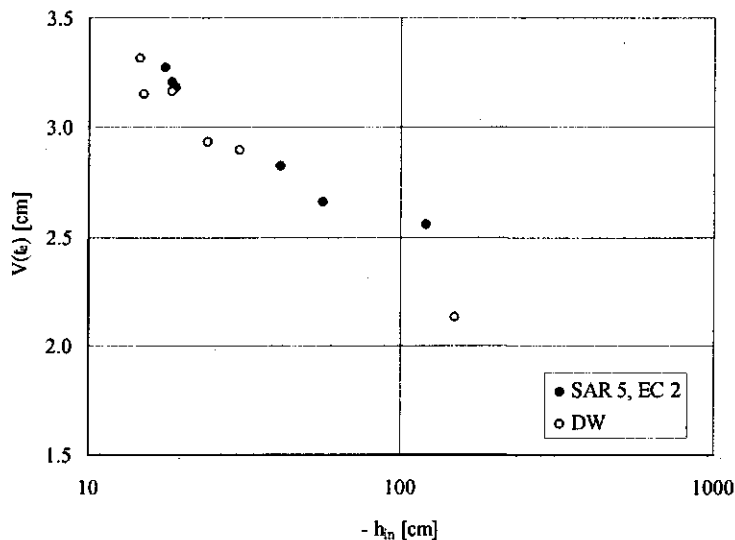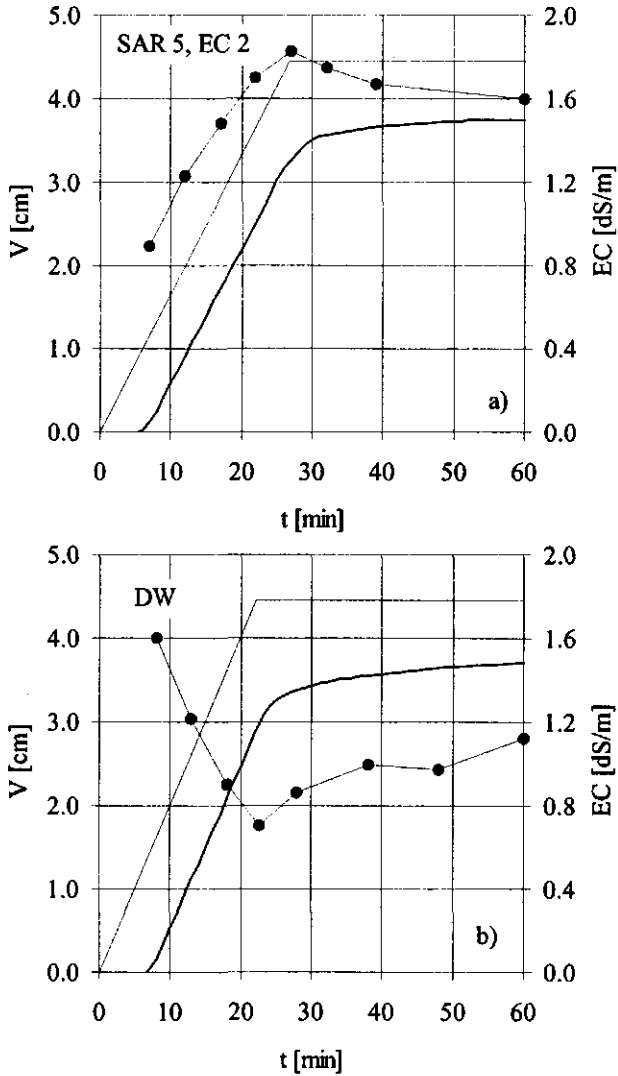Or/Ir = Ratio between outflow rate (Or) and inflow rate (Ir)

Figure 4. Total outflow, $V(t_e)$, vs. the matric potential (h_{in}) measured in the core before starting each experiment (S_1 serie).

119

Figure 5a, 5b. Cumulative outflow vs. time and EC of the effluent as measured during the experiments performed by alternating SAR 5, EC 2 and distilled water (DW).

The EC values show a maximum when water application stops (at the end of the linear outflow), and gradually decrease. The rapid increase in EC following water application, with the maximum occurring at the end of the linear outflow, is consequence of bypass flow of water and proves the occurrence of bypass flow of solutes. The subsequent

decrease in the EC after the end of water application (end of bypass flow) proves some release of solutes from the soil matrix.

In the experiments performed with DW, the measured EC shows the minimum at the end of bypass flow, increasing after water application has stopped. The rapid decrease in the EC following water application proves that leaching occurs in concomitance with bypass flow of water; the subsequent increase indicates that part of the solutes previously adsorbed by the soil matrix flow in the pore solution when bypass flow has terminated.
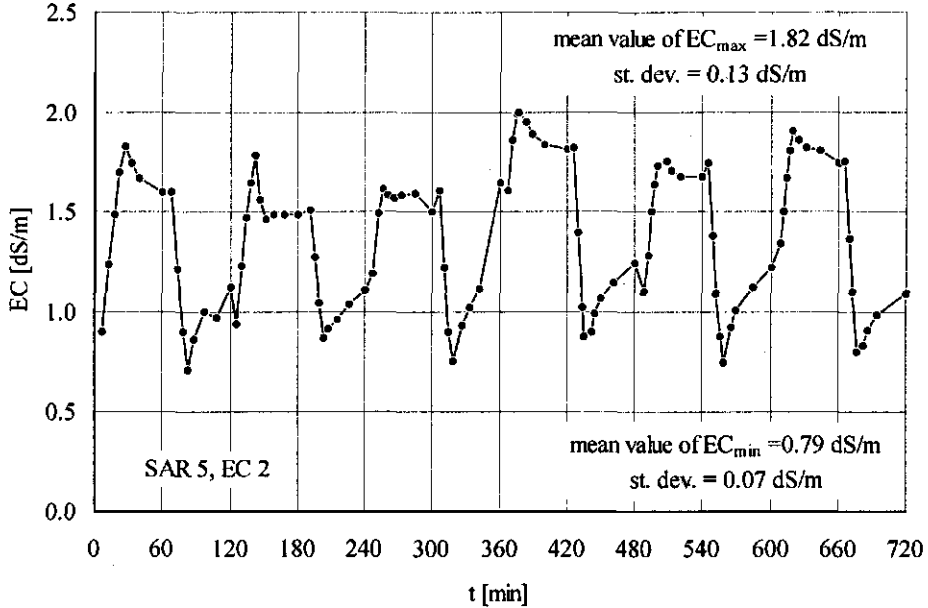

Figure 6. EC values measured in the effluent solution during the S_1 serie.

Figure 6 reports all the EC values measured in the effluent solution during the S_1 serie.

The figure shows that the EC values measured at the end of bypass flow (maximum ECs) in the experiments performed with SAR 5, EC 2, present a small variability around a value of 1.82 dS/m, with a tendency to reach the EC of the irrigation water.

The EC values measured at the end of bypass flow (minimum values of EC) in the experiments performed with DW (leaching process) present only a small variation around the value of 0.79 dS/m, which was the initial EC, as measured in the soil saturated extract.

This result indicates that application of DW alternated to the saline solution makes it possible to perform an efficient leaching of the applied solutes even in presence of water conducting macropores and/or cracks.

Although the ratio between the outflow rate (Or) and the inflow rate (Ir) during bypass flow was very close to 1, indicating very little adsorption of water at the contact surfaces between macropores and solution, dispersion and diffusion of solutes at the contact surfaces

between the macropores/cracks and the incoming solution must have occurred during bypass flow (Dekker and Bouma, 1984; Booltink et al., 1993).

This is in agreement with previous results indicating that bypass flow can contribute to leaching of nitrates (Dekker and Bouma, 1984; Booltink et al., 1993) and of solutes under field conditions (McIntire et al., 1982a,b; Prendergast, 1995).

With reference to the S_2 serie, the cumulative outflow curves, some of which are represented in Figures 7a and 7b, showed a behaviour similar to that observed during the S_1 serie.
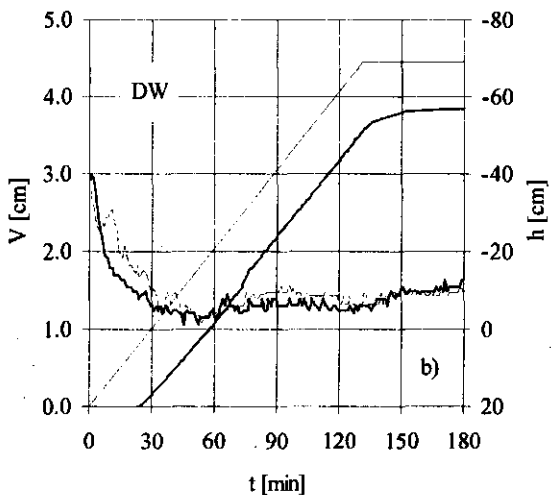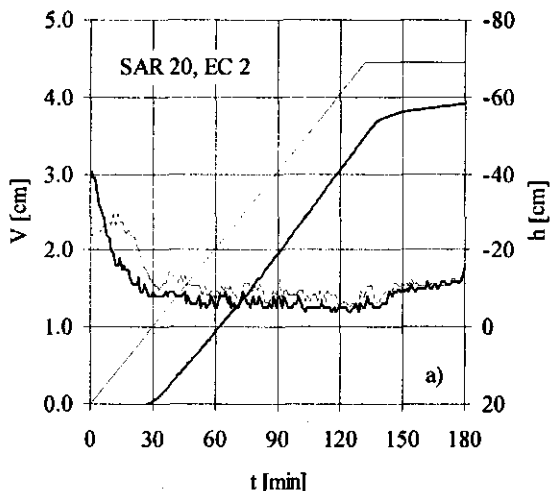

Figure 7 (a,b).
Cumulative outflow vs. time during the second sequence of bypass flow experiments (S_2 serie).

Table 3. Relevant parameters deduced from the bypass flow experiments performed with the SAR 5, EC 2 solution and with distilled water (DW).

sequence	Applied solution	h_i [cm]	t_d [min]	t_{cs} [min]	t_e [min]	$V(t_{cs})$ [cm]	$V(t_e)$ [cm]	W_s [cm]	Or/Ir [-]
1	SAR20, EC 2	-30.9	26.4	35.5	133.2	0.17	3.62	0.93	1.00
	DW	-37.5	23.2	29.0	128.5	0.13	3.46	0.79	0.99
2	SAR20, EC 2	-56.4	19.0	30.8	118.3	0.31	3.48	0.72	0.96
	DW	-146.0	24.9	37.2	117.7	0.27	3.06	0.91	0.94
3	SAR20, EC 2	-83.5	17.9	26.0	108.9	0.19	3.41	0.71	0.98
	DW	-63.5	24.8	32.0	110.6	0.32	3.42	0.97	1.00
4	SAR20, EC 2	-29.0	12.2	81.1	121.2	2.01	3.63	0.51	0.97
	DW	-278.5	26.9	62.0	111.0	1.04	2.94	1.08	0.97
5	SAR20, EC 2	-95.4	21.9	35.1	111.6	0.33	3.19	0.85	0.96
	DW	-222.3	25.5	43.6	113.7	0.42	3.04	0.96	0.99
6	SAR20, EC 2	-391.2	26.7	51.3	110.6	0.70	2.82	1.08	0.89
	DW	-437.6	26.4	37.4	102.1	0.28	2.81	1.15	0.90

h_i = Initial matric potential

t_d = Time-start of outflow

t_{cs} = Time-start of linear outflow

t_e = Time-stop of linear outflow

$V(t_{cs})$ = Cumulative outflow at the time t_{cs}

$V(t_e)$ = Cumulative outflow at the time t_e

W_s = Water stored in the soil

Or/Ir = Ratio between outflow rate (Or) and inflow rate (Ir)

Table 3 reports parameters deduced from the inflow/outflow curves. The outflow rate during steady-state, Or, was almost equal to the application rate, Ir, confirming that during the bypass flow measurements, adsorption on the macropores/cracks walls was very low.
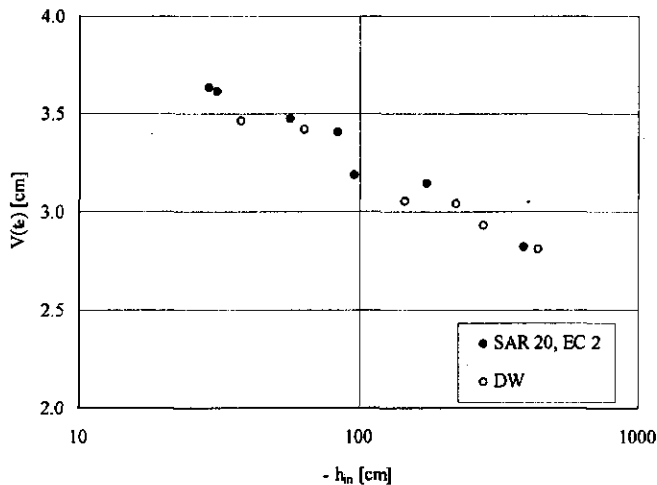

Figure 8.
Total outflow, $V(t_e)$ vs. the matric potential (h_{in}) measured in the core before starting each experiment (S_2).

Figures 8 reports the bypass flow, $V(t_e)$, vs. the matric potential (h_{in}) measured at the start of each experiment for the S_2 serie. The figure confirms the existence of a unique relationship between $V(t_e)$ and h_{in} which is independent from the chemical composition of the applied solution.

Figure 9 illustrates the EC values measured in the effluent solution during the S_2 serie. These EC values showed a behaviour similar to that observed during S_1, with the maximum ECs presenting a small variability around a value of 1.94 dS/m, which is very close to the EC of the incoming solution.
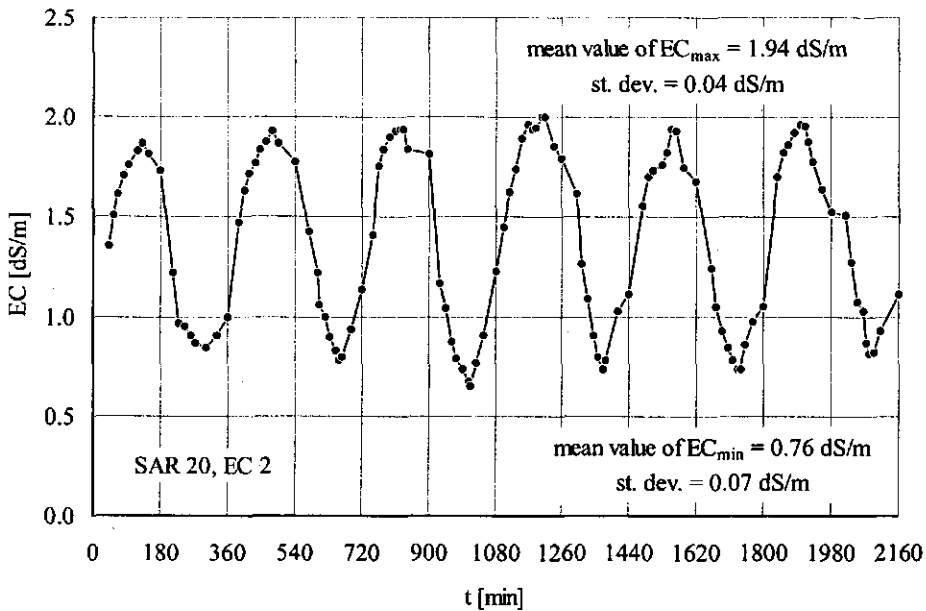

Figure 9. EC values measured in the effluent solution during the S_2 serie.

The EC values measured at the end of bypass flow (minimum EC values) in the experiments performed with DW presented only a small variation around the value of 0.76 dS/m, which was the initial EC value measured in the saturated soil extract.

These results confirm that the alternated use of DW to the SAR 20, EC 2 solution is effective to prevent accumulation of salts in the soil matrix, and indicate that leaching of solutes occurs under bypass flow conditions as a consequence of exchanges occurring at the contact surfaces between the macropores walls and the incoming solution, with subsequent dispersion and diffusion (Hillel, 1980).

With reference to the influence of bypass flow on the process of Sodium exchange, Figure 10 illustrates the values of the Sodium (Na) concentration measured in the effluent solution measured at the same time intervals at which the ECs were determined.

Being the crack volume ($\Delta V_{cr}/V$) dependent on the soil matric potential (h), according to the relationship reported in Figure 2, concentration of the outcoming Na could depend on

the matric potential (h_{in}) measured in the soil before application of DW, which is expressive of the degree of cracking at the time starting of bypass flow.
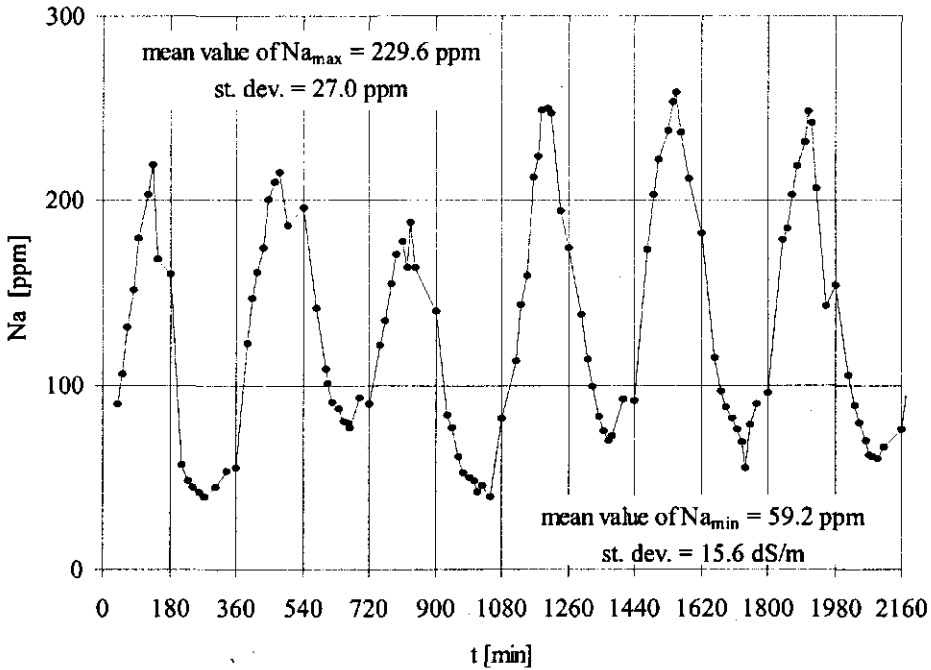

Figure 10. Na values measured in the effluent solution during the S_2 serie.

Figure 11 illustrates the relationship between the concentration (ppm) of the outcoming Sodium (Na1), recorded at the initial stage of each bypass flow event occurring under application of DW, and the initial matric potential measured in the soil core (h_{in}). Na1 represents the amount of Na released from the soil at the maximum degree of soil cracking.
As can be seen in the Figure, the Na1 concentration shows some dependency on h_{in}. A threshold behaviour can be observed, with Na1 increasing at decreasing h_{in} in the range – 30cm<h_{in}<-150 cm, showing no variability in the range -150 cm<h_{in}<- 437 cm.
A possible explanation for this threshold behaviour could be in the fact that according to the relationship illustrated in Figure 2, the crack volume (ΔV_{cr} /V) ranges between 2.4 and 4.9 (%) in the range –30cm<h_{in}<-150 cm, while only a variation from 4.9 to 6.2 (%) in ΔV_{cr} /V occurs in the range -150 cm<h_{in}<- 440 cm.
Figure 12 illustrates the relationship between the Na1 concentration and the crack volume (ΔV_{cr}/V). The figure confirms the previously observed threshold behaviour, showing the dependency of the released Sodium on the degree of soil cracking at the moment of water application.
Being the contact surfaces between the soil and the incoming solution increasing at increasing ΔV_{cr}/V, these results mean that the mechanism of Sodium release during the

125

bypass flow events depends on the magnitude of the contact surfaces between the crack walls and the incoming solution.

Figure 11.
Relationship between the Sodium concentration (Na1) measured in the effluent solution at the initial stage of bypass flow, and the matric potential (h_{in}) measured before application of DW.

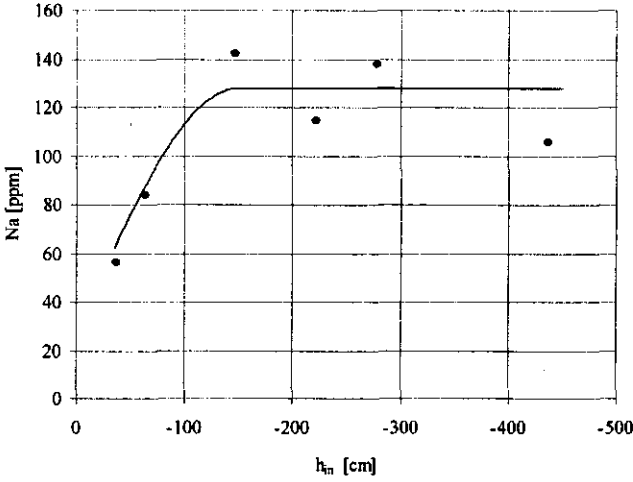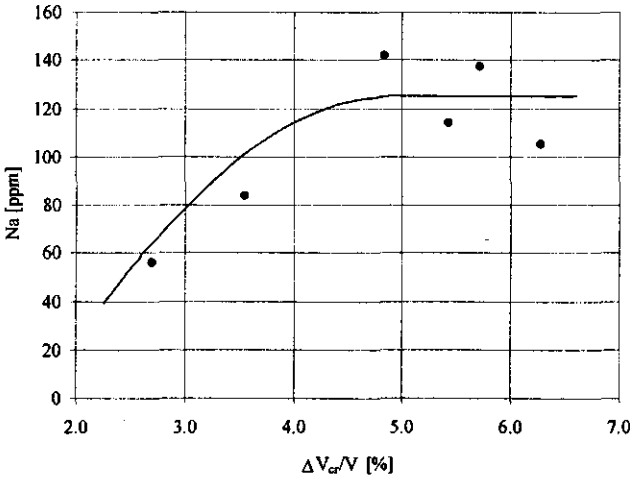**Figure 12.**
Relationship between the Sodium concentration (Na1) measured in the effluent solution at the initial stage of bypass flow, and the initial crack volume ($\Delta V_{cr}/V$).
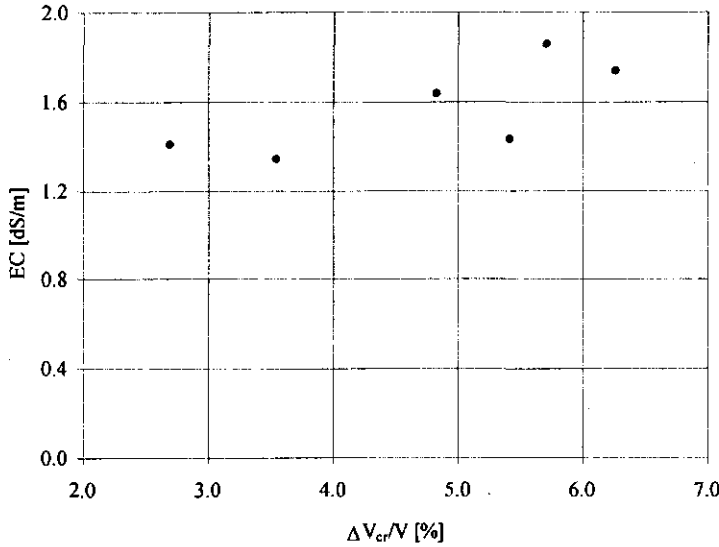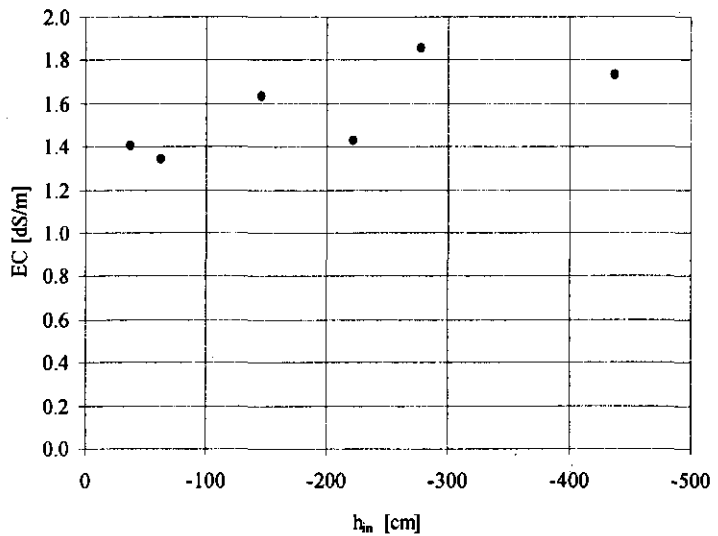
Figure 13. Relationship between the electrical conductivity (EC1) measured in the effluent solution at the initial stage of bypass flow, and the matric potential (h_{in}) measured before application of DW.

Figure 14. Relationship between the electrical conductivity (EC1) measured in the effluent solution at the initial stage of bypass flow, and the crack volume ($\Delta V_{cr}/V$) before application of DW.

Concerning the role of the macropores/cracks in the mechanism of leaching of the soluble salts, Figure 13 illustrates the relationship between the EC (called EC1) (dS/m) of the effluent solution, recorded at the initial stage of each bypass flow event occurring under application of DW, and the initial matric potential (h_{in}). EC1 indirectly represents the amount of soluble salts leached from the soil at the maximum degree of soil cracking.

As can be seen in the Figure, EC1 shows a certain dependency on the initial matric potential within the h_{in} range where the dependency of Na on h_{in} was observed..

127

Figure 14 illustrates the EC1 values as a function of $\Delta V_{cr}/V$. Analysis of Figures 12 and 14 evidences the stronger dependency of Na on $\Delta V_{cr}/V$ compared to that of EC on $\Delta V_{cr}/V$. A difference of about 217% in Na1 occurs in the $\Delta V_{cr}/V$ range between 2.2 and 4.9%, while in the same $\Delta V_{cr}/V$ range a variation of about 30% only in EC1 is found.

These results give new insight on the mechanism of exchange of solutes and of Sodium under bypass flow conditions, indicating the relevant role of cracking on the process of exchange of solutes and expecially of Sodium.

Conclusions

Bypass flow measurements performed in a Mediterranean cracking soil under alternated use of a high salinity solution to distilled water showed that exchange of solutes occurred at the contact surfaces between the macropores/cracks walls and the incoming solution in concomitance with bypass fluxes.

As a consequence of these exchanges, indicating dispersion and diffusion of the solutes during bypass flow, alternating a low salinity waters to a high salinity solution was effective in determining leaching of the applied solutes and in preventing salt-accumulation.

The experiments performed also indicated that the mechanism of release of Sodium, as well as of soluble salts, during the bypass flow measurements performed using distilled water, depended on the magnitude of the soil crack volume, which is expressive of the magnitude of the contact areas between the cracks and the incoming solution.

These results indicated that in management of irrigation in cracking soils, under the occurrence of bypass fluxes, alternating a low salinity/sodicity water to a high salinity/sodicity solution can be effective for preventing both salinization and sodification. In addition, the investigation showed that the higher efficiency of solutes/Sodium removal can be obtained if application of the leaching solution is performed when the soil is at a considerable degree of cracking.

Extension of bypass flow measurements using solutions of different composition under different degree of initial cracking could make it possible to generalize the presented results through derivation of (pedotransfer)-functions predicting the amount of Sodium and/or of soluble salts adsorbed or removed from the soil when bypass fluxes occur. These equations could be linked to models predicting the hydrological behaviour of cracking soils, allowing a generalization of the results obtained and illustrated in this paper.

Chapter 8

Effect of irrigation on soil structure and bypass flow phenomena in a Mediterranean cracking soil

Effect of irrigation on soil structure and bypass flow phenomena in a Mediterranean cracking soil

G. Crescimanno[1], G. Provenzano[1] , A. De Santis[1] and H.W.G. Booltink[2]

[1] Università di Palermo, Dipartimento ITAF, Sezione Idraulica. Palermo, Italy
[2] Wageningen University, Laboratory of Soil Science and Geology, Wageningen, The Netherlands.

Abstract

Water flow and solute transport in cracking soils may be affected by the presence of macropores and/or cracks, determining the occurrence of bypass flow.

The objective of this paper was to investigate the influence of two different irrigation systems, i.e. drip and micro-sprinkler, on soil structure and bypass flow phenomena in a Mediterranean cracking soil irrigated with saline/sodic waters.

Field application of methylene blue showed the presence of cracks terminating at a depth ranging between 5 and 10 cm from the soil surface in the micro-sprinkler irrigated field. Instead, cracks penetrating up to depths of 20-25 cm from the soil surface were found in the field where the drip system was in use.

In agreement with the observed vertical distribution of cracks in the two fields, no bypass flow was measured in laboratory in cylindrical soil cores (20 cm diameter, 20 cm height) taken from the irrigated micro-sprinkler field. Instead, high rates and amounts of bypass flow were measured in the cores taken from the drip irrigated field.

The higher intensity and the non-point water application involved in the micro-sprinkler irrigation system were responsible for the different depth of penetration of the macropores/cracks in the two fields and for the subsequent different flow behaviour observed in the undisturbed soil cores.

Dispersion of the clay particles, detachment of these particles from the surface and their movement into the cracks were the mechanisms responsible for the partial or total occlusion of some (macro) pores in the micro-sprinkler irrigated field.

Key words: Bypass flow, Soil structure, Drip irrigation, Micro-sprinkler irrigation

Introduction

Desertification is "land degradation in arid, semi-arid and dry sub-humid areas resulting from climatic variations and human activities", with the term "land" including soil, water resources, crops and natural vegetation (UNEP, 1991).

Irrigation with saline/sodic waters is increasingly practised in many arid and semi-arid regions of the world. According to the estimates 10 million Ha of irrigated lands are abandoned yearly as a consequence of the adverse effect of irrigation, mainly secondary salinization and sodification (Szabolcs, 1989).

Sustainable land management practices are urgently needed all over the world to preserve

131

the production potential of agricultural lands while safeguarding environmental quality (FAO, 1993; UNEP, 1991). Sustainable land management combines technologies, policies and activities aimed at integrating socio-economic principles with environmental concern so as "to protect the potential of natural resources and prevent degradation of soil and water quality" (FAO, 1993).

Sodium in the exchange complex may negatively affect soil structure, and aggregate stability (Abu-Sharar et al., 1987a; Baiamonte and Crescimanno, 1997), causing swelling (Murray and Quirk, 1980), dispersion of the clay particles (Shainberg et al., 1981), and slaking of unstable aggregates (Abu-Sharar et al., 1987b; Agassi et al., 1981).

When the cationic concentration (C) of the applied water decreases and/or the Soil Exchangeable Percentage (ESP) increases, clay dispersion is enhanced (Cass and Sumner, 1982) and the dispersed particles migrate with the percolating water clogging some of the water-conducting pores (Shainberg et al., 1981). Clay dispersion and migration of the detached particles may affect soil structure and modify (macro)pores distribution, decreasing the soil hydraulic conductivity (Crescimanno et al., 1995; Lima et al. 1990) and affecting water flow and/or solute transport (Crescimanno and Iovino, 1995; McCoy and Cardina, 1997).

Movement of free water along macropores or cracks through an unsaturated soil matrix has been defined as bypass flow (Bouma, 1991), while sub-surface infiltration of bypass flow at the bottom of dead-end macropores has been referred as internal catchment (Bouma, 1984; Van Stiphout et al., 1987).

Flow patterns associated with bypass flow have been morphologically characterized using tracers such as methylene blue (Bouma and Dekker, 1978). Booltink and Bouma (1991) studied bypass flow and internal catchment in undisturbed cores and added methylene blue to stain macropores' walls. Hatano and Booltink (1992) showed the importance of morphology of flowpaths in prediction of bypass flow and the feasibility of using fractal dimension of morphological staining patterns, established during bypass flow phenomena, to predict bypass flow.

The objective of this paper is to investigate the influence of two irrigation systems, i.e. drip and micro-sprinkler, on soil structure and bypass flow phenomena in a Mediterranean cracking soil irrigated by saline/sodic waters. The two irrigation systems are expected to induce differences in soil structure in terms of clay dispersion, compaction under raindrop impact and surface sealing (Al-Quinna and Abu-Awwad, 1998), detachment of soil particles with (macro)pores' occlusion and changes in the macropores or cracks distribution.

Field application of methylene blue and laboratory outflow measurements are used to investigate the effect of the two irrigation systems on the macropores/cracks distribution and on the bypass flow behaviour of some soil cores taken from the two fields.

Materials and methods

Two neighbouring fields were selected in a Sicilian area where investigation aimed at preventing land degradation and desertification is being conducted (Crescimanno, 1998).

The two fields are irrigated with the same water (SAR=5 ; EC= 2dS/m) under two irrigation systems, i.e. drip irrigation (field 1, 30m*85m) and micro-sprinkler (field 2, 40m*85m). The drip system supplies a specific flow rate of 22 m^3/hr/Ha. The micro-sprinkler system is realized by perforated pipes (20 mm diameter) supplying a specific flow rate of 104 m^3/hr/Ha.

Figure 1 depicts the topography of the area as well as the locations selected for the measurements.
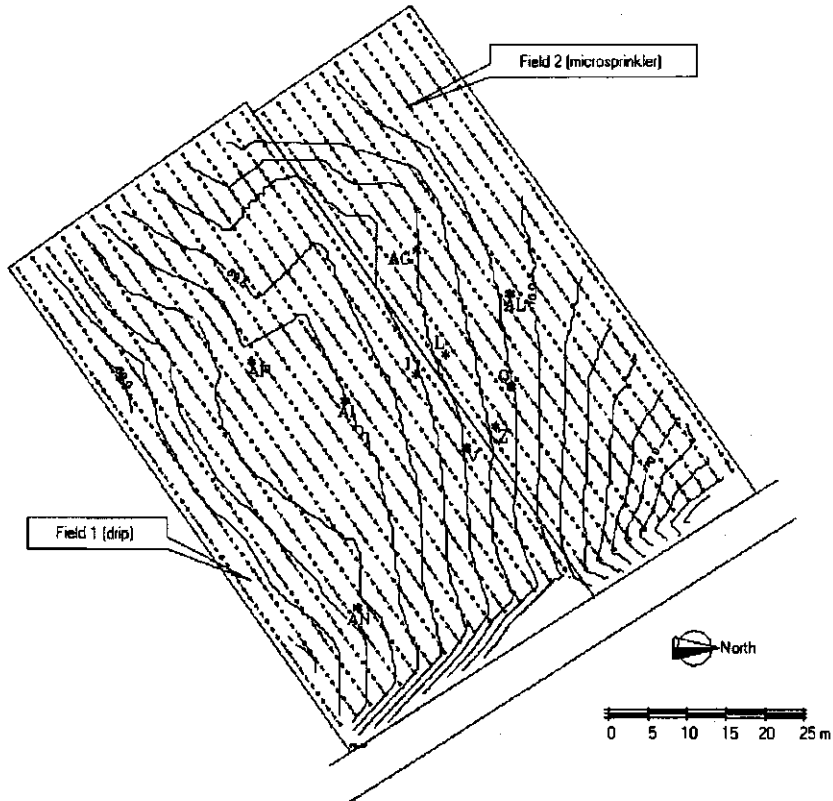
Fig.1 Map of the two fields with the locations of the considered sites

Field experiments

Five locations, the position of which is represented in Figure 1, were randomly selected in each field for application of methylene blue and analysis of the vertical distribution of macropores/cracks.

Rings with a diameter of 25 cm were inserted in each location and a 0.01 M solution of methylene blue was ponded on top of the soil surface into the rings to ensure an infiltration

process where the infiltration rate exceeded the infiltration capacity of the soil matrix and drainage was accounted by the macropores (Bouma and Dekker, 1978). After 1 day the soil was removed in layers of 5, 10, 15, 20 and 25 cm depth from the surface and pictures were taken at each layer showing the methylene blue patterns.

Laboratory measurements

Undisturbed soil cores (200-mm diameter by 200-mm long) were sampled in each field from the five selected locations from the C1 horizons nearby the points where application of methylene blue had been performed. The hydraulic conductivity of the soil matrix at saturation, $K_{(sat)}$, was determined on each soil core by the suction crust infiltrometer method (Booltink et al., 1991).

After measuring $K_{(sat)}$, each core was placed on a funnel connected to an outflow collector equipped with a pressure transducer and two tensiometers were installed at -4 cm and -8 cm from the top. These tensiometers provided information on: (i) the initial pressure head in the soil; (ii) the time when water started to infiltrate in the macropores (top tensiometer) and (iii) the hydraulic conditions in the upper part of the soil column.

Rain showers with intensities (I_r) higher than the measured $K_{(sat)}$ were applied on top of the samples using a small rain simulator (Crescimanno et al., 2000) in order to induce bypass flow (Booltink et al., 1993).

After the bypass flow measurements had been performed, the cores were dried to the initial conditions prior to the experiments, and a 0.01 M methylene blue solution was applied on top of the samples. The cores were left air-drying for one day, then peeled-off in layers of two cm from the top, and pictures were taken at each layer showing the methylene blue patterns.

Undisturbed soil cores (8.5 cm diameter by 11.5 cm long) were sampled from the same locations into fields 1 and 2 for measurement of the soil shrinkage characteristic curve (SSCC), which was determined by measuring vertical and horizontal shrinkage (Crescimanno and Provenzano, 1999).

The coefficient of linear extensibility, COLE, was calculated according to Grossman et al. (1968):

$$COLE = \left(\frac{V_{wet}}{V_{dry}}\right)^{\frac{1}{3}} - 1$$

with V_{wet} volume at saturation and V_{dry} volume at the air-dry condition.

Results and discussion

Field experiments

Table 1 presents the soil textural composition at the selected locations in the two fields.

Analysis of variance showed that the mean values of clay (C), sand (SA) and silt (Si) measured in field 1 did not significantly differed from those measured in field 2 (probability level P=0.05).

Table 1 Classification and physical characteristics of the soils

Horizon		Ap (0-15 cm)			C1 (15-40 cm)				
Classification †		Vertic Chromoxerert							
	Soil site	Sa [%]	Si [%]	C [%]	Sa [%]	Si [%]	C [%]	$K_{(sat)}$ [cm/h]	D_{max} [cm]
Field 1	V	36	32	32	28	37	35	3.70	25
(drip)	I	35	33	32	32	34	34	3.78	20
	AN	36	33	31	35	33	32	2.58	20
	AF	34	33	33	38	32	30	2.69	22
	AI	41	30	29	35	34	32	1.34	20
	mean	36.4	32.2	31.4	33.5	34.0	32.5		
	st. dev.	3.0	1.4	1.6	3.5	1.7	2.0		
Field 2	Z	38	32	31	27	37	36	0.26	5
(micro-sprinkler)	L	35	33	33	31	34	35	2.01	10
	Q	39	31	30	33	34	33	0.43	10
	AG	39	32	29	36	32	33	1.18	10
	AL	36	33	31	31	34	35	0.91	6
	mean	37.3	31.9	30.7	31.7	34.2	34.1		
	st. dev.	1.9	0.8	1.3	3.2	2.0	1.4		

† Soil Taxonomy (Soil Survey Staff, 1992)
Sa=Sand (2-0.02 mm)
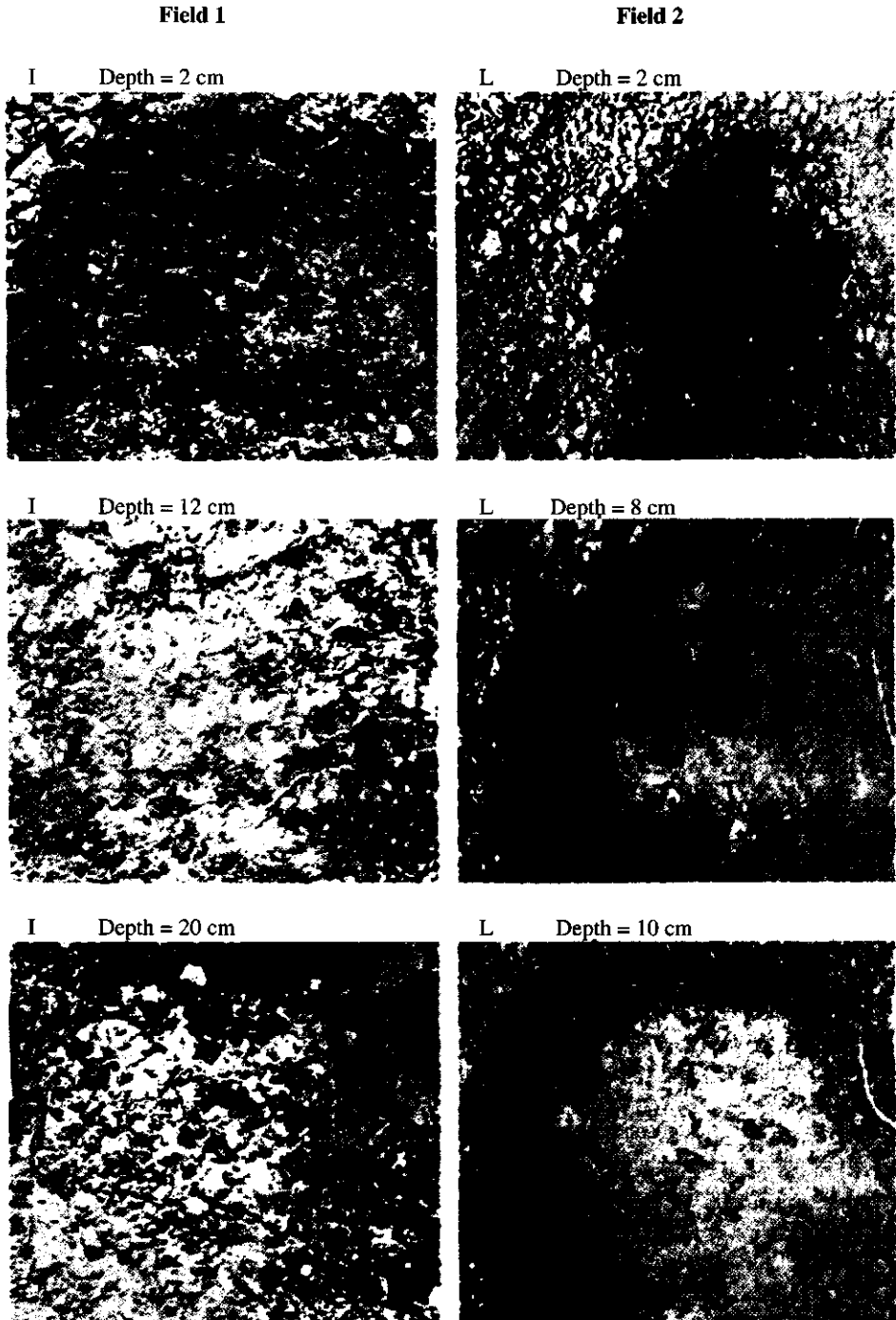Si=Silt (0.02-0.002 mm)
C=Clay (<0.002 mm)
$K_{(sat)}$=saturated hydraulic conductivity [cm/h]
D_{max}=maximum macropores/cracks depht measured in the field [cm]

Figure 2 illustrates some pictures taken in the two fields and showing the methylene blue patterns at two of the locations (I and Q) where the cores for the bypass flow measurements were sampled. The Figures show the different depth of penetration of the macropores/cracks in the two fields, the maximum value of which, D_{max}, as reported in Table 1, was about 20 cm for the I location, and of 10 cm for the Q location. Analysis of the pictures taken at the other locations in the two fields evidenced D_{max} values, which are reported in Table 1, ranging from 20 to 25 cm (mean value 21.4 cm) in field 1, and from 3 to 10 (mean value 6.8 cm) in field 2.

These results evidenced the larger depth of penetration of the macropores/cracks in the field where the drip irrigation was practiced.

Fig.2 Soil sections at different dephts showing the methylene blue distibution

Field 1

Field 2

I   Depth = 2 cm

L   Depth = 2 cm

I   Depth = 12 cm

L   Depth = 8 cm

I   Depth = 20 cm

L   Depth = 10 cm

Laboratory measurements

The mean value of the COLEs determined on the basis of the SSCCs measured on the cores taken from field 1 was 0.082, and the mean value of the COLEs determined on the cores taken from field 2 was 0.084. No significant differences (P=0.05) were found between the two mean COLE values (P=0.05). According to Parker et al. (1977), the cores from the two fields were both classified as having a high rate of shrink-swell potential.
Table 1 reports the hydraulic conductivity of the soil matrix at saturation, $K_{(sat)}$. As can be seen in the Table, systematically higher $K_{(sat)}$ values, indicating less compaction, were measured in the cores from field 1.
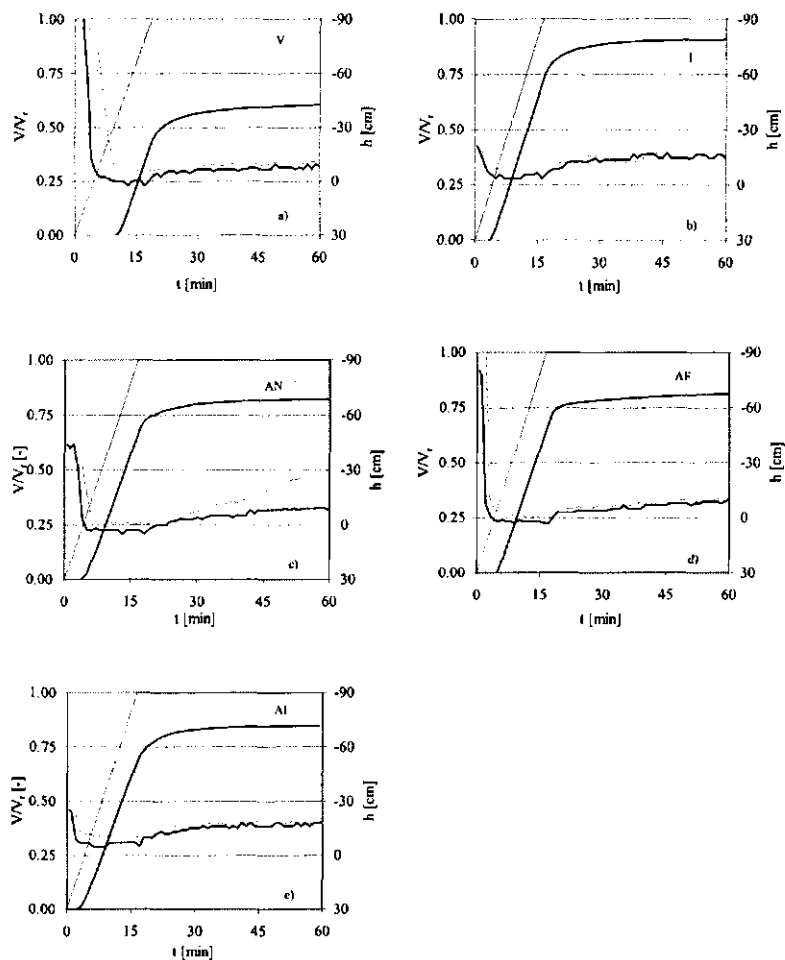
Fig. 3 a-e

Fig.3(a-e) Cumulative outflow volume relative to the volume of applied water, and matric potential as a function of time (cores from field 1)

Figures 3a, 3b, 3c, 3d and 3e show the results of the bypass flow experiments performed on the V, I, AN, AF and AI cores of field 1 under an almost constant rate of water application. The figures report the outflow volume, V, divided by the volume of the applied water, Vr, as a function of time, together with the matric potential (h) recorded by the tensiometers.

Table 2: Relevant parameters deduced from bypass flow experiments

	Soil cores	h_i [cm]	l_r [cm/h]	t_r [min]	t_d [min]	t_{cs} [min]	t_e [min]	$V(t_{cs})/V_r$ [%]	$V(t_e)/V_r$ [%]	W_s/V_r [%]	O_r [cm/h]	O_r/l_r [-]	D'_{max} [cm]
Field 1	V	-90.4	10.2	18.8	10.3	11.9	18.5	5.4	40.9	55.6	10.2	1.00	16
(drip)	I	-21.0	11.7	16.4	3.4	6.3	15.0	13.0	64.5	20.9	11.3	0.97	16
	AN	-44.0	11.5	16.7	3.8	6.1	16.7	7.5	68.8	23.0	10.5	0.92	16
	AF	-93.0	11.6	16.5	4.8	4.9	16.4	0.4	64.2	28.9	10.6	0.92	14
	AI	-26.0	11.7	16.4	2.3	6.0	17.0	13.0	70.9	14.2	10.1	0.86	14
Field 2	Z	-68.4	11.2	17.0	24.0					100.0	1.2	0.11	8
(micro-sprinkler)	L	-49.0	11.5	16.7	6.9					41.4	7.3	0.64	16
	Q	-90.0	11.0	17.4	12.3					70.4	1.2	0.11	10
	AG	-82.0	11.8	16.2	18.8					100.0	1.7	0.15	12
	AL	-26.0	10.8	17.6	7.8					44.4	1.2	0.11	8

h_i = initial matric potential
t_r = Rainfall duration
t_d = Time-start of outfow
t_{cs} = Time-start of linear outflow
t_e = Time-stop of linear outflow
$V(t_{cs})$ = Cumulative outflow at the time t_{cs} [cm]
$V(t_e)$ = Cumulative outflow at the time t_e [cm]
W_s = Water stored in the soil at t_d [cm]
V_r = rainfall volume [cm]
l_r = Inflow rate [cm/h]
O_r = Outflow rate [cm/h]
D'_{max} = maximum macropores/cracks depht measured in the soil cores [cm]

The cumulative outflow curves all show identical behaviour. After the point when outflow starts, t_d, an exponential progression (ESO) between the times t_d and t_{cs} (start of linear outflow) could be observed. Between t_{cs} and t_{ce} (end of linear outflow) there was a nearly linear outflow pattern, and after t_{ce} an exponential fade out pattern was evident. The linear outflow occurring between t_{cs} and t_e (i.e. the time derivative of outflow is constant) had been observed in earlier measurements (van Stiphout et al., 1987; Booltink et al., 1993; Crescimanno et al., 1999, 2000).

Table 2 reports some relevant parameters deduced from the inflow/outflow curves. As can be seen in the Table, for the cores from field 1 the outflow process starts during the rainfall application ($t_d<t_r$), and occurs when the bottom tensiometer records a negative matric

potential (h). The outflow volume $V(t_e)$, which represents the bypass flow, is a relevant percentage of the applied rainfall volume (1000 cm³), ranging from 40.9% to 70.9%. The outflow rate during steady-state, O_r, as reported in Table 2, is almost equal to the application rate, I_r, indicating the very low adsorption of water on the macropores/cracks walls during the bypass flow process, and confirming the occurrence of bypass flow (Booltink et al., 1993; Crescimanno et al., 1999).

Figures 4a, 4b, 4c, 4d and 4e show the results of the bypass flow experiments performed on the Z, L, Q, AG and AL cores of field 2.
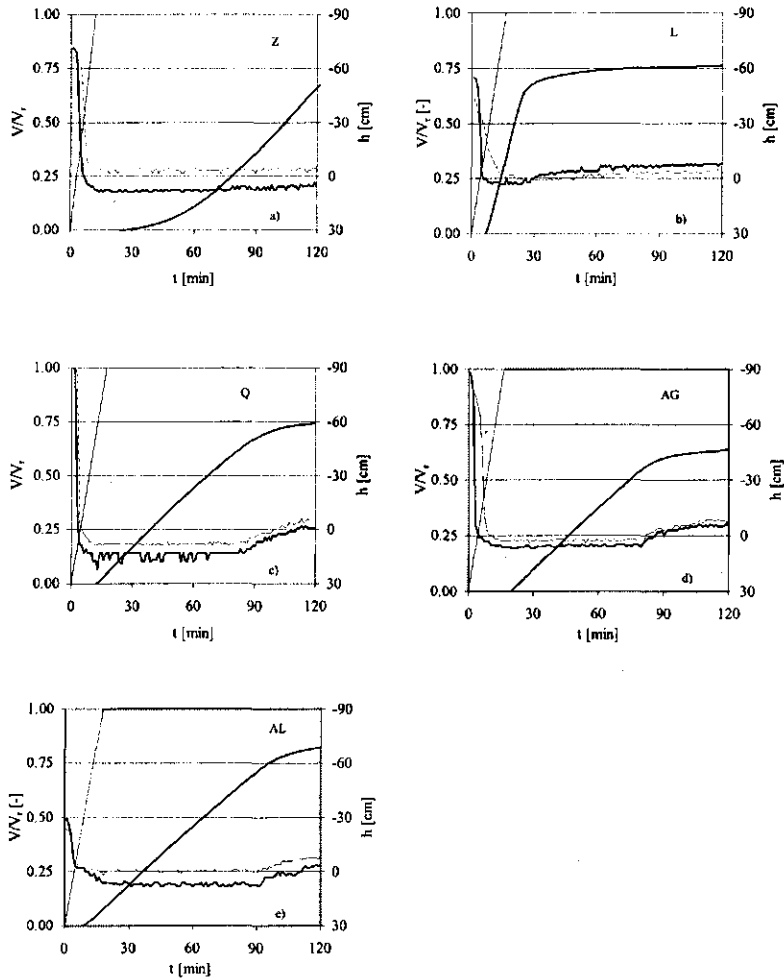
Fig. 4 a-e

Fig.4(a-e) Cumulative outflow volume relative to the volume of applied water, and matric potential as a function of time (cores from field 2)

Analysis of Table 2 for the cores taken from field 2 evidences that for the Z, L, Q, and AG cores the outflow process starts when the bottom tensiometer evidences conditions of saturation or ponding (h>=0), and that O_r is much lower than I_r. These conditions evidence the absence of bypass flow, and the occurrence of Darcian flow.

This flow behaviour is in agreement with the morphological patterns generally observed in the micro-sprinkler irrigated field, which evidenced less penetrating macropores/cracks into field 2, and confirms the role of continuous macropores on the rate and amount of bypass flow (Bouma, 1991).

Only for the L sample the outflow curves showed a behaviour intermediate between that observed in the cores from field 1 and those from field 2. The outflow process started during the rainfall application ($t_d<t_r$) when the bottom tensiometer indicated unsaturated conditions (h<0). The outflow rate during steady-state, O_r, was lower than those observed in the cores from field 1 but higher than the O_r rates found in the cores of field 2. This behaviour, indicating a certain occurrence and amount of bypass flow, could be the consequence of a greater depth of penetration of cracks in the L core compared to that found in the other samples taken from field 2.

Application of methylene blue in the cores where bypass flow measurements had been performed confirmed a different vertical penetration of the cracks in the two fields. Figures 5(a, e) and 6(a,e) illustrate the maximum depth of penetration of methylene blue in the cores where the bypass flow measurements have been performed. The maximum depth of cracks, D_{max}, which is reported in Table 2, ranged from 14 to 16 cm (mean value 15.2 cm) in the V, I, AN, AF and AI cores, and from 8 to 12 (mean value 9.5cm) in the Z, AQ, AG and AL cores.

A D_{max} equal to 16 cm was found only in the L core, but in this case there was evidence of a root crossing the sample. The relatively high O_r found for this soil was evidently determined by the presence of this macropore.

Additional parameters describing macroporosity (number of pores, area, perimeter) should be derived from the staining patterns (Droogers et al., 1998) to better explain the flow behaviour observed in the L core.

The presented results evidenced a different morphological and flow behaviour in the cores taken from the drip and micro-sprinkler irrigated fields which can be attributed to the higher intensity and to the non-point water application involved in the micro-sprinkler irrigation system compared to the drip system.

Dispersion of the clay particles (Frenkel et al., 1978), detachment of these particles from the surface and their movement into the pores (Shainberg et al, 1992) could be the mechanisms responsible for the partial or total occlusion of the (macro)pores/cracks in the micro-sprinkler irrigated field. These mechanisms have been previously recognized to alter soil structure (Shainberg et al., 1981; Baiamonte and Crescimanno, 1997), decreasing the soil hydraulic conductivity (Crescimanno et al., 1995; Lima et al. 1990) and affecting water flow and/or solute transport (Crescimanno and Iovino, 1995; McCoy and Cardina, 1997).
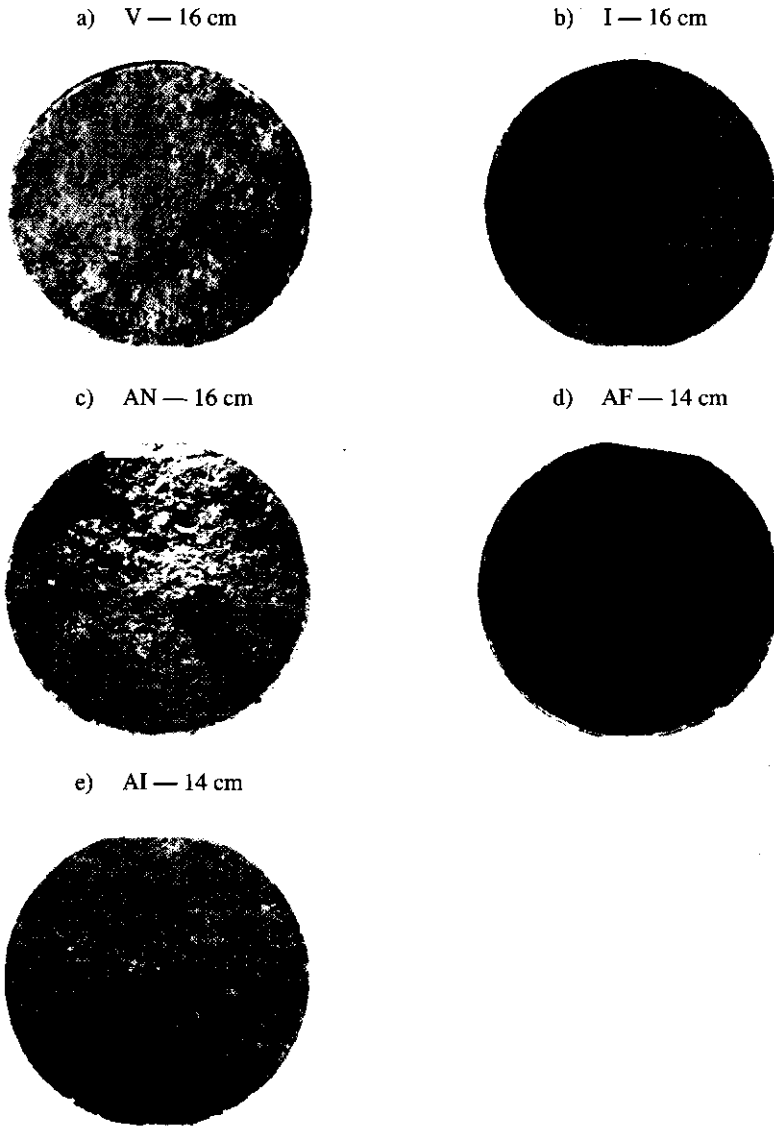
a)   V — 16 cm

b)   I — 16 cm

c)   AN — 16 cm

d)   AF — 14 cm

e)   AI — 14 cm

Fig.5a-e Sections showing the maximum depth of
penetration of methylene blue in the cores from field 1

To check the hypothesis that detachment of soil particles and their movement into the soil macropores/cracks were the mechanisms inducing the structural modifications determining the absence of bypass flow in the soils from field 2, two samples taken from field 1 were exposed to the micro-sprinkler irrigation. The presence of detached particles in the effluent solution confirmed that the higher intensity and the non-point water application involved in the micro-sprinkler irrigation system compared to the drip system was responsible for the

141

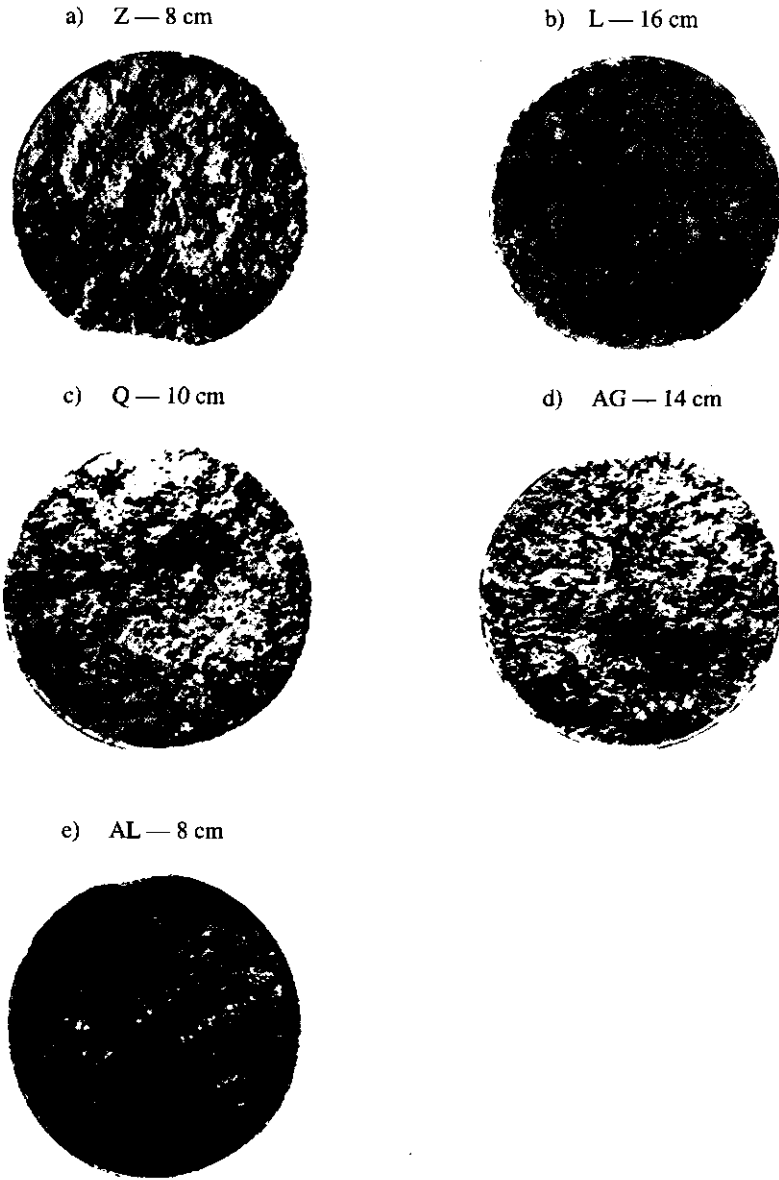partial or total occlusion of the (macro) pores under field conditions.

a)   Z — 8 cm

b)   L — 16 cm

c)   Q — 10 cm

d)   AG — 14 cm

e)   AL — 8 cm

Fig.6a-e Sections showing the maximum depth of
penetration of methylene blue in the cores from field 2

Conclusions

This investigation explored the effect of irrigation on soil structure and bypass flow phenomena in a Mediterranean cracking soil under two irrigation systems, i.e. drip and micro-sprinkler, with the objective of finding management strategies suitable to prevent the hazard of salinization and desertification.

Field application of methylene blue showed the presence of macropores/cracks terminating at a depth ranging between 5 and 10 cm from the soil surface in the micro-sprinkler irrigated field. Instead, cracks penetrating up to a depth of 20-25 cm from the soil surface were found in the field where the drip system was in use.

In agreement with the different vertical distribution of cracks in the two fields, no bypass flow was generally measured in laboratory on cylindrical soil cores taken from the irrigated micro-sprinkler field. Instead, a high rate and amount of bypass flow was measured in the cores taken from the drip irrigated field.

Being the conditions in the two fields comparable in terms of pedological and textural characteristics, topography and quality of water used for irrigation, as well as of crop and tillage, the differences found in soil structure and bypass flow phenomena were attributed to the different irrigation systems.

The higher intensity and the non-point water application involved in the micro-sprinkler irrigation system were found to be responsible for the partial or total occlusion of the (macro) pores, for the different depth of penetration of the macropores/cracks and for the observed absence of bypass flow.

Being bypass flow a mechanism inducing leaching of solutes (Crescimanno et al., 2000), these results indicate that in management of clay soils, irrigation systems such as micro-sprinkler or sprinkler should be avoided.

Further research is being performed by extending the application of methylene blue to some other locations in the two fields in order to analyse the distribution of cracks at a larger scale. Parameters describing macroporosity from staining patterns will be also derived to check the possibility to predict bypass flow from morphology.

The influence of the different flow behaviour observed in the two fields under the two different irrigation systems on the spatial distribution of water content and salinity at the field scale will be the object of further investigation finalized to find management strategies suitable to prevent irreversible land degradation at a larger scale.

Chapter 9

General Conclusion

General conclusions

1. In clay soils, knowledge of the *Soil Shrinkage Characteristic Curve* (SSCC) is fundamental to calculate the volumetric water content and to incorporate volume changes occurring upon changing water content in the soil hydraulic characteristics (HC).
Comparison between measurement techniques used for determination of the SSCC showed that measurement of vertical and horizontal shrinkage in confined soil cores is suitable to incorporate shrinkage in the soil hydraulic parameters/functions determined on confined undisturbed soil samples.

2. The multi-step outflow method with inverse modeling is increasingly used to determine the soil hydraulic properties, but for cracking soils physical parameters accounting for the presence of macropores and/or cracks need to be included in the optimization procedure in order to obtain reliable hydraulic parameters/functions. An optimization procedure was developed accounting for structural porosity and shrinkage processes on the basis of hydraulic conductivity values determined by the Suction Crust Infiltrometer Method and of the SSCC determined on confined soil cores.

3. An Exchangeable Sodium Percentage (ESP) greater than 15 is traditionally considered to affect the soil structural and hydraulic characteristics, but investigations performed on two Sicilian Vertisols showed that the concept of *critical threshold* needs reconsideration, because soil degradation at increasing ESP appears to be a continuum, and a major hazard of deterioration of structural and hydraulic peoperties may occur even at low ESP values (ESP<5) in dilute solutions.

4. Models simulating water flow and solute transport can be used to evaluate the influence that the reductions in hydraulic conductivity due to salinity and/or sodicity may have on water transport in the soil-crop system. Application of the LEACHM model, which did not account for bypass flow, showed the large influence that the reductions in the soil HC, occurring at ESP values ranging from 0 to 15, may have on the water balance in clay soils. The possibility to run the LEACHM model to predict the hazard of salinization/sodification due to irrigation with saline/sodic waters was tested, and the need to improve predictions by application of models accounting for the occurrence of bypass flow was evidenced by results obtained.

5. Quantitative evaluation of the relevance that bypass flow may have on the water balance in a Mediterranean context like Sicily, was performed by the simulation model FLOCR. This context is characterized by high values of the rainfall intensity, low amounts of the annual rainfall, and cracking soils. The results showed that bypass flow corresponded with about 70-74% of the cumulative yearly rainfall, and that models not accounting for bypass flow may lead to a serious overprediction of crop (evapo)transpiration, and subsequent underestimation of the hazard of land degradation and desertification. In these soils, internal catchment of water in dead-end pores, as reported for other soils, is not significant.

6.   The results of bypass flow measurements performed in a Sicilian cracking soil under alternated use of a high salinity solution to distilled water, showed that exchange of solutes occurred at the contact surfaces between the macropores/cracks walls and the incoming solution in concomitance with bypass fluxes. The results indicated that alternating low salinity/sodicity water with a high salinity/sodicity solution is effective for preventing salinization and sodification, and that the higher efficiency of removal of Sodium and other soluble salts can be obtained if the leaching solution is applied when the soil is dry and contains many cracks.

7.   Combined use of morphometric and physical techniques made it possible to explore the effect of irrigation on soil structure and bypass flow phenomena in a Sicilian cracking soil under two different irrigation systems, i.e. drip and micro-sprinkler. The vertical distribution of cracks under the two irrigation systems was different. In agreement with these observations, different flow behaviour was observed in the laboratory in cylindrical soil cores taken from the irrigated micro-sprinkler field. In contrast with the drip-irrigated field, no bypass flow was observed in the micro-sprinkler irrigated field. Chemical dispersion of clay particles and detachment of these particles from the surface and their movement into the cracks were the mechanisms responsible for the partial or total occlusion of the (macro)-pores in the micro-sprinkler irrigated field.

CHAPTER 10

REFERENCES

References

Abu-Sharar, T.M., F.T. Bingham, and J.D. Rhoades. 1987a. Stability of soil aggregates as affected by electrolyte concentration and composition. Soil Sci. Soc. Am. J. 51:309-314.

Abu-Sharar, T.M., F.T. Bingham, and J.D. Rhoades. 1987b. Reduction in hydraulic conductivity in relation to clay dispersion and disaggregation. Soil Sci. Soc. Am. J. 51:342-346.

Agassi, M., J. Morin, and I. Shainberg. 1985. The effect of water drop impact energy and water salinity on the infiltration rates of sodic soils. Soil Sci. Soc. Am. J. 49:186-190.

Agassi M., I. Shainberg, and J. Morin. 1981. Effect of electrolyte concentration and soil sodicity on the infiltration rate and crust formation. Soil Sci. Soc. Am. J. 45: 848-851

Ahuja L.R., S.A. El-Swaify and A. Rahman. 1991. Characteristics and importance of preferential macropore transport studied with the ARS Root Zone Water Quality Models. 32-49. In T.H. Gish and A. Shirmohammadi (ed). Proceedings of National Symposium on preferential flow, Chicago. 16-17 Dec. ASAE, St. Joseph, MI.

Akaike, H., 1974. A new look at the statistical model identification. IEEE Trans. Autom. control, 19: 716-723.

Al-Qinna M.I., and A.M. Abu-Awwad. 1998. Soil water storage and surface runoff as influenced by irrigation method in arid soils with surface crust. Agric. Water Manage., 37: 189-203

Allbrook, R.F. 1992. Shrinkage of some New Zealand soils and its implications for soil physics. Aust. J. Soil Res. 31:111-118.

Baiamonte G., and G. Crescimanno. 1997. Assessing the influence of salinity and sodicity on wet aggregate stability and water dispersible clay to prevent soil crusting and erodibility. Int. Conf. on "Water management, salinity and pollution control towards sustainable irrigation in the Mediterranean region". MAI.Bari- 22-26 September, 1997

Belmans C., J.G. Wesseling, and R.A. Feddes. 1983. Simulation model of the water balance of a cropped soil: SWATRE. Journal of Hydrology, 63:271-286.

Benjamin, J.R., and C.A. Cornell. 1970. Probability, statistics and decision for civil engineers. McGraw Hill, New York, 684 pp.

Berndt, R.D., and K.J. Coughlan. 1976. The nature of changes in bulk density with water content in a cracking clay. Aust. J. Soil Res. 15:27-37.

Beven, K., and P. Germann. 1982. Macropores and water flow in soils. Water Resour. Res. 18:1311-1325.

Boels, D.J., H.M. van Gils, G.J. Veerman, and K.E. Wit. 1978. Theory and system of automatic determination of soil moisture characteristic and unsaturated hydraulic conductivities. Soil Sci. 126 (4): 191-199.

Bohne, K., C. Roth, F.J. Leij, and M.Th. van Genuchten. 1993. Rapid method for estimating the unsaturated hydraulic conductivity from infiltration measurements. Soil Sci. 155 (4):237-244.

Booltink H.W.G., and J. Bouma. 1991. Physical and morphological characterization of bypass flow in a well-structured clay soil. Soil Sci. Soc. Am. J. 55:1249-1254.

Booltink H.W.G., and J. Bouma. 1993. Sensitivity analyses on processes affecting bypass flow. Hydrol. Processes, 7:33-43.

Booltink, H.W.G., J. Bouma and D. Gimenez. 1991. A suction crust infiltrometer for measuring hydraulic conductivity of unsaturated soil near saturation. Soil Sci. Soc. Am. J. 55, 566-568.

Booltink HWG, R. Hatano and J. Bouma. 1993. Measurement and simulation of bypass flow in a   structured clay soil: a physico-morphological approach. J. of Hydrol. 148:149-16

Borcher, C.A., J. Shopp, D. Watts, and J. Schepers. 1987. Unsaturated hydraulic conductivity determination by one-step outflow for fine-textured soils. Trans. ASAE, vol.30(4):1038-1042.

Bouma, J. 1983. Use of soil survey data to select measurement techniques for hydraulic conductivity. Agric. Wat. Man., 6: 177-190.

Bouma J. 1984. Using soil morphology to develop measurement methods and simulation techniques for water movement in heavy clay soils. In: J. Bouma and P.A.C. Raats (eds), Water and solute movement in heavy clay soils. Int. Soc. Soil Science (ISSS) Symp. Inst. Land Reclamation and Irrigation (ILRI), Wageningen, The Netherland. 37:298-316

Bouma, J. 1991. Influence of soil macroporosity on environmental quality. Advances in Agronomy, 46: 1-37.

Bouma, J., and L.W. Dekker. 1978. A case study on infiltration into dry clay soil. I. Morphological observations. Geoderma 20: 27-40.

Brasher, B.R., D.R. Franzmeier, V. Valassis, and S.E. Davidson. 1966. The use of SARAN resin to coat natural soil clods for bulk density and water retention measurements. Soil Sci. 101:108.

Bronswijk, J.J.B. 1988. Modeling of waterbalance, cracking and subsidence on clay soils. J. Hydrol., 97:199-212.

Bronswijk JJB. 1989. Prediction of actual cracking and subsidence in clay soils. Soil Science 148:87-93.

Bronswijk, J.J.B. 1990. Shrinkage geometry of a heavy clay soil at various stresses. Soil Sci. Soc. Am. J. 54:1500-1502.

Bronswijk, J.J.B., and J.J. Evers-Vermeer. 1990. Shrinkage of dutch clay soil aggregates. Neth. J. Agr. Sci. 38:175-194.

Brutsaert, W. 1966. Probability laws for pore-size distribution. Soil Sci. 101, 85-92.

Cass, A., and M.E. Sumner. 1982. Soil pore structural stability and irrigation water quality. I. Empirical sodium stability model. II. Sodium stability data. Soil Sci. Soc. Am. J., 46:503-512.

Chan, K.J. 1982. Shrinkage characteristics of soil clods from a grey clay under intensive cultivation. Aust. J. Soil Res. 20:65-68.

Clemente, R.S., R. De Jong, H.N. Hayhoe, W.D. Reynolds and M. Hares. 1994. Testing and comparison of three unsaturated soil water flow models. Agric. Wat. Manag. 25:135-152.

Collis-George, N., and B.S. Figueroa. 1984. The use of high energy moisture characteristic to assess soil stability. Aust. J. Soil Res. 22:349-56.

Coughlan, K.J., D. McGarry, R.J. Loch, B. Brideg, and G.D. Slith. 1991. The measurement of soil structure: some practical initiatives. Aust. J. Soil Res. 29:869-89.

Crescimanno G. 1998. An integrated approach for for sustainable management of irrigated land susceptible to degradation/desertification. Proc. of the European Climate Science Conference. Vienna, City Hall, 19-23 October 1998.

Crescimanno, G. 2000. Irrigation with saline/sodic waters in Mediterranean regions: soil quality degradation and desertification. 2000. Procs. of the International Conference on Mediterranean Desertification, Crete, Oct 29-Nov.1. 1996.

Crescimanno, G., and M. Iovino. 1995. Determining the hydrological characteristics of saline-sodic soils by the parameter estimation method. International Symposium on Water Quality Modeling, Orlando, Florida, 2-5 April.

Crescimanno, G., and M. Iovino. 1995. Evaluating the effects of saline-sodic waters on the hydrological characteristics of soil. International Symposium on Water Quality Modeling. Orlando, Florida, 2-5 April.

Crescimanno, G., and M. Iovino. 1995. Parameter estimation by inverse method based on outflow one-step and multistep outflow experiments. Geoderma 68:257-277

Crescimanno, G., M. Iovino and E. Marcone. 1995. Irrigation with saline-sodic waters: water and salt-balance in a Sicilian field. Int. Symp. on Salt-affected Lagoons ecosystems, ISSALE 95, Valencia, sept. 18-25, 1995

Crescimanno, G., M. Iovino and G. Provenzano. 1995. Influence of salinity and sodicity on soil structural and hydraulic characteristics. Soil Sci. Soc. Am. J.59:1701-1708

Crescimanno, G., and G. Provenzano. 1995. Fenomeni di rigonfiamento e contrazione dei terreni argillosi: indagime sperimentale nell'ambiente siciliano. Rivista di Ingeneria agraria, Anno XXVI, n. 3.

Crescimanno, G., and G. Provenzano. 1998. Clay soils susceptible to bypass flow: influence of sodicity on water balance. XIIIth Int. Congress on Agricultural Engineering, Rabat, Marocco, February 2-3.

Crescimanno, G., and G. Provenzano. 1998. La gestione dell'irrigazione con acque salino/sodiche in terreni suscettibili a processi di degradazione. Rivista Irrigazione e drenaggio 1:21-24.

Crescimanno, G., and G. Provenzano. 1999. Soil shrinkage characteristic in clay soils: measurement and prediction. Soil Science Society of American Journal, 63:25-32.

Crescimanno G., G. Provenzano, and H.W.G. Booltink. 1999. Bypass flow of water and solutes in Mediterranean swelling and shrinking soils. XXIV General Assembly of the European Geophysical Society. Den Haag, The Netherlands, 19-23 April.

Crescimanno G. and G. Provenzano. 2000. Hydrological processes affecting land degradation in the Mediterranean environment. Third International Congress of the European Society for Soil Conservation (ESSC). Valencia, Spain, 28 March- 1 April (in press).

Crescimanno G and G. Baiamonte. 1999. Hydraulic characterization of swelling/shrinking soils by a combination of laboratory and optimization techniques. Procs. Of the

International Workshop "Modelling of transport processes in soils at various scales in time and space". Leuven (Belgium), November 24-26.

Crescimanno G., G. Provenzano, and H.W.G. Booltink. 2000. The effect of alternating different water qualities on accumulation and leaching of solutes in Mediterranean cracking soils. Accepted for pubblication on Hydrological Processes (in press).

Crescimanno G., Provenzano G., De Santis A. and H.W.G. Booltink. 2000. Effect of irrigation on soil structure and bypass flow phenomena in a Mediterranean cracking soil. Submitted to Agricultural Water Management.

Cresswell, H.P., D.E. Smiles, and J. Willians. 1992. Soil structure, soil hydraulic properties and the soil water balance. Aust. J. Soil Res. 30:265-283.

Dasog, G.S., D.F. Acton, A.R. Mermuth, and E. De Jong. 1988. Shrink-swell potential and cracking in clay soils of Saskatchewan. Can. J. Soil Sci. 68:251-260.

De Jong, E., L.M. Kozak, and H.B. Stonehouse. 1992. Comparison of shrink-swell indices of some Saskatchewan soils and their relationships to standard soil characteristics. Can. J. Soil Sci. 72:429-439.

Dekker L.W., and J. Bouma, 1984. Nitrogen leaching during sprinkler irrigation of a Dutch clay soil. Agricultural Water Management, 9:37-45.

Droogers, P. and J. Bouma, 1996. Biodynamic vs. conventional farming effects on soil structure expressed by simulated potential productivity. Soil Sci. Soc. Am. J. 60: 1552-1558.

Droogers P., A. Stein, J. Bouma, and G. de Boer. 1998. Parameters for describing soil macroporosity derived from staining patterns. Geoderma 83: 293-308

Durner, W. 1994. Hydraulic conductivity estimation for soils with heterogeneous pore structure. Water Resour. Res., vol. 30(2):211-223.

Eching, S.O., and J.W. Hopmans. 1993. Optimization of hydraulic functions from transient outflow and soil water pressure data. Soil Sci. Soc. Am. J. 57:1167-1175.

Eching, S.O., J.W Hopmans, and O. Wendroth. 1994. Unsaturated hydraulic conductivity from transient multi-step outflow and soil water pressure data. Soil Sci. Soc. Am. J. 58: 687-695.

FAO. 1993. FESLM. An international framework for evaluating sustainable land management. World Soil Resources Reports, 73, Rome.

Fitzpatrick, R.W., S.C. Boucher, R. Naidu, and E. Fritsch. 1994. Environmental consequences of soil sodicity. Aust. J. Soil Res. 32:1069-93.

Frenkel H., J.O. Goortzen, and J.D. Rhoades. 1978. Effects of clay type and content, exchangeable sodium percentage and electrolyte concentration on clay dispersion and soil hydraulic conductivity. Soil Sci. Soc. Am. J. 42:32-39

Gardner, W.R. 1958. Some steady state solutions of the unsaturated moisture flow equation with application to evaporation from a water table. Soil Sci. 85, 228-232.

Garnier P., M. Rieu, P. Boivin, M. Vauclin, and P. Baveye. 1997. Determining the hydraulic properties of a swelling soil from a transient evaporation experiment. Soil Sci. Soc. Am. J. 61: 1555-1563.

Grossman, R.B., B.R. Brasher, D.P. Franzmeier, and J.L. Walker. 1968. Linear extensibility as calculated from natural-clod bulk density measurements. Soil Sci. Soc. of Am. Proc. 32:570-573.

Haines, W.B. 1923. The volume change associated with variations in water content in soil. J. of Agr. Sci. (Cambridge) 13: 296-311.

Hargreaves G.H. 1983. Closure of estimating potential evapotranspiration. Journal of Irrigation and Drainage. Div. Am. Soc. Civ. Eng., 109:343-344

Hatano R., and H.W.G. Booltink. 1992. Using fractal dimensions of stained flow patterns in a clay soil to predict bypass flow. J. Hydrol. 135:121-131

Hedden, K.F. 1986. Example field testing of soil fate and transport model, PRZM, Dougherty Plain, Georgia. In: Hern, S.C. and S.M. Melancon (eds.), Vadose zone modeling of pollutants. Lewis Publishers Inc., Essex, UK, pp. 81-101.

Hillel, D. 1980. Fundamental of Soil Physics. Academic Press, inc., NY

Hoogmoed W.B., and J. Bouma. 1980. A simulation model for predicting infiltration into cracked clay soil. Soil Sci. Soc. Am. J. 44: 458-461.

Hopmans, J.W., T. Vogel, and P.D. Koblik. 1992. X-ray tomography of soil water distribution in one-step outflow experiments. Soil Sci. Soc. Am. J. 56: 355-362.

Hornung, U. 1983. Identification of non-linear physical parameters from input-output experiment. In: P. Deyuflhard and E. Haier (Editors) Workshop on Numerical Treatments of Inverse Problems in Differential and Integral Equations. Birkhauser, Boston, Mass. pp. 227-237.

Hudson, D.B., M.H. Young, P.J. Wierenga, and Hills, R.H. 1991. Transient method for estimating soil water parameters of unsaturated soil cores. In: Agronomy Abstracts. ASA, Madison, WI. 221 pp.

Hutson, J.L., and R.J. Wagenet. 1995. A multiregion model decribing water flow and solute transport in heterogeneous soils. Soil Sci. Soc. Am. J. 59: 743-751.

Jarvis N.J., P.B. Leeds-Harrison. 1987. Modelling water movement in drained clay soil. I. Description of the model, sample output and sensitivity analysis. J. Soil Sci. 38:487-489.

Jaynes, D.B., and E.J. Tyler. 1980. Comparison of one-step outflow laboratory method to an in-situ method for measuring hydraulic conductivity. Soil Sci. Soc. Am. J. 44: 903-907.
61: 1555-1563.

Kim, D.J., H. Vereecken, J. Feyen, D. Boels, and J.J.B. Bronswijk. 1992. On the characterization of properties of an unripe marine clay soil. I. Shrinkage processess of an unripe marine clay soil in relation to physical ripening. Soil Sci. 153:471-481.

Kim, D. J., H. Vereecken, J. Feyen, D. Boels, and J.J.B. Bronswijk. 1992. On the characterization of properties of an unripe marine clay soil. II. A method on the determination of hydraulic properties. Soil Sci. 154:59-71.

Kirby, J.M., and B.G. Blunden. 1991. Interaction of soil deformations, structure and permeability. Austr. J. Soil Res. 29:891-904.

Klute, A. 1986. Water retention: laboratory methods. pp. 635-662. In A. Klute (ed.): Methods of soil analysis, Part 1, ASA-SSSA.

Klute, A., and C. Dirksen. 1986. Hydraulic conductivity and diffusivity: laboratory methods. In: A. Klute (Editor) Methods of soil analysis. Part 1. Agron. Monogr. 9, ASA-SSSA (2nd edition). Madison, WI, pp. 687-734.

Kool, J.B., and J.C. Parker. 1987. FLOFIT. Environmental Systems & Technologies, Inc.-USA, 56 pp.

Kool, J.B., and J.C. Parker. 1988. Analysis of the inverse problem for transient unsaturated flow. Water Resour. Res., 24(6):817-830.

Kool, J.B., J.C. Parker, and M.Th. van Genuchten. 1985. Determining soil hydraulic properties from one-step outflow experiments by parameter estimation: I. Theory and numerical studies. Soil Sci. Soc. Am. J. 49:1348-1354.

Kool, J.B., J.C. Parker, and M.Th. van Genuchten. 1985. Determining soil hydraulic properties from one-step outflow experiments by parameter estimation: II. Experimental studies. Soil Sci. Soc. Am. J. 49:1354-1359.

Kool, J.B., J.C. Parker, and M.Th. van Genuchten. 1987. Parameter estimation for unsaturated flow transport models - A review. J. Hydrol., 91:255-293.

Lauren, J.G., R.J. Wagenet, J. Bouma, and J.H.M. Wosten. 1988. Variability of saturated hydraulic conductivity in a Glossaquic Hapludalf with macropores. Soil Sci. 145(1): 20-28.

Lima, L.A., M.E. Grismer, and D.R. Nielsen. 1990. Salinity effects on Yolo loam hydraulic properties. Soil Sci. 150:451-458.

Little, T.M., and F.J. Hills. 1978. Agricultural experimentation. Design and analysis. pp. 53-65. J. Wiley and Sons Inc, NY.

Maas, E.V. 1990. Crop salt tolerance. In Agricultural Salinity Assessment and Management manual, K.K. Tanji (eds), ASCE, New York. 262-304.

McCoy, E.L., J.Cardina. 1997. Characterizing the structure of undisturbed soils. Soil Sci. Soc. Am. J. 61:280-286.

McGarry, D. 1988. Quantification of the effects of zero and mechanical tillage on a vertisol by using shrinkage curve indices. Aust. J. Soil Res. 26:537-542.

McGarry, D., and I.G. Daniells. 1987. Shrinkage curve indices to quantify cultivation effects on soil structure of a Vertisol. Soil Sci. Soc. Am. J. 51:1575-1580.

McGarry, D., and K.W.J. Malafant. 1987. The analysis of volume change in unconfined units of soils. Soil Sci. Soc. Am. J. 51:290-297.

McIntyre, D.S. 1979. Exchangeable sodium, subplasticity and hydraulic conductivity of some Australian soils. Aust. J. Soil Res. 17:115-120.

McIntire D.S., J. Loveday, and C.L. Watson. 1982. Field studies of water and salt movement in an irrigated swelling clay soil. 1. Infiltration during ponding. Aust. J. Soil Res. 20:81-90.

McIntire D.S., J. Loveday, and C.L. Watson. 1982. Field studies of water and salt movement in an irrigated swelling clay soil. III. Salt movement during ponding. Aust. J. Soil Res. 20:101-105.

McNeal, B.L., and N.T. Coleman. 1966. Effect of solution composition on soil hydraulic conductivity. Soil Sci. Soc. Am. Proc., 30:308-312.

Mishra, S., and J.C. Parker. 1989. Effects of parameter uncertainity on predictions of unsaturated flow. J. of Hydrol., 108: 19-33

Mitchell, A.R. 1992. Shrinkage terminology: Escape from "normalcy". Soil Sci. Soc. Am. J. 56:993-994.

Mitchell, A.R., and M.Th. van Genuchten. 1992. Shrinkage of bare and cultivated soil. Soil Sci. Soc. Am. J. 56:1036-1042.

Mohanty, B.P., R.S. Kanwarand, and R. Horton. 1991. A robust- resistant approach to interpret spatial behaviour of saturated hydraulic conductivity of a glacial till soil under no-tillage system. Water Resour. Res., vol. 27(11): 2979-2992.

Mous, S.L.J. 1993. Identification of the movement of water in unsaturated soils: the problem of identifiability of the model. J. of Hydrol., 143:153-167.

Mualem, Y. 1976. A new model for predicting the hydraulic conductivity of unsaturated porous media. Wat. Resour. Res., 12:513-522.

Mu'azu, S., J. Skopp, and D. Swartzendruber. 1990. Soil water diffusivity determination by a modified one-step outflow method. Soil Sci. Soc. Am. J. 54:1184-1186.

Murray, R.S., and J.P. Quirk. 1980. Clay-water interactions and the mechanism of soil swelling. Colloids and Surfaces. 1:17-32.

Nelder, J.A. 1961. The fitting of a generalization of the logistic curve. Biometrics. 17:89-110.

Nelder, J.A. 1962. An alternative form of a generalized logistic equation. Biometrics. 18:614-616.

Northcote, K.H., and J.K.M. Skene. 1972. Australian soils with saline and sodic properties. CSIRO Aust. Soil Publication 27.

Oostindie K., and J.J.B. Bronswijk. 1992. FLOCR: a simulation model for the calculation of water balance cracking and surface subsidence of clay soils. DLO The Winand Staring Centre. Wageningen, The Netherlands, Report n. 47.

Oostindie K., and J.J.B. Bronswijk. 1995. Consequences of preferential flow in cracking clay soils for contamination risk of shallow acquifers. J. Environ. Manag. 43:359-373.

Oster, J.D. 1994. Irrigation with poor quality water. Agric. Wat. Manag. 25: 271-197

Parker, J.C., D.F. Amos, and D.L. Kaster. 1977. An evaluation of several methods of estimating soil volume change. Soil Sci. Soc. Am. J. 41: 1060-1064

Passioura, J.B. 1976. Determining soil water diffusivity from one-step outflow experiments. Aust. J. Soil Res., 15: 1-8.

Pierson, F.B., and D.J. Mulla. 1989. An improved method for measuring aggregate stability of a weakly aggregate Loessian soil. Soil Sci. Soc. Am. J. 53:1825-1831.

Prendergast J.B. 1995. Soil water bypass and solute transport under irrigated pasture. Soil Sci. Soc. Am. J. 59:1531-1539.

Quirk, J.P., and R.K. Schofield. 1955. The effect of electrolyte concentration on soil permeability. J. Soil Sci. 6:163-178.

Reeve, N.J., D.G.M. Hall, and P. Bullock. 1980. The effect of soil composition and environmental factors on the shrinkage of some clayey British soils. J. of Sci. 31:429-442.

Rengasamy, P., R.S.B. Green, G.W. Ford, and A.H. Mehanni. 1984. Identification of dispersive behaviour and the management of the red-brown earths. Aust. J. Soil Res. 22:413-431.

Rengasamy, P., and K.A. Olsson. 1991. Sodicity and soil structure. Aust. J. Soil Res. 29:935-952.

Rhoades, J. D. 1989. Effect of salts on soils and plants. Proc. National Water Conference IR & WR Division, ASCE.

Rijniersce, K. 1983. A simulation model for physical soil ripening in the Ijsselmeerpolders. Rijksdienst voor de Ijsselmeerpolders. Lelystad, The Netherlands. 216 pp.3

Russo, D., 1988. Determining soil hydraulic properties by parameter estimation: On the selection of a model for the hydraulic properties. Wat. Resour. Res., 24:453-459.

Schafer, W.M., and M.J. Singer. 1976. Influence of physical and mineralogical properties on swelling soils in Yolo County, California. Soil Sci. Soc. Am. J. 40:557-562.

Shainberg, I., and A. Caiserman. 1971. Studies on Na/Ca montmorillonite systems. 2. The hydraulic conductivity. Soil Sci. Vol. III, 5:276-281.

Shainberg I., G.J. Levy, P. Rengasamy, and H. Frenkel. 1992. Aggregate stability and seal formation as affected by drops' impact energy and soil amendments. Soil Sci.154: (2).

Shainberg, I., J.D. Rhoades, and R.J. Prather. 1981. Effect of low electrolyte concentration on clay dispersion and hydraulic conductivity of a sodic soil. Soil Sci. Soc. Am. J. 45:273-277.

So, H.B., and L.A.G. Aylmore. 1993. How do sodic soils behave? The effects of sodicity on soil physical behavior. Aust. J. Soil Res. 31:761-777.

Soil Survey Staff, 1992. Keys to soil taxonomy, 8th edition. SMSS technical monograph n. 19, Blacksbourg, Virginia, Pocahontas Press Inc., 556 pp.

Stakman, W.P., G.V. Valk, and G.G. Van der Harst. 1969. Determination of soil moisture retention curves. I. Sandbox apparatus. Range pF 0 to pF 2.7. ICW, Wageningen, The Netherlands.

Statistix. 1994. User's manual, Version 4.1 Edition. Analytical Software. Tallahassee, FL. 320 pp.

Steenhuis, T.S., and J.Y. Parlange. 1991. Preferential flow in structured and sandy soils. In Proc. National Symp. Preferential flow, Chicago, IL. T.J, Gish and Shirmohammady (eds), 16-17 Dec. 1991, Am. Soc. Agric. Eng., St. Joseph, MI; 12-21

Stolte, J., J.I. Freyer, W. Bouten, C. Dirksen, J. Halbersma, J.C. van Dam, J.A. van den Berg, G.J. Veerman, and J.H.M. Wosten. 1994. Comparison of six methods for determining unsaturated soil hydraulic conductivity. Soil Sci. Soc. Am. J. 58: 1596-1603.

Stolte, J., and G. Veerman. 1991. Manual of soil physical measurements. Vers. 2.0. The Winand staring Centre, Wageningen, The Netherlands.

Sumner, M.E. 1993. Sodic soils: new perspectives. Aust. J. Soil Res. 31:683-750.

Systat. 1992. Statistics, Version 5.2, Ed. Evanstone, IL: Systat, Inc, 724 pp.

Szabolcs, I. 1989. Amelioration of soils in salt-affected areas; Soil Technology, vol. 2:331-334,Cremlingen

Szabolcs, I. 1989. Salt affected soils. CRC press. Boca Raton, Florida.

Szabolcs, I. 1992. Salinization and desertification. Acta Agronomica Hungarica, 41:137-148

Szabolcs, I. 1994. Prospects of soil salinity for the 21st century. 15th International Congress of Soil Science, Acapulco, Mexico

Tanton T.W., D.W. Rycroft, and F. Wilkinson. 1988. The leaching of salts from saline heavy clay soils: factors affecting the leaching process. Soil Use Management, 4:133-139.

Thorburn, P.J., C,W. Rose. 1990. Interpretation of solute profile dynamics in irrigated soils. III: a simple model of bypass flow. Irrig. Sci. 11:219-225.

Toorman, A.F. and P.J. Wierenga. 1992. Parameter estimation of hydraulic properties from one-step outflow data. Water Resour. Res. 28(11):3021-3028.

UNEP. 1984. Status of desertification and implementation of the United Nations plan of action to combat desertification.. Governing Council, 12th session, Nairobi.

UNEP 1991. Status of desertification and implementation of the United Nations plan of action to combat desertification. UNEP, Nairobi.

US Salinity Laboratory Staff. 1954. Saline and alkali soils. US Dept. Agr. Handbook n.60. 160 p.

Valiantzas, J.D., P.G. Kerkides, and A. Poulovassilis. 1988. An improvement to the one-step outflow method for the determination of soil water diffusivities. Water Resour. Res. 24(11):1911-1920.

van Dam, J.C., J.N.M. Stricker, and P. Droogers. 1990. From one-step to multi-step. Determination of soil hydraulic functions by outflow experiments. Report 7. Agricultural Univ., Wageningen, the Netherlands.

van Dam, J.C., J.N.M. Stricker, and P. Droogers. 1994. Inverse method to determine soil hydraulic functions from multi-step outflow experiments. Soil Sci. Soc. Am. J. 58: 647-652.

van Dam, J.C., J.N.M. Stricker, and A. Verhoef. 1992. Inverse method for determining soil hydraulic functions from one-step outflow experiments. Soil Sci. Soc. Am. J. 56:1042-1050.

van der Molen, W.H. 1973. Salt balance and leaching equipment. In Drainage principles and application. Pub. 16 Int. Inst. for Land reclamation and Improve., Wageningen, The Netherlands.

van der Tak, L. and M.E. Grismer. 1987. Irrigation, drainage and soil salinity in cracking soils. Transaction of the ASAE, 30:740-744.

van Genuchten, M. Th. 1980. A closed-form equation for predicting the hydraulic conductivity of unsaturated soils. Soil Sci. Soc. Am. J. 44:892-898.

van Stiphout, T.P.J., H.A.J. van Lanen, O.H. Boersma, and J. Bouma. 1987. The effect of bypass flow and internal catchment of rain on the water regime in a clay loam grassland. J. of Hydrology 95:1-11.

Vereecken, H., J. Maes and J. Feyen, 1990. Estimating unsaturated hydraulic conductivity from easily measured soil properties. Soil Science, 149 [1], 1-12.

Wagenet, R.J. and J.L. Hutson. 1992. LEACHM: A process based model of water and solute movement, transformation, plant uptake and chemical reactions in the

unsaturated zone. Centre of Environmental Research, Cornell University, Ithaca New York, USA.

White, R.E. 1985. The influence of macropores on the transport of dissolved and suspended matter through soil. Adv. Soil Sci. 3:95-120

Yasuda, H., R. Berntsson, A. Bahri, and K. Jinno. 1994. Plot-scale solute transport in a semiarid agricultural soil. Soil Sci. Soc. Am. J. 58:1052-1060.

Yates, S.R., M. Th. van Genuchten, A.W. Warrick, and F.J. Leij. 1992. Analysis of measured, predicted and estimated hydraulic conductivity using the RETC computer program. Soil Sci. Soc. Am. J. 56: 347-354.

Yeh, W.G., 1986. A review of parameter estimation procedures in groundwater hydrology: the inverse problem. Wat. Resour. Res., 22:95-108.

Yong, R.N., and B.P. Warkentin. 1975. Soil properties and behaviour. Elsevier Scientific Publishing Co. Amsterdam. The Netherlands. 449pp.

Yule, D.F., and J.T. Ritchie. 1980. Soil shrinkage relationship of Texas Vertisols: I Small cores. Soil Sci. Soc. Am. J. 44:1285-1291.

Yule, D.F., and J.T. Ritchie. 1980. Soil shrinkage relationship of Texas Vertisols: I Large cores. Soil Sci. Soc. Am. J. 44:1291-1295.

Zachmann, D.W., P.C. Duchateau, and A. Klute. 1982. Simultaneous approximation of water capacity and soil hydraulic conductivity by parameter identification. Soil Sci., 134:157-163.

Summary

The available amount of water for agriculture, and specifically for irrigation, is decreasing all over the world. The quality of irrigation water is also deteriorating, and saline/sodic waters are increasingly used in many arid and semi-arid regions of the world.

Salinization is closely associated with desertification, which is defined as "land degradation in arid, semi-arid and dry sub-humid areas resulting from climatic variations and human activities", with the term "land" including soil, water resources, crops and natural vegetation.

Sustainable land management practices are urgently needed to preserve the production potential of agricultural land while safeguarding environmental quality.

This thesis is a contribution to hydrological and environmental research focused on prevention of land degradation and desertification in arid and semi-arid regions, with special attention to some peculiar conditions occurring in Sicily, where irrigation with saline-sodic waters in cracking soils is increasingly practised.

Swelling/shrinking clay soils change volume with changes in water content, and during dry periods extensive cracks will form in the field. Soil cracks alter the pore-size distribution through intermittent wetting, acting as significant pathways for water and solutes and determining the occurrence of bypass flow, i.e. the rapid transport of water and solutes via shrinkage-cracks to subsoil and to groundwater.

Differences between the soil shrinkage curve obtained on resin-coated natural aggregates (volume 20-30 cm^3) and on cylindrical confined cores having a volume (650 cm^3) which is close to the volume of cores used for laboratory determination of soil hydraulic characteristics, were investigated on twenty-one Sicilian soils of variable shrink/swell behaviour.

The results showed that measurement of vertical and horizontal shrinkage in confined soil cores was suitable to incorporate shrinkage in the soil hydraulic parameters/functions determined on confined undisturbed soil samples. The investigation also showed the possibility to predict the soil shrinkage characteristic curve of confined cores from routinely measured soil physical properties **(Chapter 2)**.

Models simulating transport of water and solutes in unsaturated soil require the knowledge of soil hydraulic characteristics, i.e. the soil moisture characteristic curve and the hydraulic conductivity function. The multistep outflow method (MSTEP) with inverse modeling is often used to determine the soil hydraulic properties. However, specific optimization techniques accounting for the presence of preferential pathways through cracks and incorporating shinkage processes need to be developed for acccurate determination of the hydraulic conductiecvity in swelling and shrinking clay soils.

The applicability of the inverse method based on one-step and multi-step outflow experiments for determining the $\theta(h)$ and the $K(\theta)$ functions in swelling/shrinking soils was investigated.

The results showed the need for using optimization procedures incorporating structural porosity and shrinkage processes on the basis of hydraulic conductivity values determined by the suction crust infiltrometer method, and of the soil shrinkage characteristic determined on confined soil cores **(Chapter 3)**.

Interactions between soil physical properties and salinity and sodicity are complex, and still need much investigation in order to derive sustainable management options suitable to prevent irreversible land degradation phenomena.
An exchangeable sodium percentage (ESP) greater than 15 is considered to affect soil structure and hydraulic characteristics. Some investigations suggested that this threshold may need reconsideration because soil degradation can take place even at low ESP values.
Investigations performed on two Sicilian Vertisols showed that the concept of critical threshold needs to be reconsidered, because soil degradation at increasing ESP appears to be a continuum, and that a major hazard of deterioration of structural and hydraulic properties may occur even at low ESP values (ESP<5) in dilute solutions **(Chapter 4)**.

The influence that reductions in hydraulic conductivity due to salinity and/or sodicity may have on water transport in the soil-crop system was evaluated by simulations performed with the water flow version of the LEACHM model.
The results evidenced the large influence that the reductions in the soil hydraulic conductivity, occurring at ESP values ranging from 0 to 15, may have on water balance in clay soils. Application of the chemistry version of LEACHM for prediction of salinity and sodicity in the same context also demonstrated the need for improving the model, accounting for the occurrence of bypass flow **(Chapter 5)**.

Bypass flow processes can be particularly relevant in Mediterranean areas characterized by low amounts of the annual rainfall, high values of the rainfall intensity and clay soils with a low hydraulic conductivity.
Quantitative evaluation of the relevance that bypass flow may have on water balance in a case study in Sicily was performed by the simulation model FLOCR. The results showed that bypass flow corresponded with about 70-74% of the cumulative yearly rainfall, and that models not accounting for bypass flow may lead to a serious overprediction of (evapo)transpiration and to a serious underestimation of the hazard of land degradation and desertification **(Chapter 6)**.

Conjunctive or alternate use of different quality irrigation waters can be applied to reduce salt-accumulation in the root zone through adequate leaching, and to keep the cationic concentration (C) of the pore solution at thresholds compatible with the crops tolerance.
The role that bypass flow may have on salt-accumulation and salt-leaching in a Sicilian cracking soil under alternate use of a high salinity solution to distilled water was investigated in **Chapter 7**. The results showed that exchanges of solutes occurred at the contact surfaces between the macropores/cracks walls and the incoming solution in concomitance with bypass fluxes. These exchanges led to dispersion and diffusion of the solutes and were effective in leaching solutes and in preventing salt-accumulation in the soil sample.

Sustainable management of irrigation in cracking soils should take into account the influence that land use may have on structure and bypass flow phenomena.

The influence of two different irrigation systems, i.e. drip and micro-sprinkler, on soil structure and bypass flow phenomena in a Sicilean cracking soil was explored by application of dye tracers and laboratory measurements of bypass flow performed on undisturbed soil cores. Different vertical distributions of cracks were found under the two irrigation systems. In agreement with these observations, different flow behaviour was observed in the laboratory in cylindrical soil cores taken from the two fields. No bypass flow or lower amount of bypass flow was observed in the micro-sprinkler compared to the drip irrigation treatment. **(Chapter 8).**

Samenvatting

Op wereldschaal neemt de beschikbare hoeveelheid water voor landbouw en irrigatie, af. Ook de kwaliteit van irrigatiewater neemt af. Daarnaast wordt, met name, in aride en semi-aride gebieden in toenemende mate zouthoudend water voor irrigatie gebruikt.

Verzouting kan ontaarden in verwoestijning wat gedefinieerd is als "land degradatie in aride, semi-aride en droge sub-humide regio's als gevolg van klimatologische variaties en menselijke activiteiten". Met de term "land" wordt wordt hier de bodem inclusief bodemvocht, gewassen en natuurlijke vegetatie bedoelt.

Om het productie potentieel van deze landbouwgronden op peil te houden, met in acht name van milieukundige randvoorwaarden, zijn duurzame landgebruiksmethoden nodig.

Dit proefschrift is een bijdrage aan het hydrologisch en milieukundig onderzoek gericht op de preventie van land degradatie en verwoestijning in aride en semi-aride gebieden. Speciale aandacht gaat hierbij uit naar een case studie in Sicilië, waar irrigatie met zout water in gescheurde kleigronden in toenemende mate wordt toegepast.

Met het veranderen van het vochtgehalte in de bodem, veranderd het bodemvolume in zwellende en krimpende kleigronden. Gedurende droge perioden zullen hierdoor scheuren ontstaan die in natte perioden weer sluiten. Dit dynamische proces leidt tot een constant veranderende poriëngrootteverdeling in de bodem. Deze scheuren spelen daarnaast een belangrijke rol in het transport van water en opgeloste stof naar de ondergrond of het grondwater. Dit laatste proces wordt aangeduid als "bypass flow".

Verschillen in de krimpkarakteristieken zoals verkregen via hars-gecoate, natuurlijke, bodemaggregaten van circa 20 tot 30 cm^3 zijn vergeleken met volume veranderingen gemeten aan cylindrische bodemmonsters (volume 650 cm^3). Deze monsters zijn vergelijkbaar met standaard bodemmonsters zoals gebruikt voor de bepaling van bodem hydraulische karakteristieken.

Op één-en-twintig Siciliaanse bodemmonsters met verschillende krimp en zwel karakterisiteken zijn zowel de bodem hydraulische karakterisiteken als verticale en horizontale krimp bepaald. De resultaten van dit onderzoek gaven aan dat het meten van horizontale en verticale krimp in cylindrische bodemmonsters geschikt was om bodemkrimp en de daaraan gerelateerde veranderende hydraulische karakterisiteken te kwantificeren en om de krimpkarakteristiek, zoals bepaald aan de hars-gecoate monsters, af te leiden (Hoofdstuk 2).

Voor het simuleren van water en opgeloste stof transport in het onverzadigde deel van de bodem is kennis van de bodem hydraulische eigenschappen, zoals de waterretentie en doorlatendheidskarakterisitek, van groot belang. De multi-step outflow methode (MSTEP), gecombineerd met invers modeleren, wordt veelal gebruikt om deze beide karateristieken simultaan te bepalen. Echter, specieke optimalisatie technieken die rekening houden met de aanwezigheid van preferentiële stroming door scheuren ontbreken en dienen te worden

ontwikkelt voor een betrouwbare bepaling van de doorlatendheidskarakteristieken in krimpende en zwellende kleigronden.

De toepasbaarheid van invers modeleren, gebaseerd op de "one-step" en "multi-step" outflow experimenten, voor de bepaling van de waterretentie en doorlatendheiddskarakterisitek op zwellende en krimpende kleigronden is onderzocht in **Hoofdstuk 3.**

De resulten laten zien dat het inbrengen van structurele porositeit en krimpprocessen in de optimalisatie procedures, op basis van de doorlatendheidscurve waarden zoals bepaald met de "suction crust infiltrometer" en de krimpkarakteristiek op bodemkolommen met zwellende en krimpende kleigronden, noodzakelijk is.

Interacties tussen bodemfysische eigenschappen en verzouting zijn complex en behoeven nog veel onderzoek om duurzame management opties te ontwikkelen die irreversibele landdegradatie tegengaan.

Een uitwisselbaar natrium percentage (ESP) groter dan 15 wordt over het algemeen geacht de bodemstructuur en de fysieke eigenschappen van een bodem te veranderen. Sommige onderzoeken geven echter aan dat deze drempelwaarde wellicht moet worden aangepast omdat veranderingen aan bodemeigenschappen ook al oprtreden bij lagere ESP waarden.

Onderzoek verricht aan twee Siciliaanse Vertisolen gaf aan dat het concept van de kritische drempelwaarde inderdaad herbezien dient te worden omdat bodemdegradatie met toenemende ESP waarden een continue proces is en dat verslechtering van bodemstructuur en hydraulische eigenschappen al optreden bij lagere ESP waarden (< 5) (**Hoofdtuk 4**).

De afname in de doorlatendheid, als gevolg van verzouting, op het water transport in een bodem-gewas-systeem is onderzocht met behulp van simulaties met de water module van het LEACHM-model.

De resultaten demonstreerden de grote invloed op de gesimuleerde waterbalans van een afnemende doorlatendheid als gevolg van toenemende (0 tot 15) ESP waarden. Toepassing van LEACHC, de zout versie van LEACHM, ten behoeve van de voorspelling van verzouting in dezelfde context liet de noodzaak zien tot het aanpassen van het LEACHC model met betrekking to bypass stroming (**Hoofdstuk 5**).

Bypass processen kunnnen bijzonder relevant zijn in mediterane gebieden gekarakteriseerd door lage hoeveelheden jaarlijkse neerslag met hoge regenintensiteiten en kleigronden met lage hydraulische doorlatendheid.

Kwantitatieve evaluatie van de relevantie van bypass stroming op de waterbalans voor een case study op Sicilië is uitgevoerd met behulp van het simulatie model FLOCR. De resultaten lieten zien dat bypass stroming ongeveer 70-74% van de cumulatieve jaarlijkse neerslag bedroeg. Modellen die bypass stroming dan ook niet simuleren kunnen leiden tot een ernstige overschatting van (evapo)transpiratie en tot een onderschatting van het gevaar van land degradatie en verwoestijning (**Hoofdstuk 6**).

Menging van verschillende waterkwaliteiten, of het alternerend gebruik van goed en zout irrigatie water, kan woren gebruikt om zoutaccumulatie in de wortelzone tegen te gaan,

adequate uitspoeling te bevorderen en de kation concentratie van het bodemvocht beneden de drempelwaarde voor gewas tolerantie te houden.

De rol die bypass stroming kan hebben op zoutaccumulatie en uitspoeling in een Siciliaanse gescheurde kleigrond onder het afwisselend gebruik van irrigatie water met een hoge en lage zout concentratie is onderzocht in **Hoofdstuk 7**. De resultaten gaven aan dat de uitwisseling van oplossingen in samenhang met bypass stroming voorkwam op het contact oppervlak tussen macroporiën en bypass water. Deze uitwisseling leidde tot diffusie en dispersie van de oplossingen en was effectief in het doorspoelen van het bodemmonster. Zoutaccumulatie in de bodem kon op deze wijze worden voorkomen.

Duurzame management systemen voor irrigatie in gescheurde kleigronden zouden rekening moeten houden met de invloed die landgebruik heeft op de bodemstructuur en bypass stroming.

Het effect van twee verschillende irrigatiesystemen (drip en sprinkler) op de bodemstructuur en bypass stroming is onderzocht met behulp van tracers en laboratorium metingen op ongestoorde bodemmonsters in een Siciliaanse gescheurde kleigrond. De verticale verdeling van scheuren onder de twee irrigatie systemen was zeer verschillend. Deze verschillen stemden overeen met de waarnemingen verricht aan bodemmonsters genomen op beide velden en genalyseerd in het laboratorium. Geen of bijna geen bypass kon worden waargenomen in de met sprinkler geirrigeerde velden. Velden onder drip irrigatie vertoonden juist wel significante hoeveelheden bypass stroming (**Hoofdstuk 8**).

167

Curriculum Vitae of Giuseppina Crescimanno

Born in Palermo (Italy) on September 15, 1955, she graduated in Agricultural Sciences in Palermo in July 1980 (maximum cum laude).

She had a position as Researcher at the Agricultural University of Palermo from 17/11/83 to 8/9/1992, and became Associate Professor of Agro-Hydrology on 7/9/1992.

Her research activity covered the field of agro/hydrology, with a special focus on methodologies for determination of hydraulic and shrinkage characteristics, water and solute transport in cracking soils, and prevention of degradation and desertification.

She is actually coordinating the European Project: "An integrated approach for sustainable management of irrigated lands susceptible to degradation/deser-tification", funded by the Environment and Climate Programme, Area 1.1.43: "Land resources, and the threat of land degradation and desertification in Europe" (contracts ENV4-CT97-0681).

She participated to the activity of selection of projects in the frame of the programmes "Energy, Environment and Sustainable Development" and "Sustainable management and quality of water". She coordinates a Socrates/Erasmus exchange programme involving exchanges with the universities of Wageningen (NL) and Cordoba (ES).

Her teaching activity (permanently) covered the course of Agro/hydrology and (temporarily) the course of Soil and Water Conservation at the Palermo Agricultural University.

She actually has a permanent position of Associate Professor of Agro/Hydrology at the Agricultural University of Palermo, Italy.

Errata corrige

p. 7: assist to=attend

p. 26: Crescimanno and Iovino (1995) = Crescimanno and Iovino (1995a)

p. 27: eq. 3 $$v = \frac{1}{\rho_s} + \frac{a'}{\rho_s + \exp[\alpha' \rho_s U]} + b'U$$

p. 27: Fig. 1 :U=UA; U=UB

p. 28: v (m^3/Mg^{-1})= v (m^3/Mg); ρb (Mg/m^{-3})= ρb (Mg/m^3); U (Mg/Mg^{-1}) = U (Mg/Mg)

p. 50: eq.(8) = eq. (16)

p. 55: $(t_i) = \hat{V}(t_i)$

p. 55: Fig. 2: procedure 8/3= procedure 5/3

p. 57: $(t_i) = \hat{V}(t_i)$

p. 60: Fig 7b q=θ

p. 64: Crescimanno and Iovino (1995a)

p. 65: Crescimanno and Iovino (1995a)

p. 69: Fig 1A D2=A1

p. 71: Fig 3c A1=D2

p. 81: Crescimanno and Iovino (1994)= Crescimanno and Iovino (1995b)

p. 83: Fig 4 1 mol m^{-3} T = 1 mol m^{-3}

p. 104: ⊔(h) = θ (h)

p. 105: Crescimanno and Iovino (1995) = Crescimanno and Iovino (1995b)

p. 114: Crescimanno et al. (1995) = Crescimanno et al. (1995b)

p. 123: Table 3 SAR5=SAR 20

p. 132: Crescimanno et al. (1995)=Crescimanno et al. (1995b) ; Crescimanno and Iovino (1995)=
Crescimanno and Iovino (1995a)

p. 140: Crescimanno et al. (1995)=Crescimanno et al. (1995b) ; Crescimanno and Iovino (1995)=
Crescimanno and Iovino (1995a)

p. 147: ESP 0 to 15 = ESP 0 to 10

p. 162: ESP 0 to 15 = ESP 0 to 10

p. 166: ESP 0 to 15 = ESP 0 to 10

p. 153 :
Crescimanno, G., and M. Iovino. 1995a. Evaluating the effects of saline-sodic waters on the hydrological
characteristics of soil. International Symposium on Water Quality Modeling. Orlando, Florida, 2-5 April.
Crescimanno, G., and M. Iovino. 1995b. Parameter estimation by inverse method based on outflow one-step
and multistep outflow experiments. Geoderma 68:257-277
Crescimanno, G., M. Iovino and E. Marcone. 1995a. Irrigation with saline-sodic waters: water and salt-balance
in a Sicilian field. Int. Symp. on Salt-affected Lagoons ecosystems, ISSALE 95, Valencia, sept. 18-25,
1995
Crescimanno, G., M. Iovino and G. Provenzano. 1995b. Influence of salinity and sodicity on soil structural and
hydraulic characteristics. Soil Sci. Soc. Am. J.59:1701-1708
Crescimanno, G., and G. Provenzano. 1995. Fenomeni di rigonfiamento e contrazione dei terreni argillosi:
indagime sperimentale nell'ambiente siciliano. Rivista di Ingeneria agraria, Anno XXVI, n. 3.
Crescimanno, G., and G. Provenzano. 1998a. Clay soils susceptible to bypass flow: influence of sodicity on
water balance. XIIIth Int. Congress.on Agricultural Engineering, Rabat, Marocco, February 2-3.
Crescimanno, G., and G. Provenzano. 1998b. La gestione dell'irrigazione con acque salino/sodiche in terreni
suscettibili a processi di degradazione. Rivista Irrigazione e drenaggio 1:21-24.